

Antimatter and Antiparticles in the Cosmic Radiation

The Existence of Antimatter

Paul A.M. Dirac

Theory of electrons and positrons

Nobel Lecture, December 12, 1933

Relativity:

$$\frac{W^2}{c^2} - p_{r^2} - m^2 c^2 = 0$$

Quantum Theory:

$$\left[\frac{W^2}{c^2} - p_{r^2} - m^2 c^2 \right] \Psi = 0$$

$$m^2 = (m)(m) = (-m)(-m)$$

Dirac asked: What is (-m) → Theory of antimatter

Antiparticles and Antimatter

We must regard it rather as an accident that the Earth and presumably the whole solar system contains a preponderance of negative electrons and positive protons. It is quite possible that for some of the stars it is the other way about.

P. A.M. Dirac Nobel Prize lecture

History of antimatter: theory and experiments

1928: Prediction existence of positrons (Dirac)

1932: Detection of positrons (Anderson)

1955: Production of antiproton at accelerator (Chamberlain et al.)

1960's: BSU cosmologies (Klein, Alven,...)

1965: Discovery of the Microwave Background Radiation e Big Bang Cosmologies

1967: Sakharov's conditions (Sakharov)

1970's: gamma-ray limits

1979: Detection of cosmic-ray antiprotons (Golden et al., Bogomolov et al.)

1996: Antihydrogen produced in a laboratory (Baur et al.)

Baryogenesis, matter and antimatter

Theoretically:

- There is an almost exact symmetry between matter and antimatter.

Experimental facts:

- There is no evidence for significant amounts of antimatter in the Universe, e.g.:
 - The primary cosmic ray nuclei are found to be completely dominated by nuclei rather than antinuclei
 - No evidence for the intense γ - and X-ray emissions expected from matter in galaxies colliding with 'clouds' of antimatter



Simple Big Bang Model

The early Universe was a hot expanding plasma with equal number of baryons, antibaryons and photons. In thermal equilibrium the two-ways reaction was:



As the Universe expands, the density of particles and antiparticles falls, annihilation process ceases, effectively freezing the ratio:

- baryon/photon = antibaryon/photon $\sim 10^{-18}$.
- Annihilation catastrophe.

Instead, in the present real Universe:

- Baryon/photon $\sim 10^{-9}$ (from direct observ. & microwave background);
- Antibaryon/baryon $< 10^{-4}$.

Sakharov criteria

To account for the predominance of matter over antimatter, Sakharov (1967) pointed out the necessary conditions:

- *B violating interactions;*
- *non-equilibrium situation;*
- *CP and C violation.*



GUT theories ?

Leptogenesis ?

The processes really responsible are not presently understood!

What about the observations?

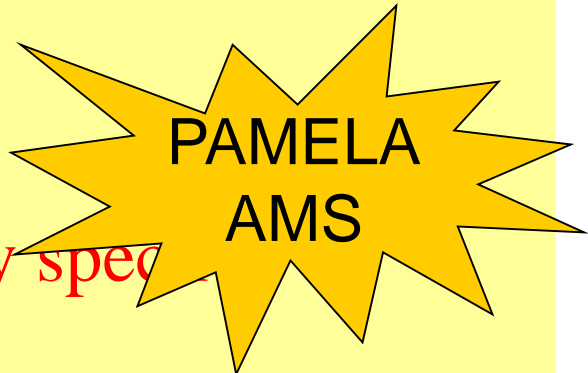
Indirect ->

By measuring: the spectrum of the Cosmic Diffuse Gamma emission

Direct ->

By searching for Antinuclei

By measuring anti-p and e⁺ energy spec



a "matter trail" from the solar system to the Galaxy

solar system

micro-meteorites and solar wind particles are continuously bombarding the earth without causing annihilation radiation. Approximating the solar wind flux with $nv \approx 2 \cdot 10^8 (d/1\text{AU})^{-2} \text{ cm}^{-2} \text{ s}^{-1}$, one can roughly estimate the annihilation radiation from an anti-planet :

$$F_\gamma(100\text{MeV}) \approx 10^8 (r/d)^2 \text{ ph cm}^{-2} \text{ s}^{-1} \quad r, d : \text{radius, distance of anti-planet}$$

example : Jupiter ($r = 7 \cdot 10^7 \text{ m}$, $d = 7 \cdot 10^{11} \text{ m}$) : $F_\gamma \approx 1 \text{ ph cm}^{-2} \text{ s}^{-1}$
FERMI features $\sim 10^{-8} \text{ ph cm}^{-2} \text{ s}^{-1}$ sensitivities

stars

Bondi Hoyle accretion of galactic gas onto an anti-star would produce detectable 100 MeV fluxes (FERMI) out to at least 100 pc, corresponding to $\sim 100'000$ stars
 \Rightarrow antimatter fraction $f_{\text{AM}} \leq 10^{-5}$

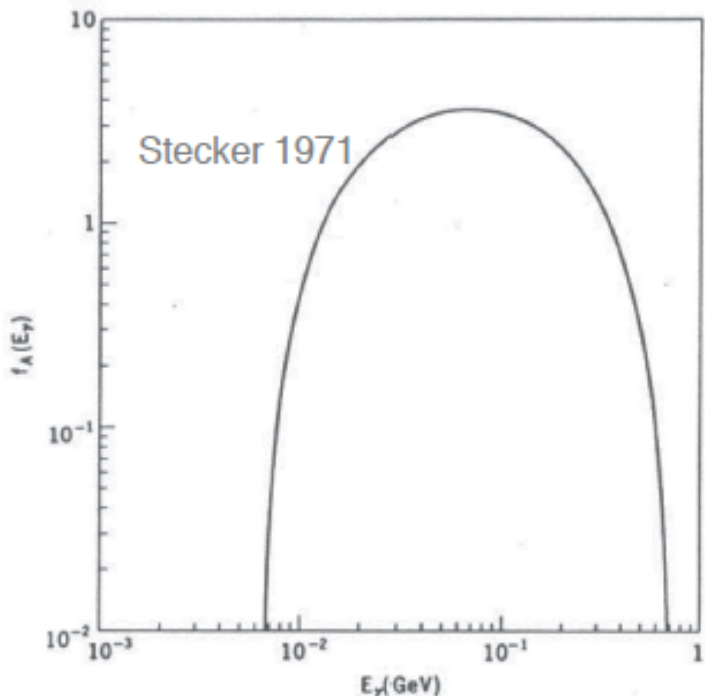
galactic gas

the observed diffuse galactic gamma ray flux (well explained by CR interaction) limits the antimatter fraction $f_{\text{AM}} \leq 10^{-15}$!

the argument can obviously be extended as long as a sufficiently dense matter trail extends out to the next bigger structure ...

gamma rays from nucleon-antinucleon annihilation

$$N - \bar{N} \rightarrow \begin{cases} \pi^0 \rightarrow \gamma + \gamma & 1/3 \text{ of } 2m_N c^2 \rightarrow 200 \text{ MeV } \gamma\text{'s} \\ \pi^\pm \rightarrow \mu^\pm + \nu_\mu (\bar{\nu}_\mu) \\ \quad \downarrow \quad \rightarrow \pi^\pm \rightarrow e^\pm + \nu_e (\bar{\nu}_\mu) + \nu_\mu (\bar{\nu}_\mu) \end{cases}$$



1/2 of $2m_N c^2 \rightarrow \nu\text{'s}$

1/6 of $2m_N c^2 \rightarrow 100 \text{ MeV } e^- / e^+$

typical rest-frame spectrum produced by $p-\bar{p}$ annihilation with π^0 decay

maximum intensity at $m_\pi c^2/2 \sim 70 \text{ MeV}$

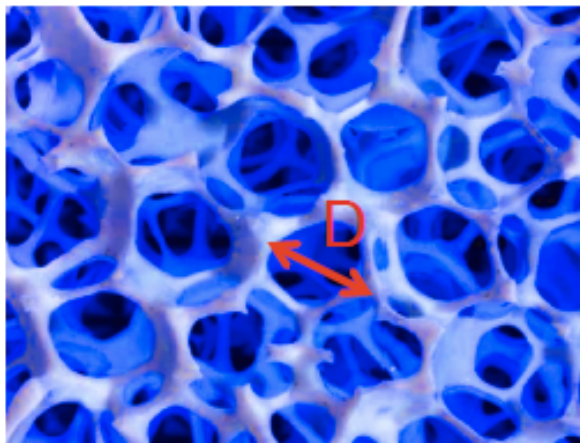
antimatter domains and the diffuse gamma-ray background

Annihilation radiation from the boundaries of matter-antimatter regions, emitted in the early Universe before - and/or - after recombination.

Stecker et al. (1971) solved the cosmological photon transport equation accounting for pair production and Compton scattering at high z.

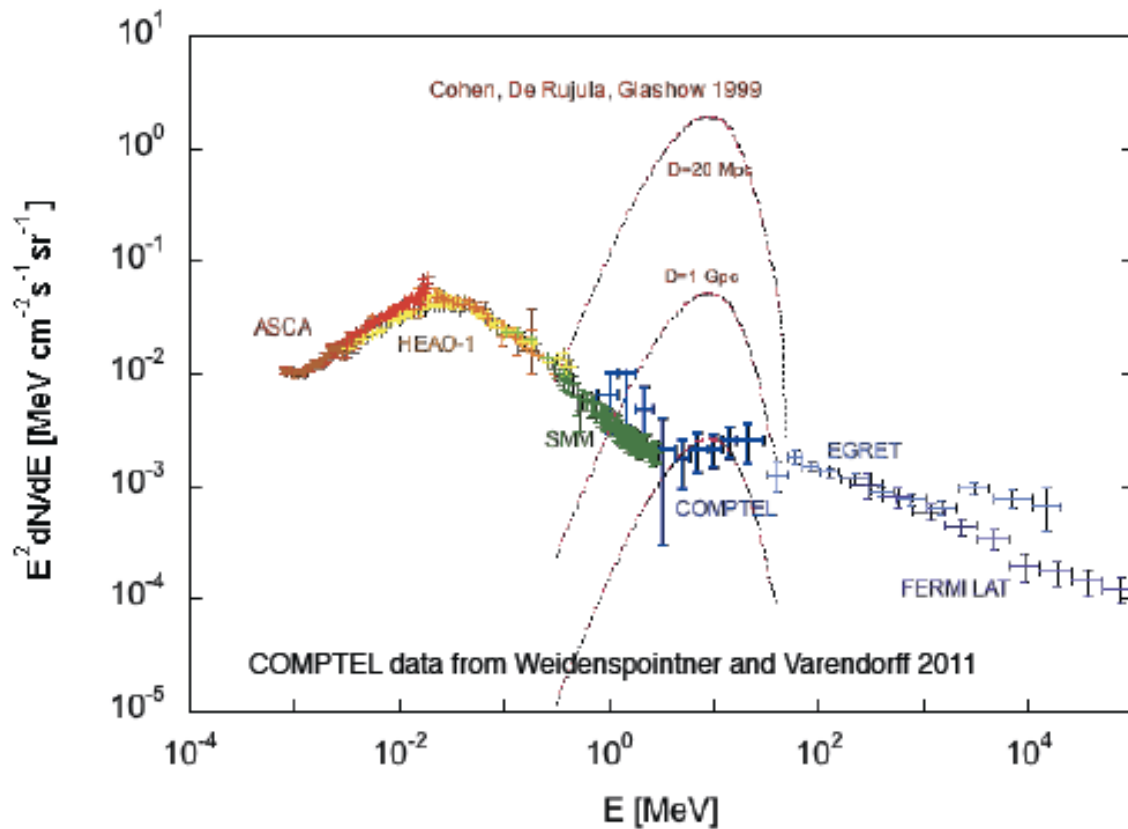
$$y \frac{\partial I}{\partial y} + \epsilon \frac{\partial I}{\partial \epsilon} = 2I + \frac{y^2 \Omega \nu}{[1 + \Omega(y - 1)]^{1/2}} \left[A(\epsilon)I - \int_{\epsilon}^{b(\epsilon)} d\epsilon' B(\epsilon|\epsilon')I(\epsilon', y) - \xi^2 \Omega n_c y^3 \nu(T(y)) \frac{\sigma_A(T(y))}{\pi r_e^2} G_A(\epsilon) \right] \dots$$

=> redshifted gamma-ray "bump" above ~ 1 MeV



what domain-size D (> 20 Mpc)
is compatible with
the observed MeV gamma-ray ?

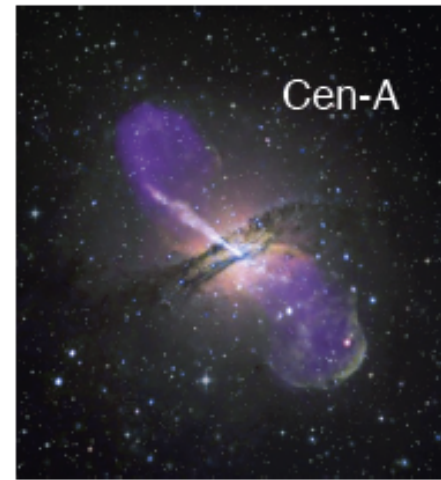
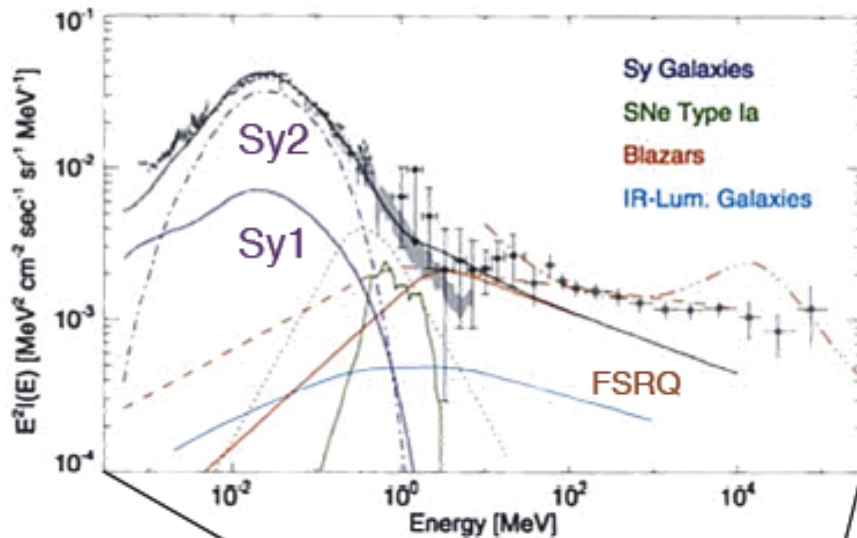
Cosmic diffuse X- and Gamma-Ray Background



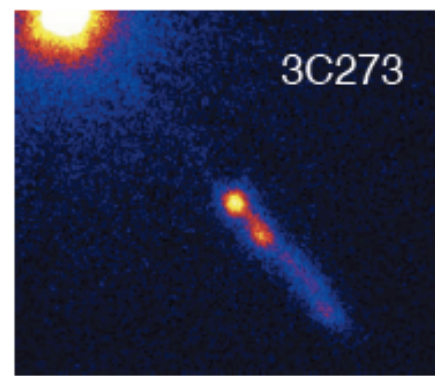
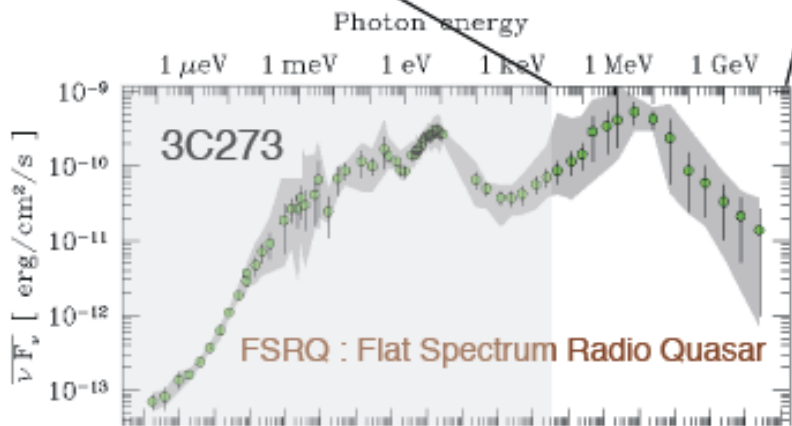
COMPTEL

- no MeV bump
- transition from a softer to a harder component at ~ 5 MeV
- no deviation from isotropy within statistics

MeV background explained as unresolved AGN's



superposition of spectra from various classes of unresolved point sources
=> no need for antimatter domains with sizes $D \approx$ the observable Universe

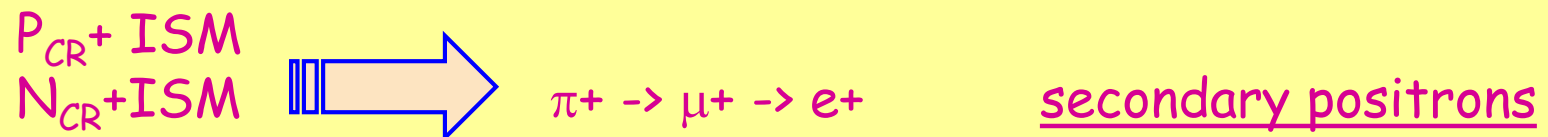


Direct searches: current status

Antiprotons: DETECTED! secondary production



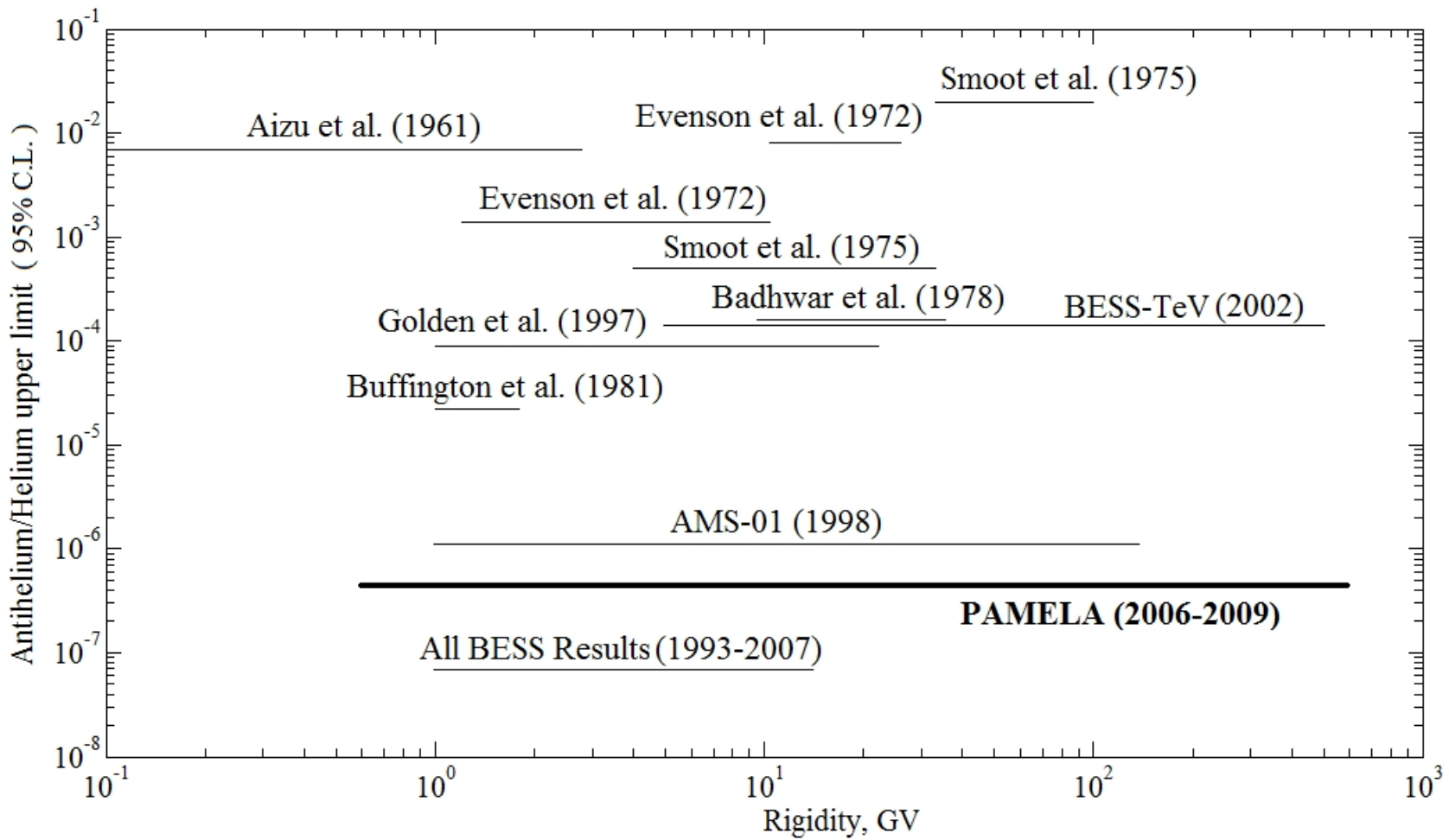
■ Positrons: DETECTED! secondary production



■ Anti-nuclei: never detected!

■ They would be the real signature of antistars because their production by “spallation” is negligible

Antihelium Searches



Antiparticles

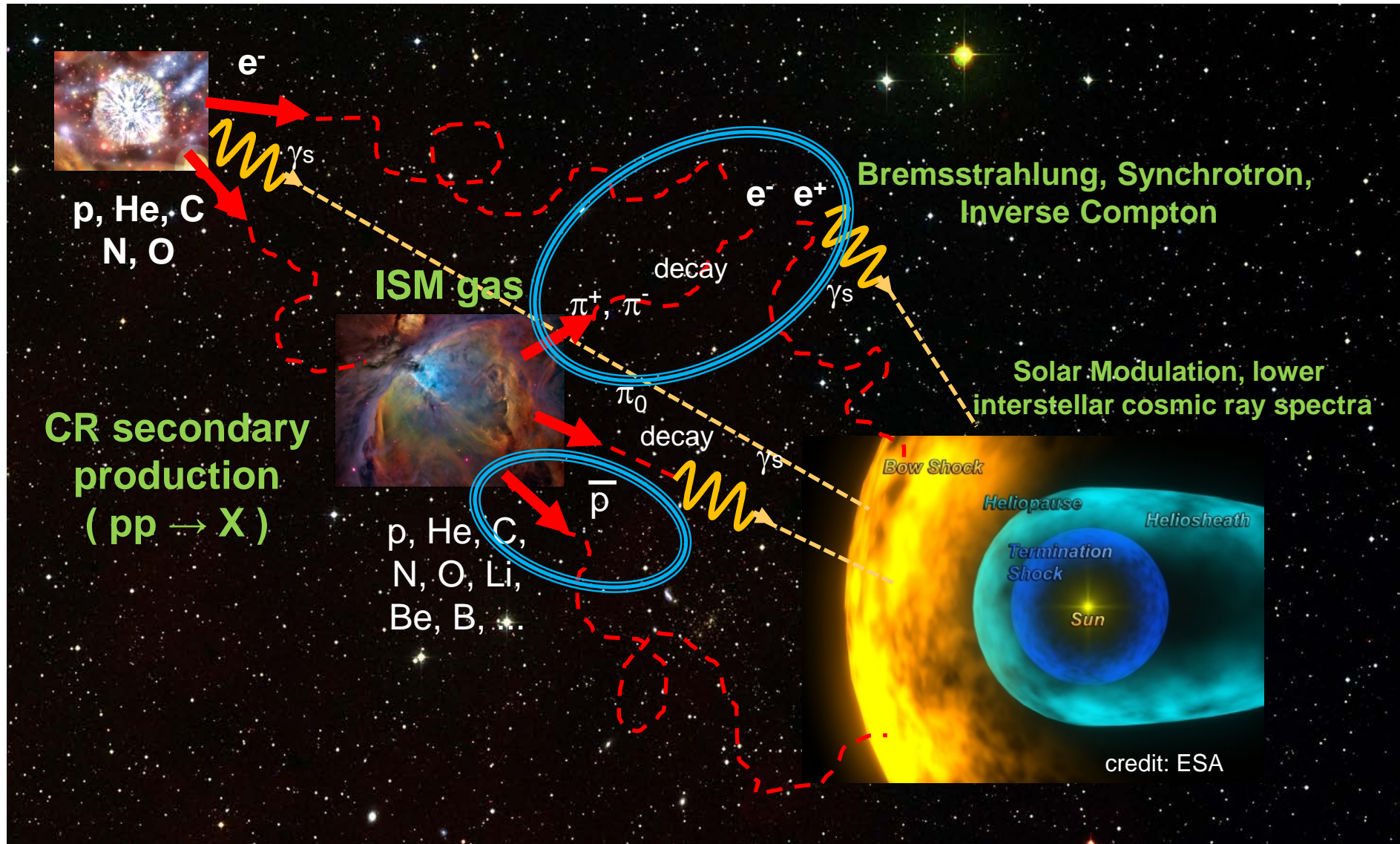
Astrophysics and Cosmology compelling Issues

*Origin and propagation of the cosmic
radiation*

*Nature of the Dark Matter that
pervades the Universe*

*Apparent absence of cosmological
Antimatter*

Cosmic Rays and Anti-Particles



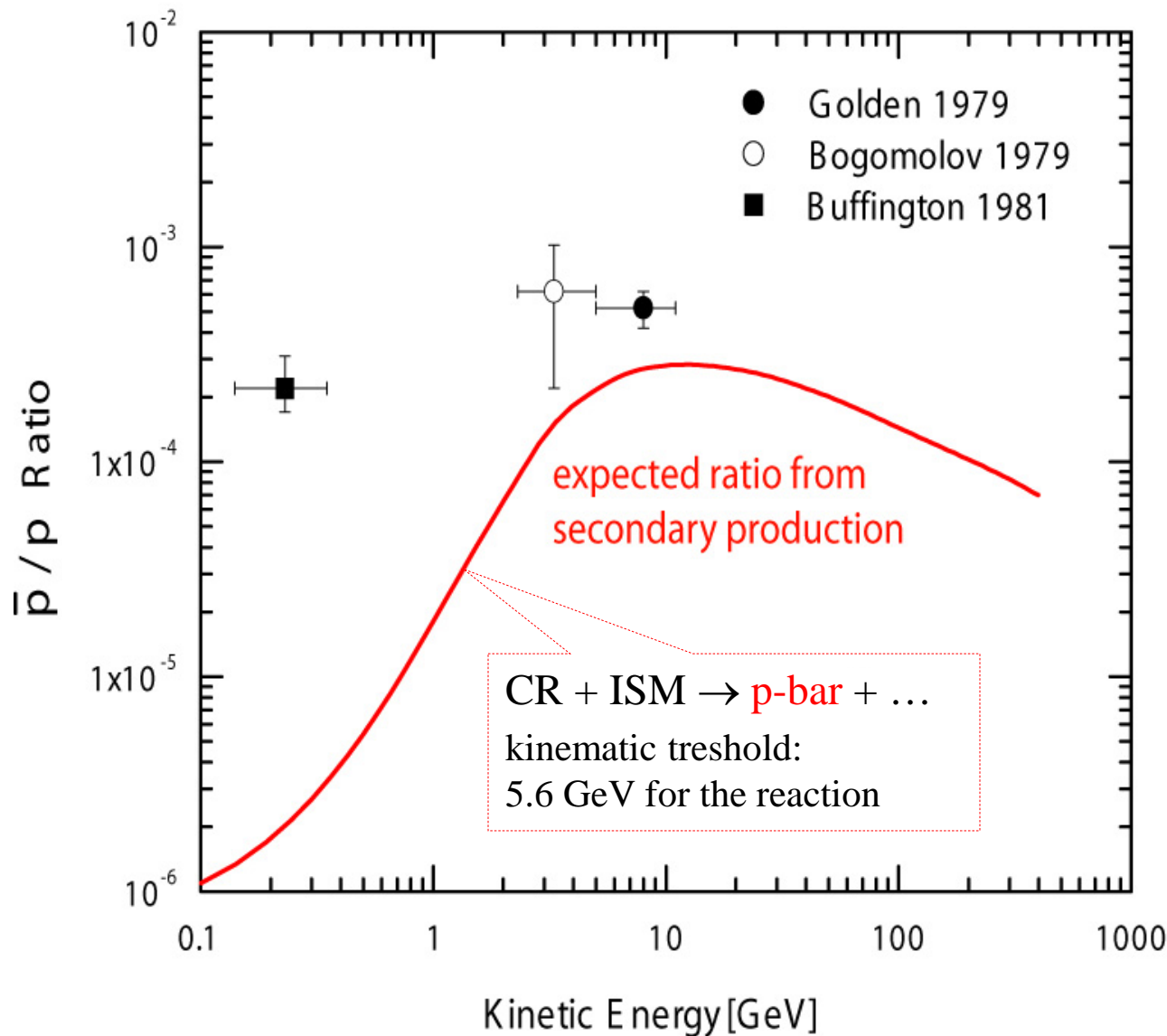
First Detection in the Cosmic Rays



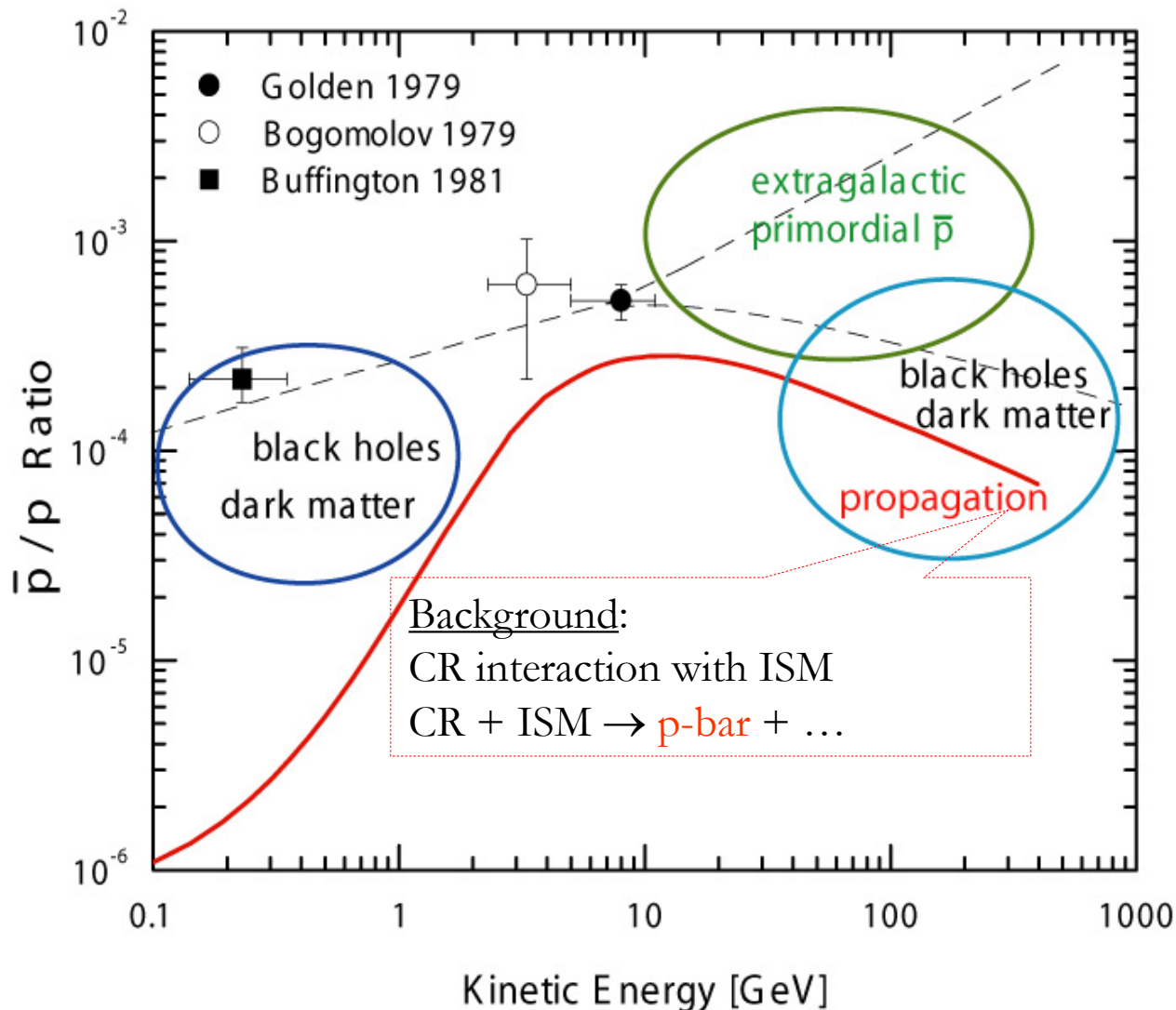
First detection of positrons in the cosmic radiation in 1964 by J.A. De shong, R.H. Hildebrand & P. Meyer (Phys. Rev. Let. **12**, 3, 1964)

First detection of antiprotons in the cosmic radiations in 1979 by R.L. Golden et al. Phys. Rev. Let. **43**, 1264, 1964) and by E. Bogomolov et al.

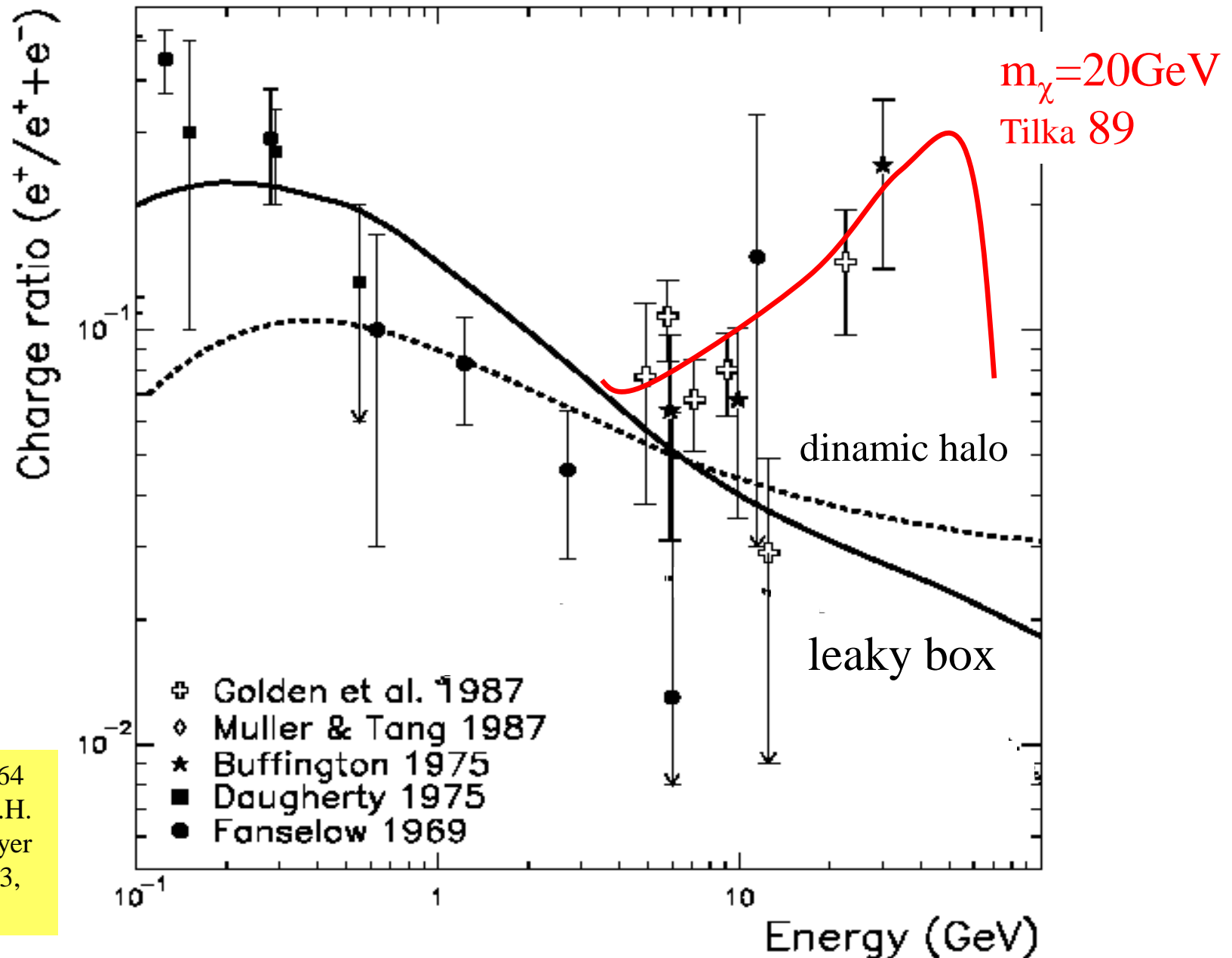
The first historical measurements on galactic antiprotons



The first historical measurements of the \bar{p}/p - ratio and various Ideas of theoretical Interpretations



Balloon data : Positron fraction before 1990



Antiparticle Experiments

(old and new)

Antimatter and Dark Matter Research

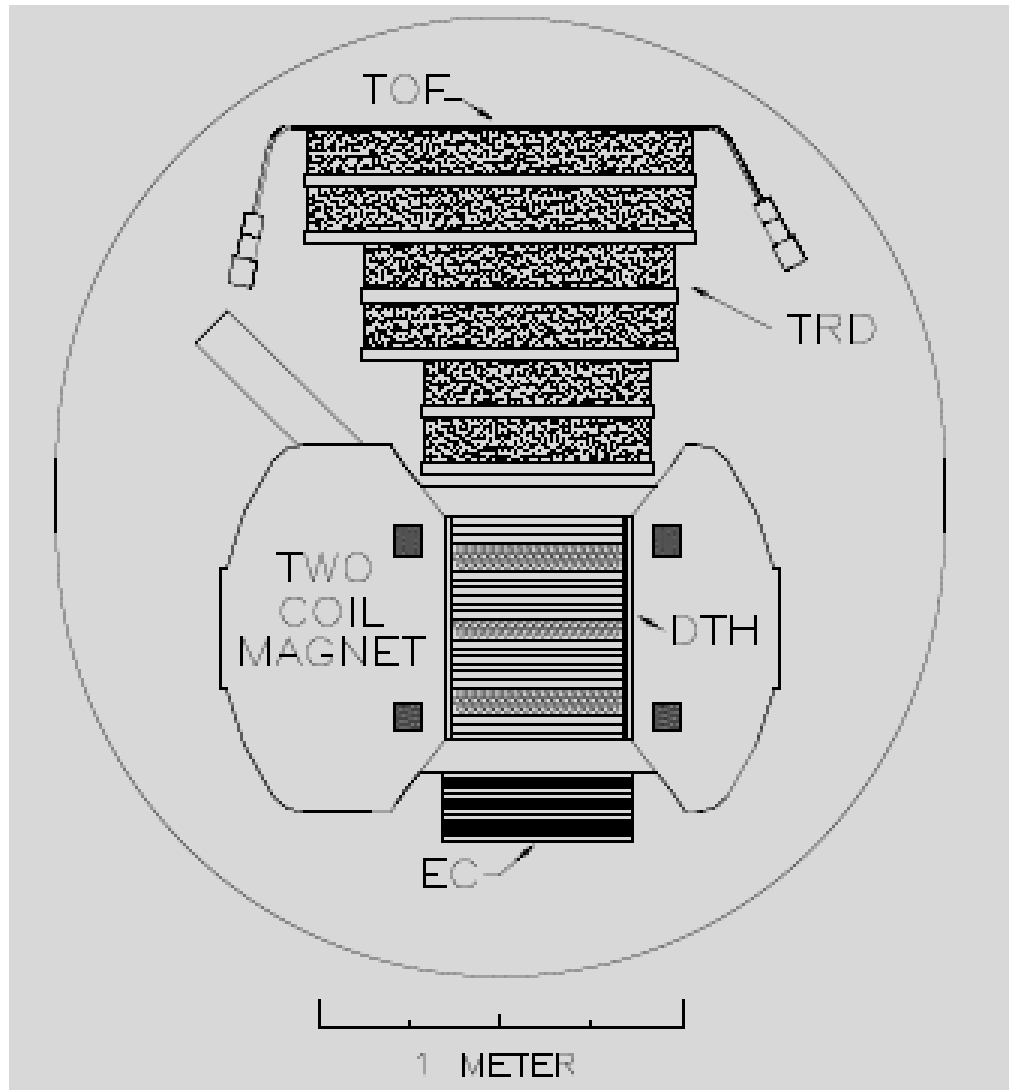
Wizard Collaboration

- ✓ MASS - 1,2 (89,91)
- ✓ TrampSI (93)
- ✓ CAPRICE (94, 97, 98)
- ✓ PAMELA (2006-)
- ✓ BESS (93, 95, 97, 98, 2000
2004,2007)
- ✓ Heat (94, 95, 2000)
- ✓ IMAX (96)
- ✓ BESS LDF (2004, 2007)
- ✓ AMS-01 (1998)
- ✓ AMS-02 (2011-)

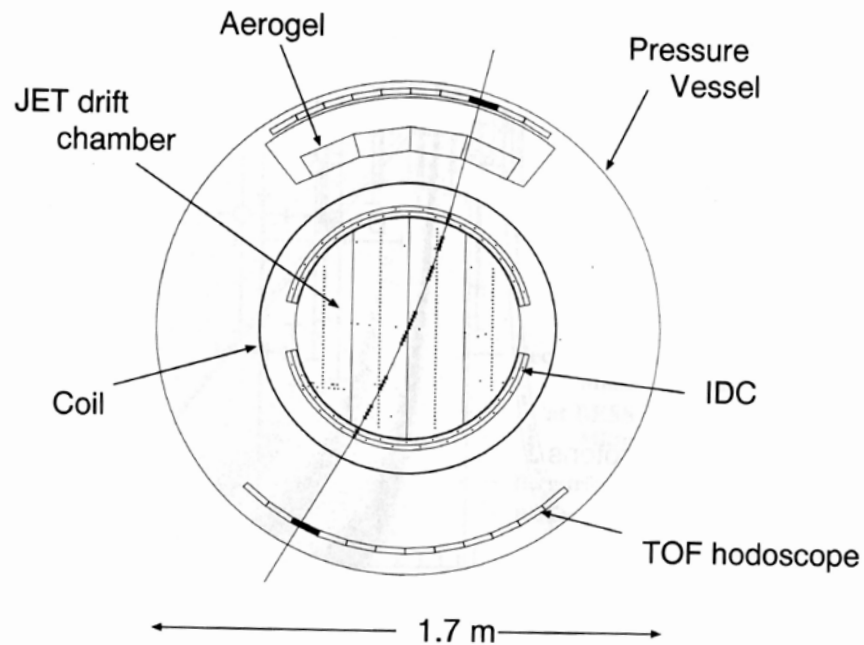
HEAT 94-95

Subnuclear Physics Techniques in Space Experiments

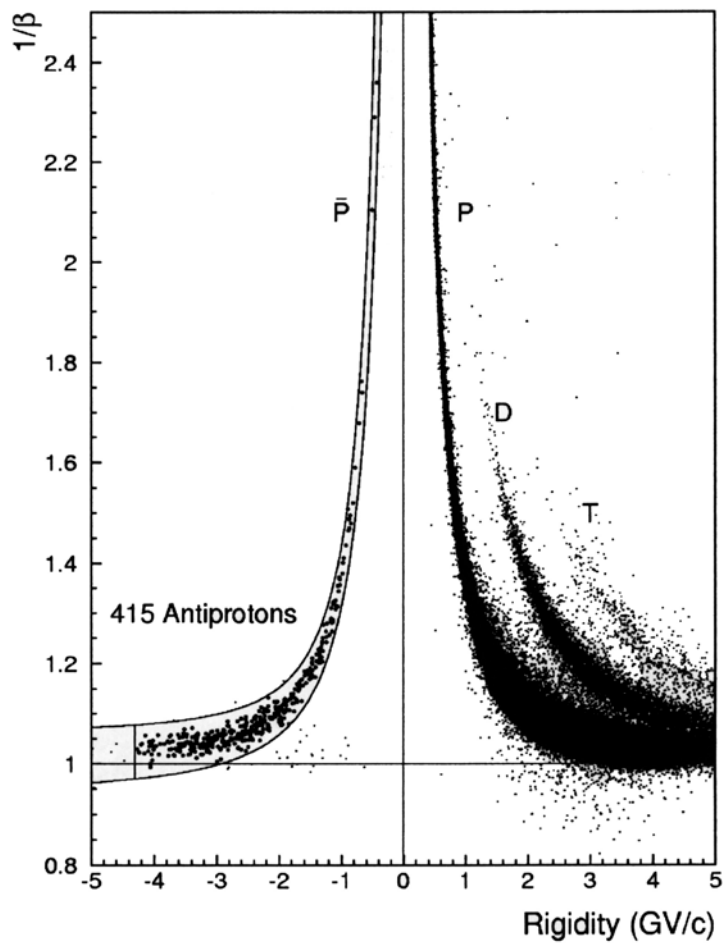
- Charge sign and momentum
- Beta selection
- Z selection
- hadron – electron discrimination



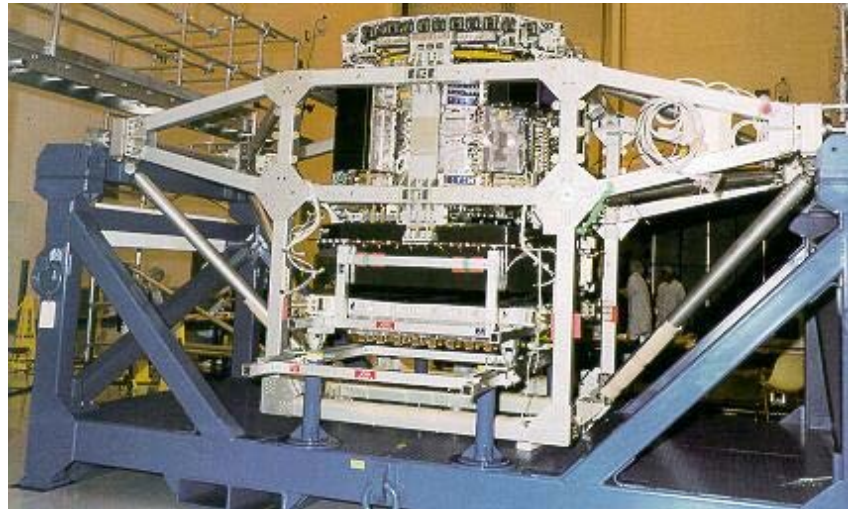
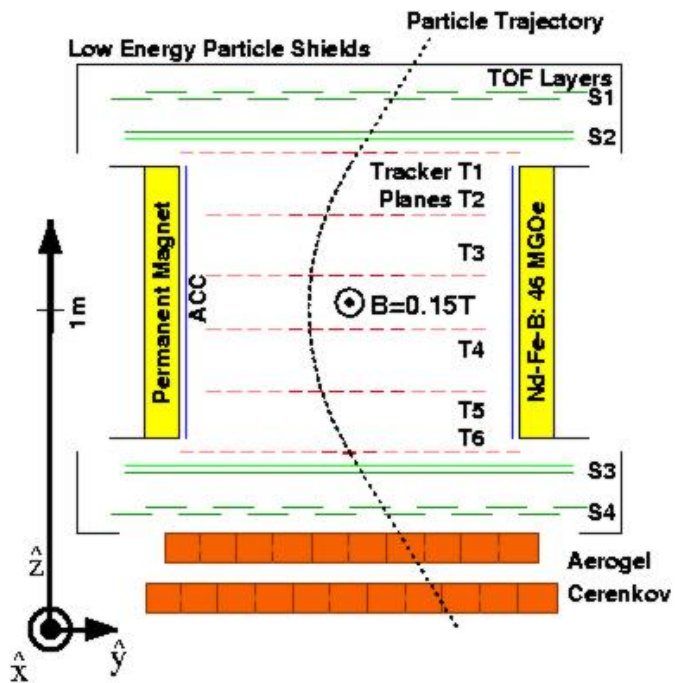
RESS97/98 Apparatus



T. Maeno et al., Astropart. Phys. 16 (2001) 121

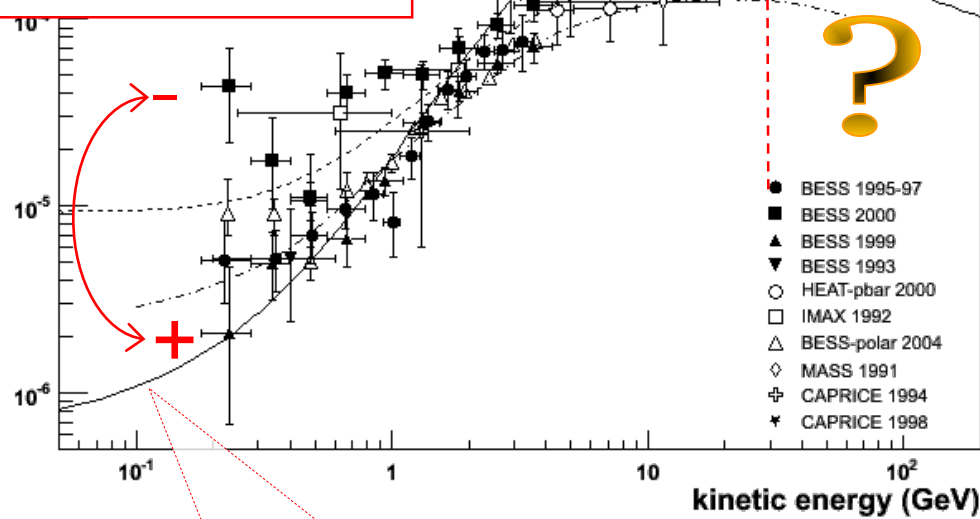
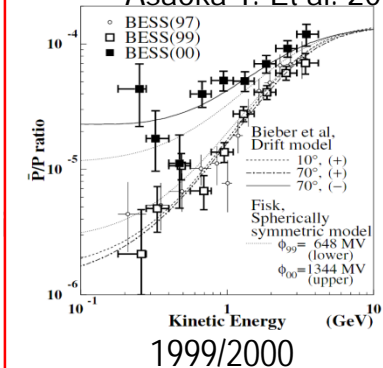


AMS-01 : the Detector



- Acceptance: $\Omega \gg 0.15 \text{ m}^2\text{sr}$
- Bending power $\gg 0.14 \text{ Tm}^2$
- TOF : trigger + β and dE/dx meas.
- Tracker: sign Z + Rigidity + dE/dx meas.
- Cherenkov: e/p separation up to $\sim 3 \text{ GeV}$.

Charge-dependent
solar modulation
Asaoka Y. Et al. 2002



$\text{CR} + \text{ISM} \rightarrow \bar{p} + \dots$
kinematic threshold:
5.6 GeV for the reaction
 $p\bar{p} \rightarrow \bar{p}ppp$

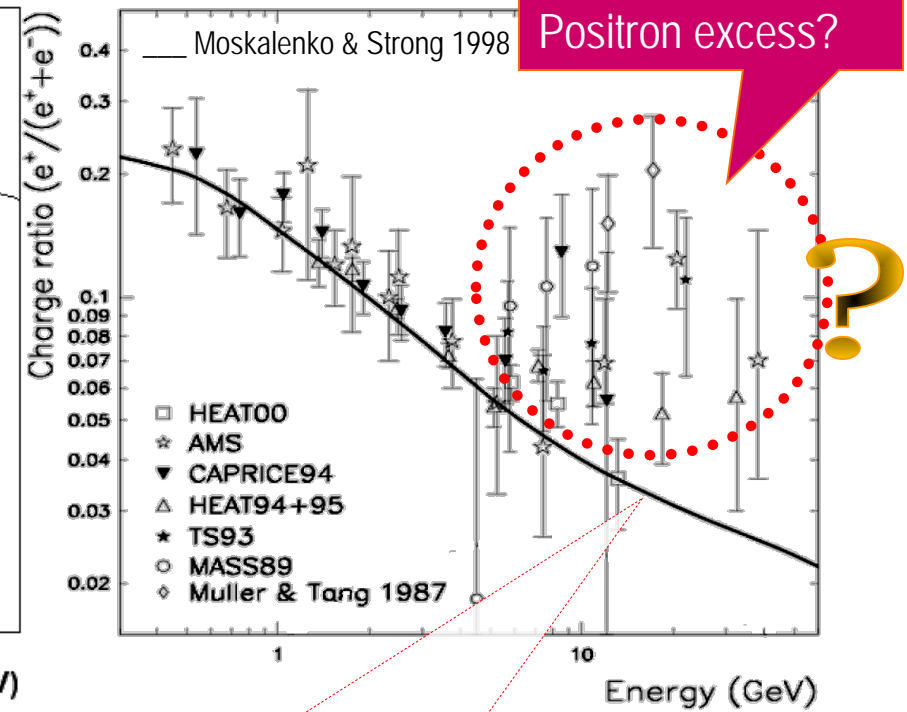
CR antimatter

Antiprotons

Status in 2006

Positrons

Positron excess?



$\text{CR} + \text{ISM} \rightarrow \pi^\pm + x \rightarrow \mu^\pm + x \rightarrow e^\pm + x$
 $\text{CR} + \text{ISM} \rightarrow \pi^0 + x \rightarrow \gamma\gamma \rightarrow e^\pm$

Antimatter Missions in “Space”

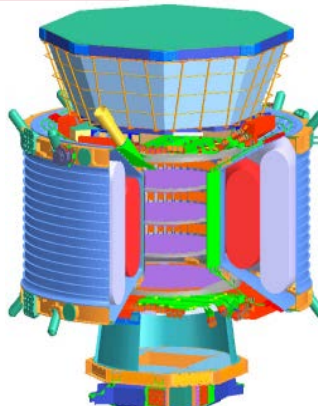
BESS LDBF
2004, 2007



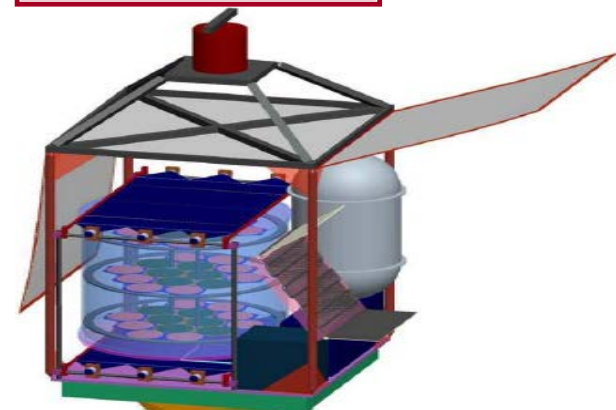
PAMELA
2006-



AMS-02
2011-



GAPS
2020?



BESS-Polar Program

Status of the BESS-Polar I Flight

Observation Time: 8.5 days

Float Time: 8.5 days (12/13/2004-12/21/2004)

Events recorded: $> 0.9 \times 10^9$

Data volume: ~ 2.1 terabytes

Data recovery: **completed** 2004

Payload recovery: **completed** 2004



Status of the BESS-Polar II Flight

Observation Time: 24.5 days

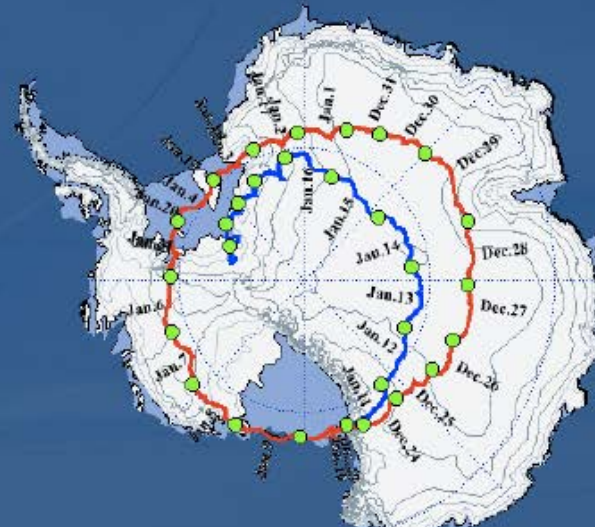
Float Time: 29.5 days (12/23/2007-01/21/2008)

Events recorded: $> 4.7 \times 10^9$

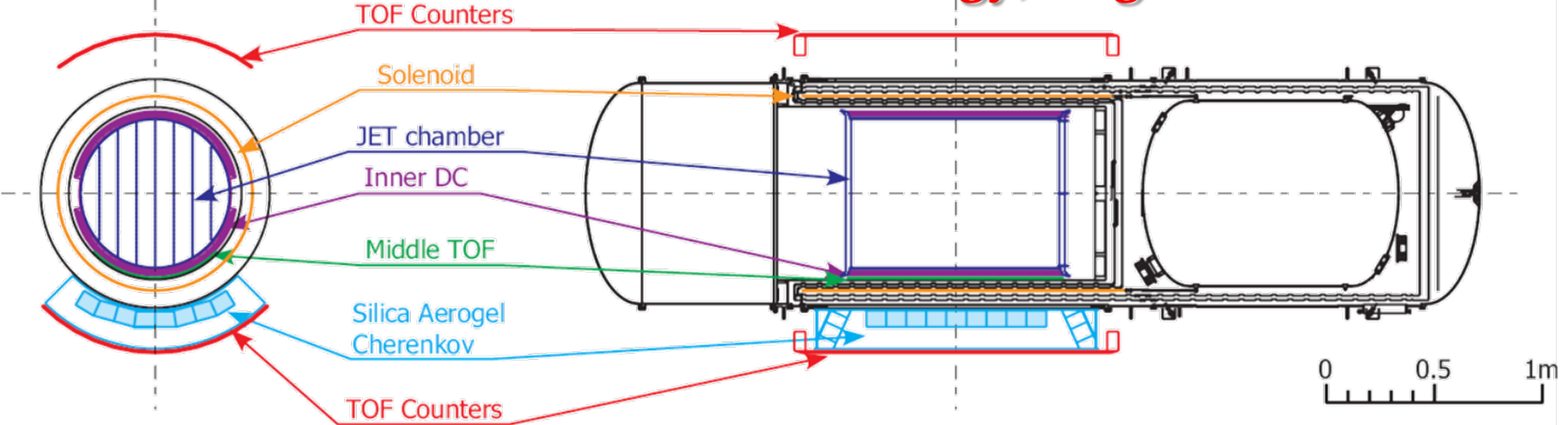
Data volume: ~ 13.5 terabytes

Data recovery: **completed** Feb 3, 2008

Payload recovery: **completed** Jan 16, 2010

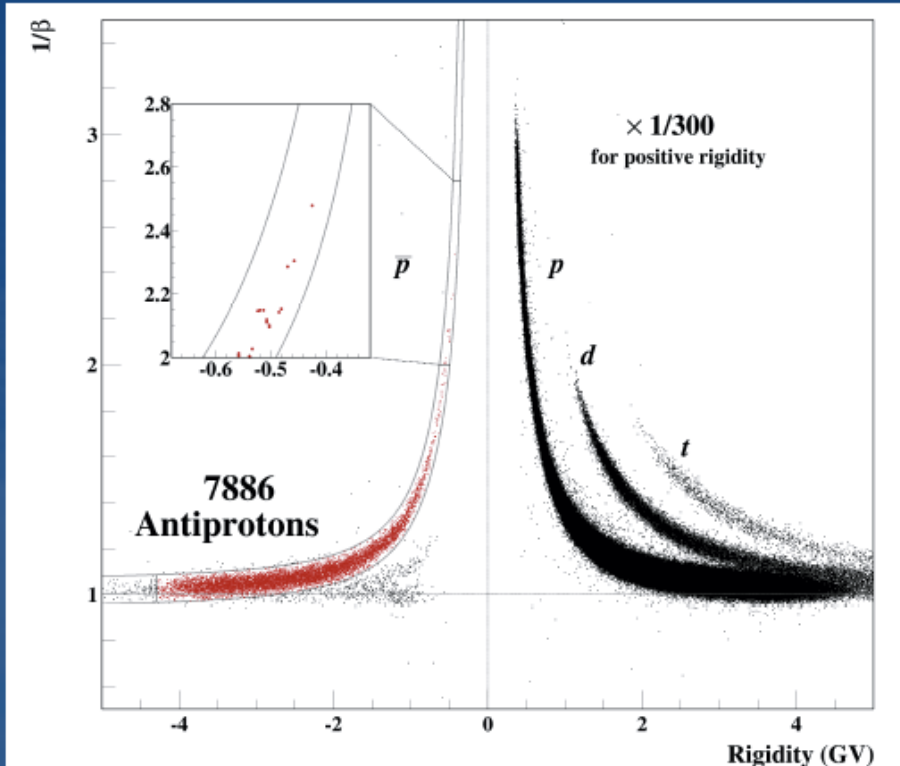


BESS-Polar II: Lower Energy, High Statistics



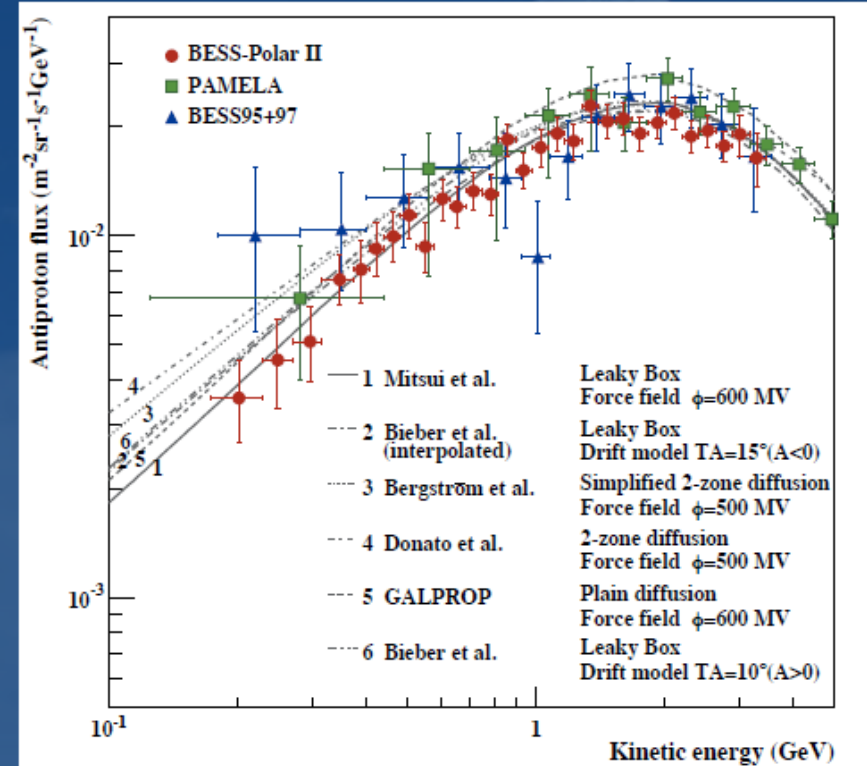
Antiproton Measurement

BESS-Polar II Z=1 Particle Id

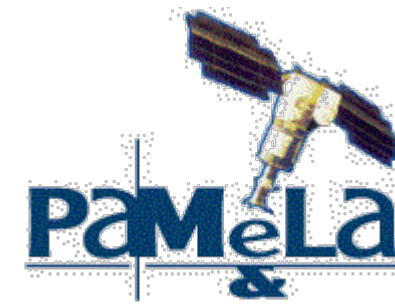
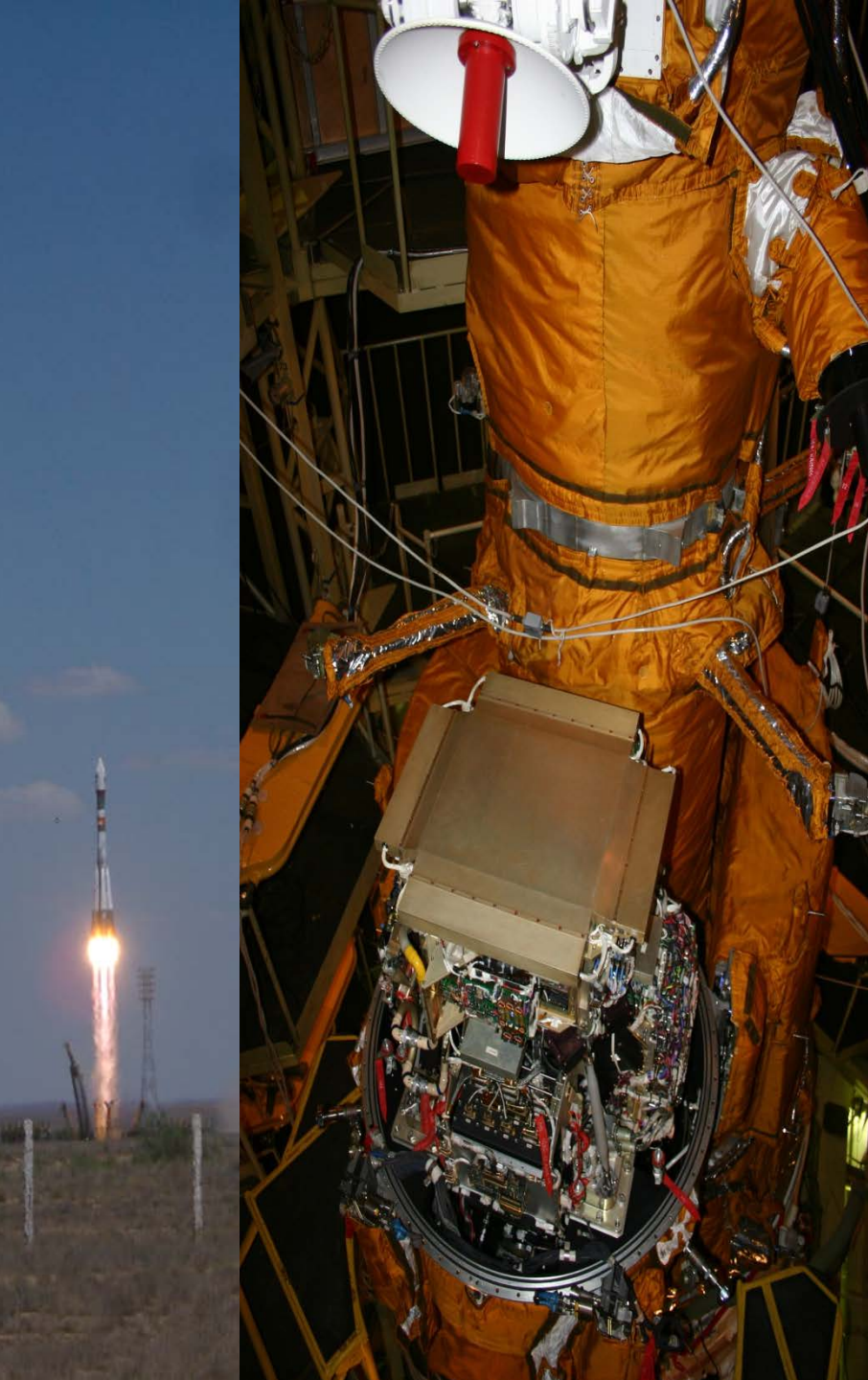


- MDR 240 GV, TOF 120 ps, ACC rejection 6100
- 7886 Antiprotons \sim 10-20 times previous Solar minimum dataset

Antiproton Spectrum

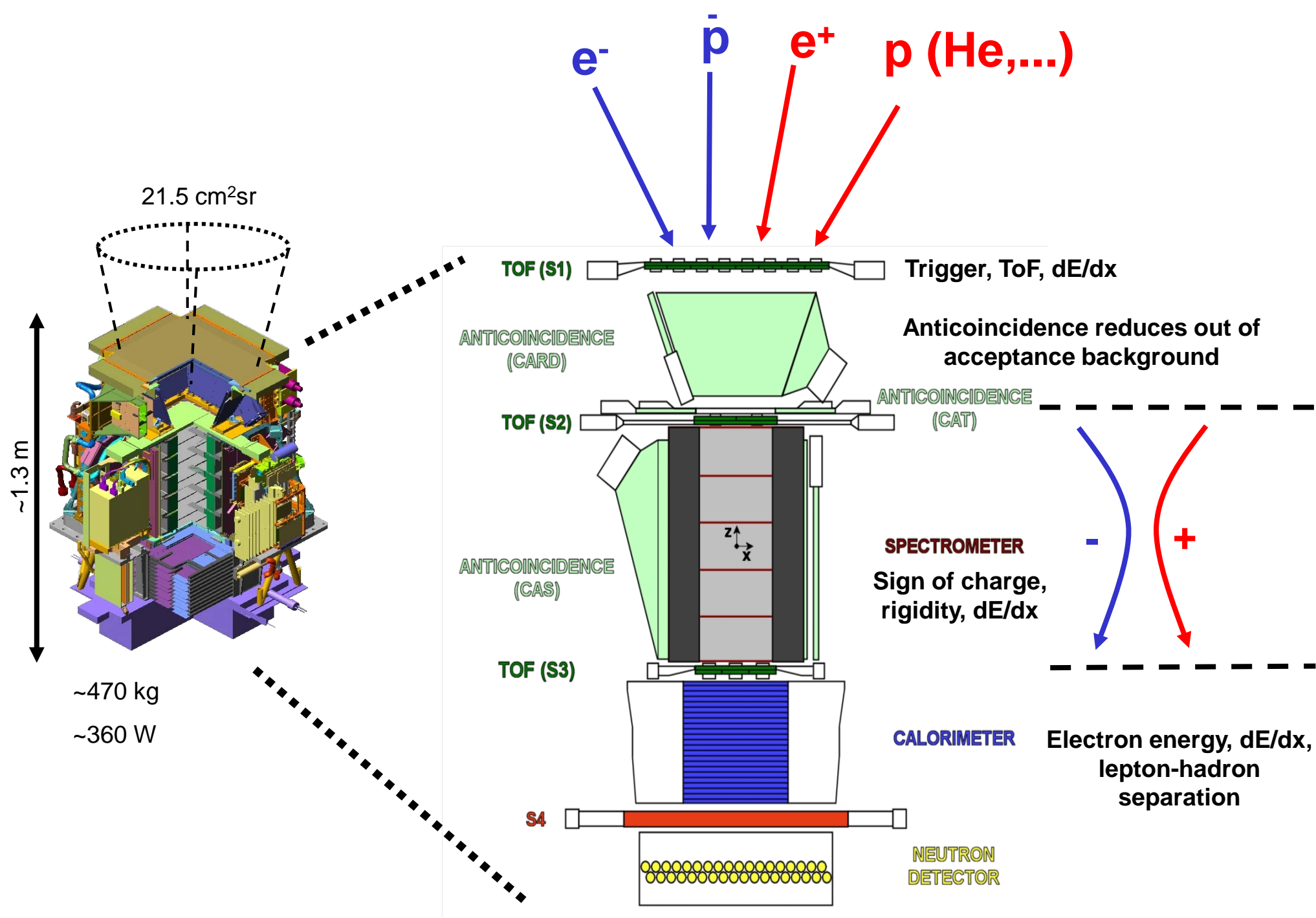


- BESS-Polar II and PAMELA spectra agree in shape but differ \sim 14% in absolute flux
- Both agree in shape with secondary

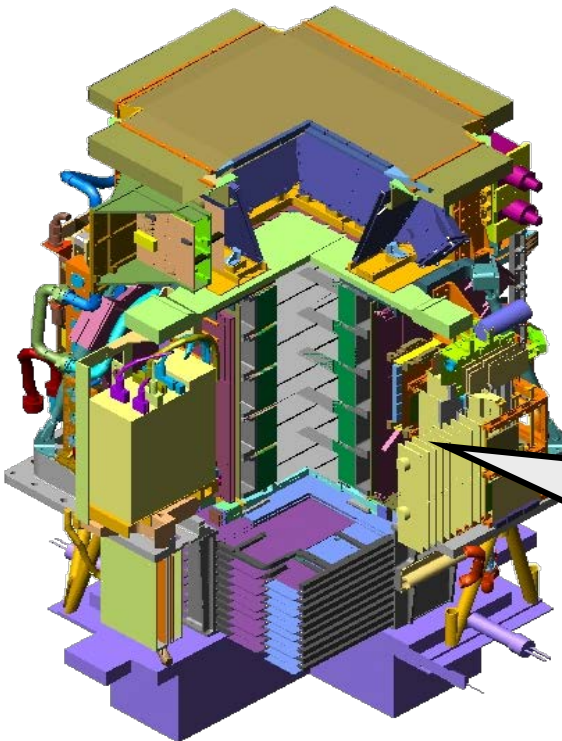


P A M E L A

**Payload for Antimatter /
Matter Exploration and
Light-nuclei Astrophysics**

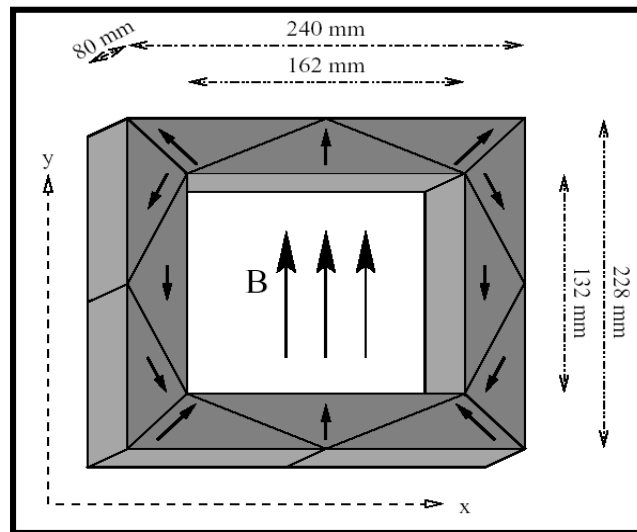
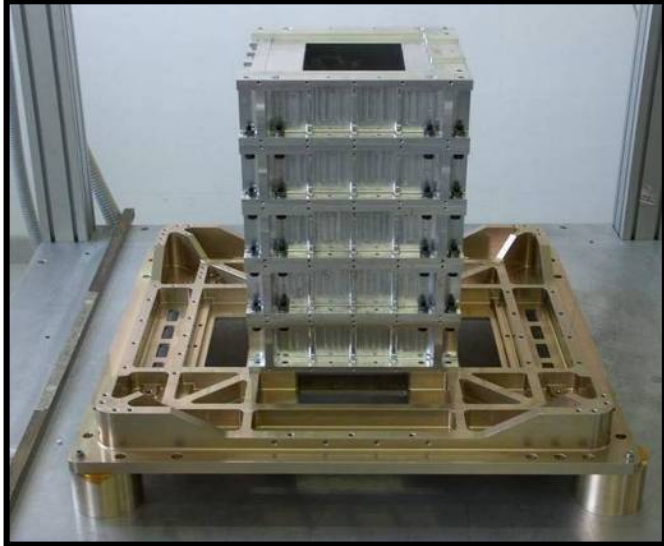


The magnet

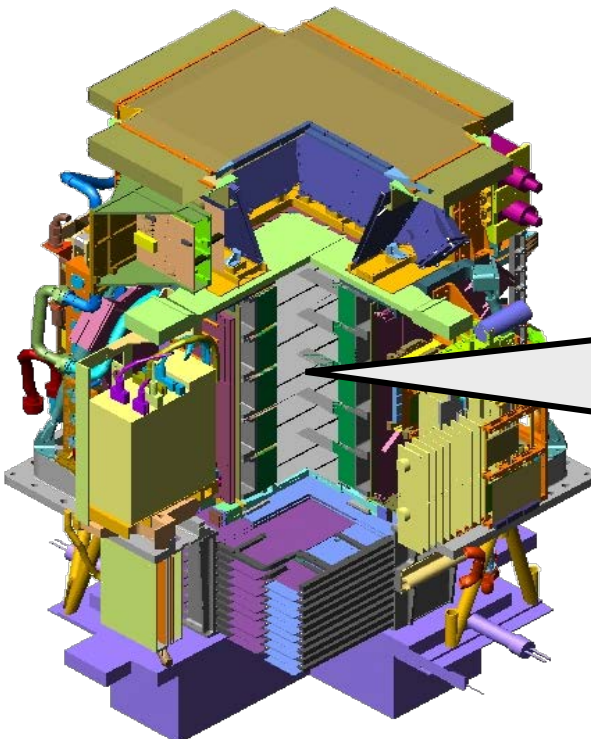


Characteristics:

- **5 modules of permanent magnet (Nd-B-Fe alloy) in aluminum mechanics**
- Cavity dimensions $(162 \times 132 \times 445) \text{ cm}^3$
→ $\text{GF} \sim 21.5 \text{ cm}^2\text{sr}$
- Magnetic shields
- 5mm-step field-map on ground:
 - **B=0.43 T (average along axis),**
 - **B=0.48 T (@center)**



The tracking system



Main tasks:

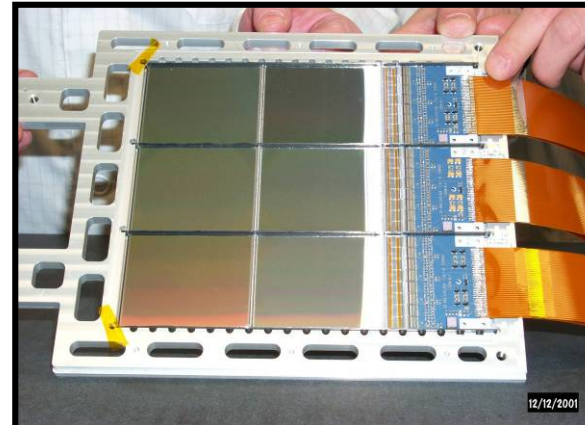
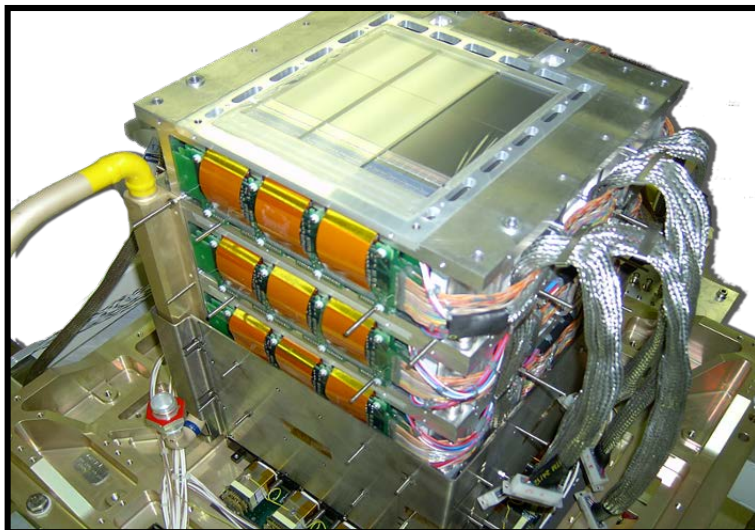
- Rigidity measurement
- Sign of electric charge
- dE/dx (ionisation loss)

Characteristics:

- 6 planes double-sided (x&y view) microstrip Si sensors
- 36864 channels
- Dynamic range: 10 MIP

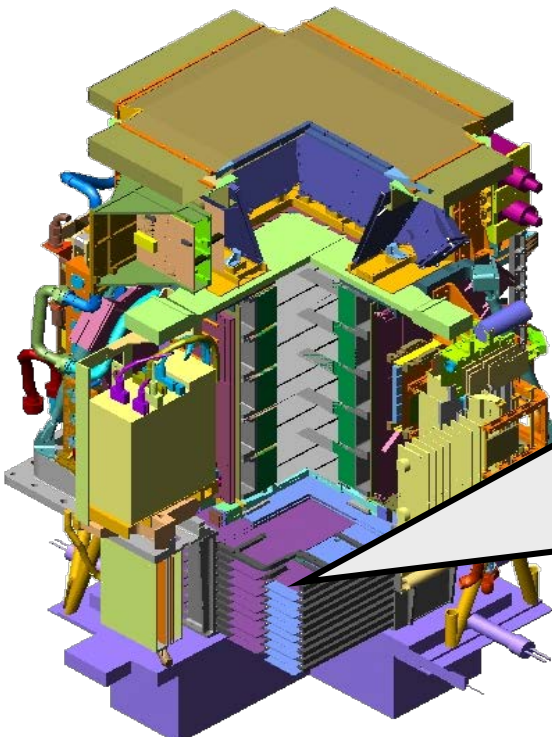
Performance:

- Spatial resolution: $\sim 3 \mu\text{m}$ (bending view)
- MDR $\sim 1 \text{ TV}/\text{c}$ (from test beam data)



12/12/2001

The electromagnetic calorimeter



Main tasks:

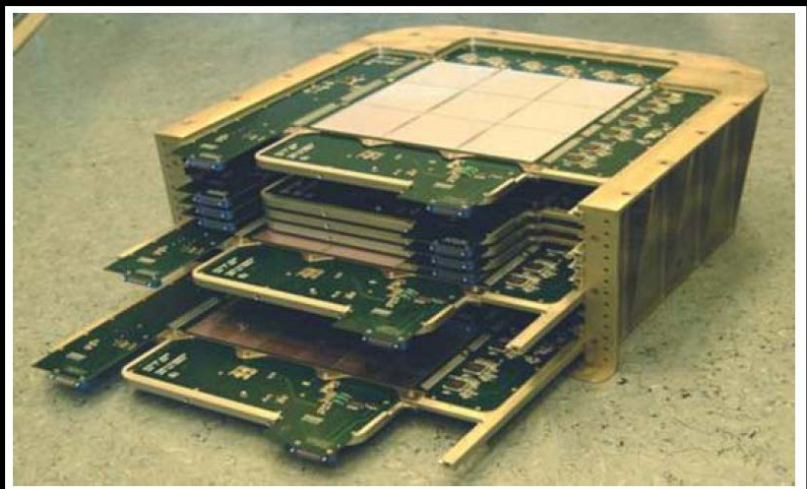
- lepton/hadron discrimination
- $e^{+/-}$ energy measurement

Characteristics:

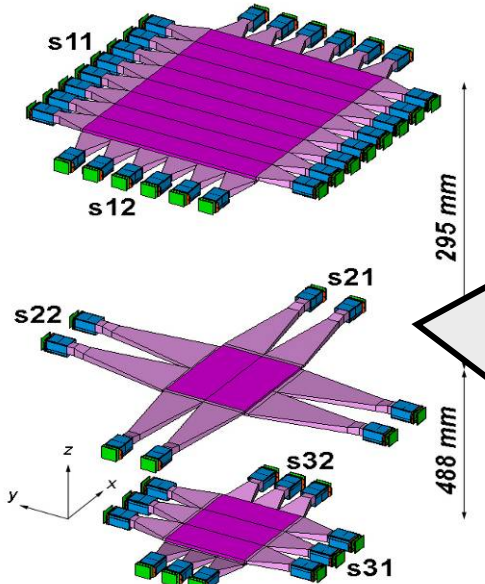
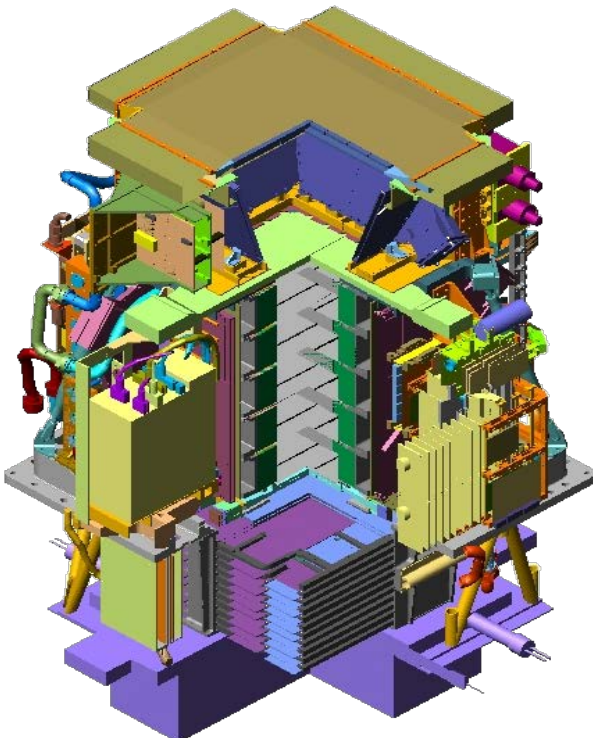
- 44 Si layers (x/y) + 22 W planes
- $16.3 X_0 / 0.6 \lambda_L$
- 4224 channels
- Dynamic range: 1400 mip
- Self-trigger mode (> 300 GeV; GF~ 600 cm 2 sr)

Performance:

- p/e $^+$ selection efficiency ~ 90%
- p rejection factor ~ 10^5
- e rejection factor > 10^4
- Energy resolution ~5% @ 200 GeV



The time-of-flight system



Main tasks:

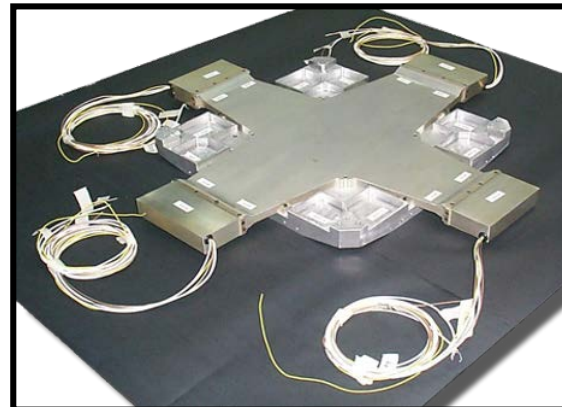
- First-level trigger
- Albedo rejection
- dE/dx (ionisation losses)
- Time of flight particle identification ($<1\text{GeV}/c$)

Characteristics:

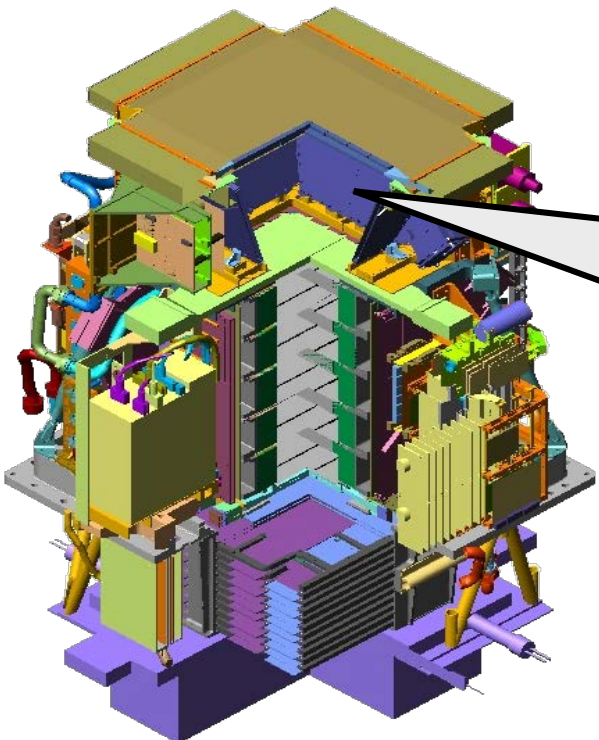
- 3 double-layer scintillator paddles
- x/y segmentation
- Total: 48 channels

Performance:

- $\sigma(\text{paddle}) \sim 110\text{ps}$
- $\sigma(\text{ToF}) \sim 330\text{ps}$ (for MIPs)



The anticounter shields



Main tasks:

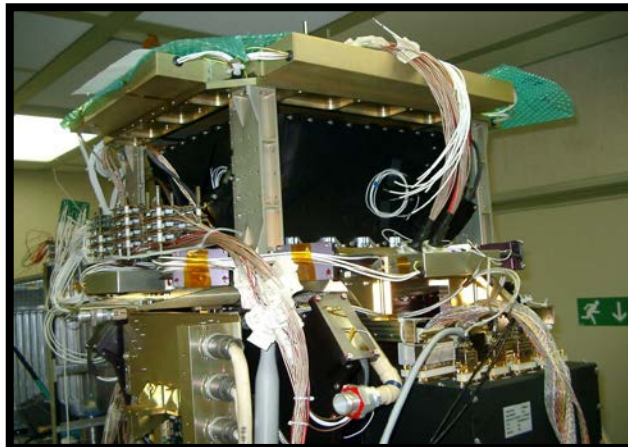
- **Rejection of events with particles interacting with the apparatus** (off-line and second-level trigger)

Characteristics:

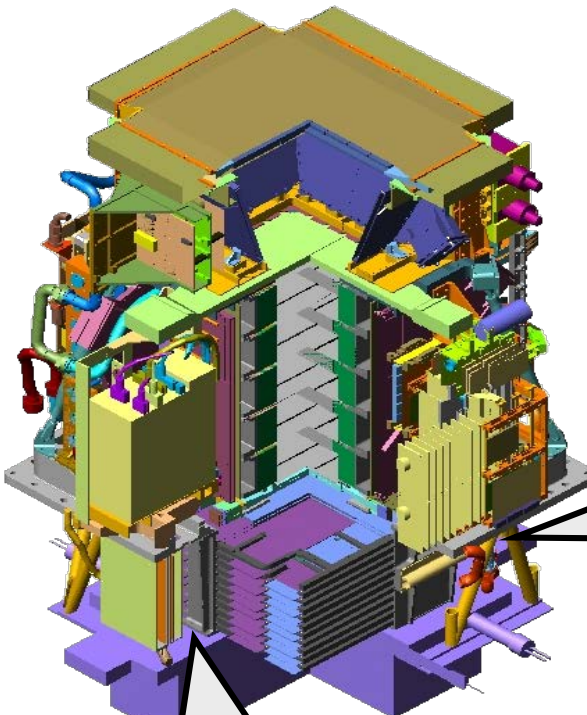
- **Plastic scintillator paddles, 8mm thick**
- 4 upper (CARD), 1 top (CAT), 4 side (CAS)

Performance:

- MIP efficiency > 99.9%



Neutron detector



Main tasks:

- e/h discrimination at high energy

Characteristics:

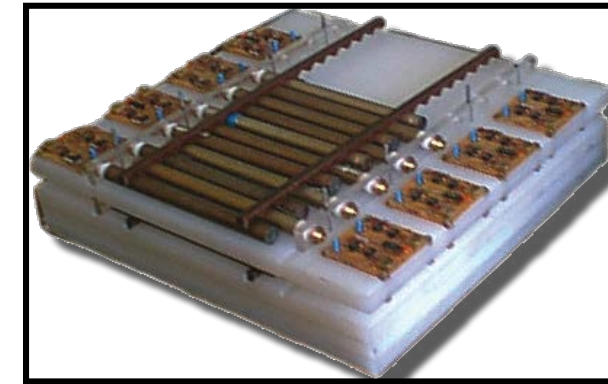
- 36 ^3He counters:
 $^3\text{He}(n,p)\text{T}$ - $E_p=780 \text{ keV}$
- 1cm thick polyethylene + Cd moderators
- n collected within 200 μs time-window

Main tasks:

- Neutron detector trigger

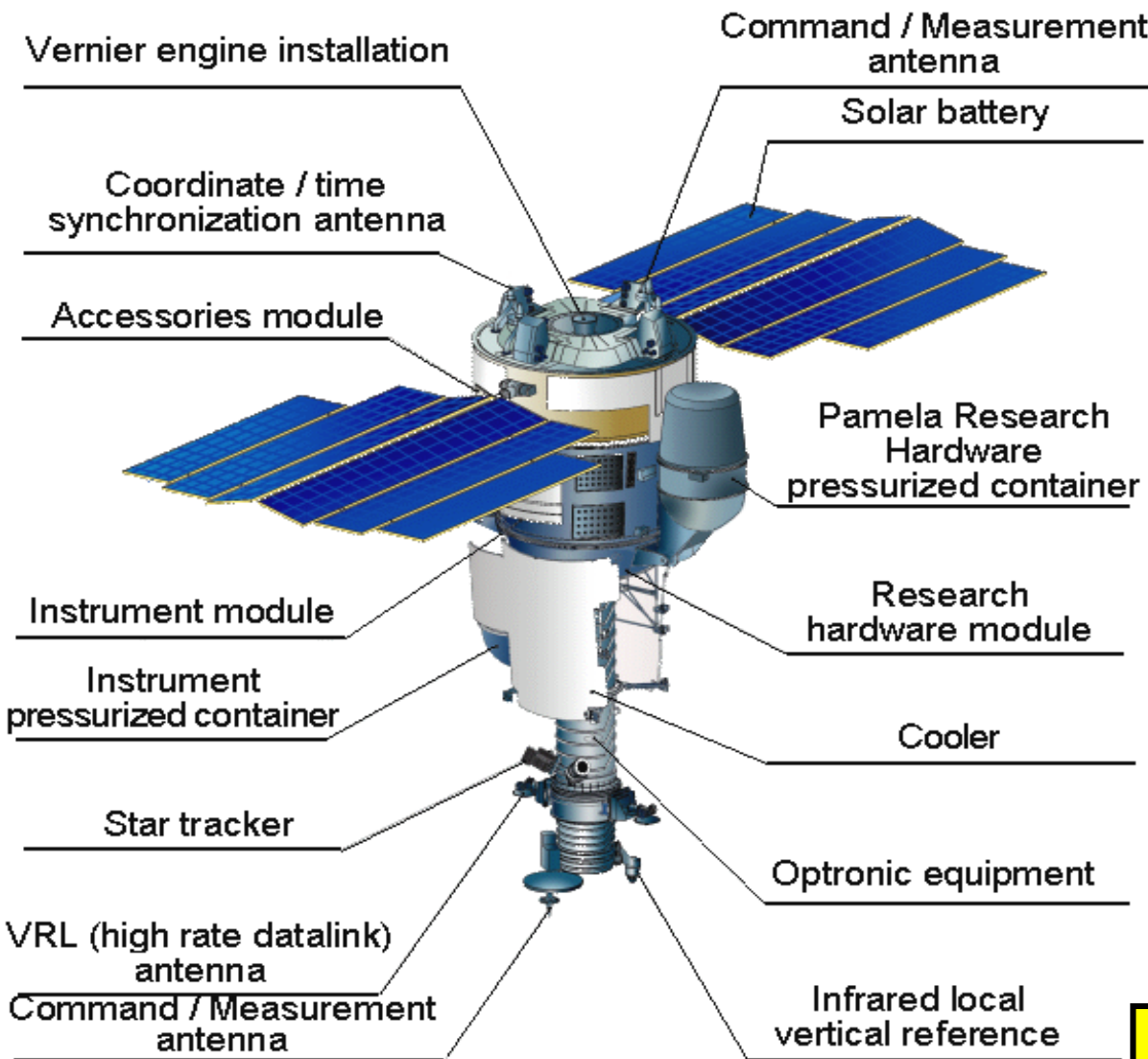
Characteristics:

- Plastic scintillator paddle, 1 cm thick



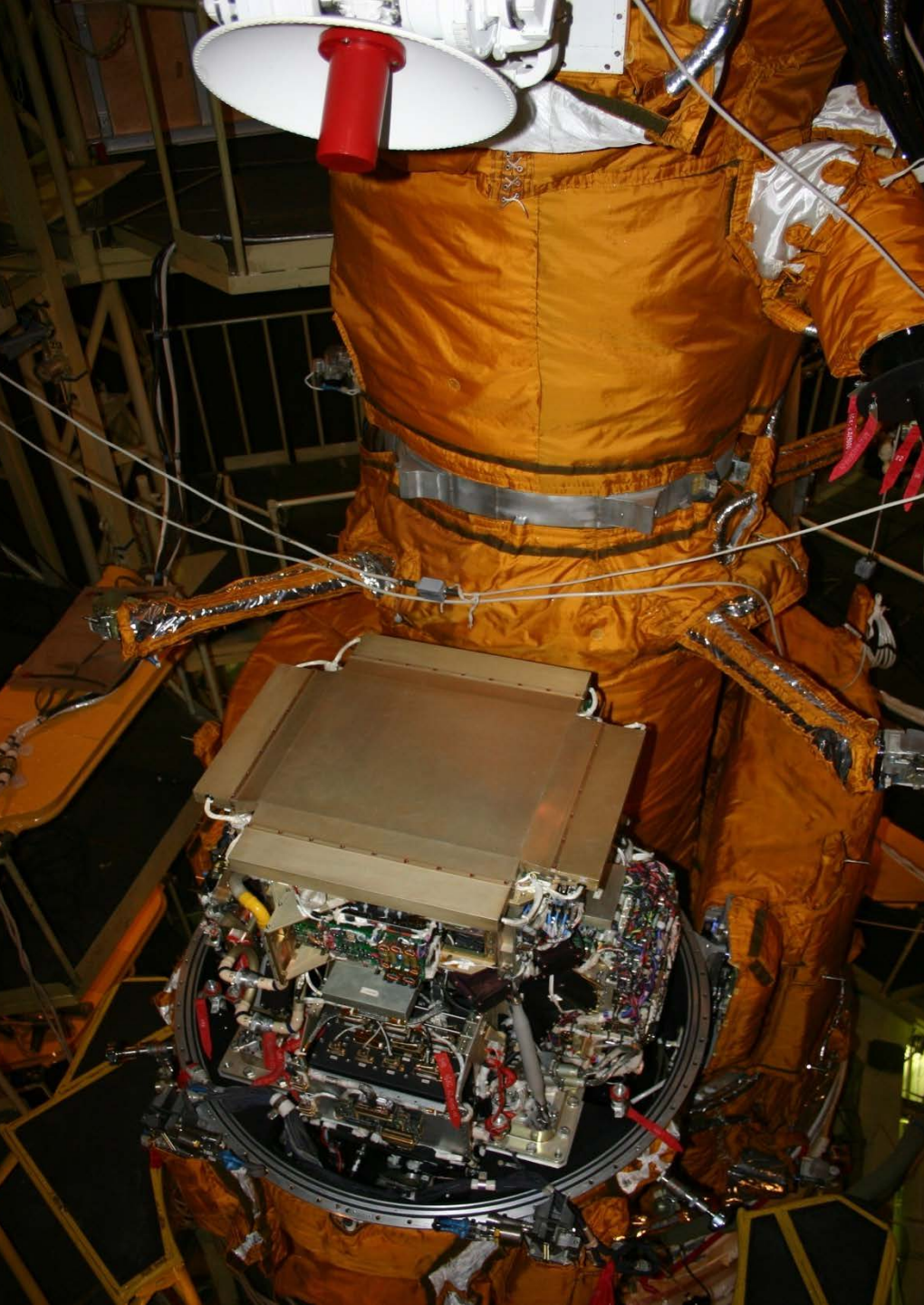
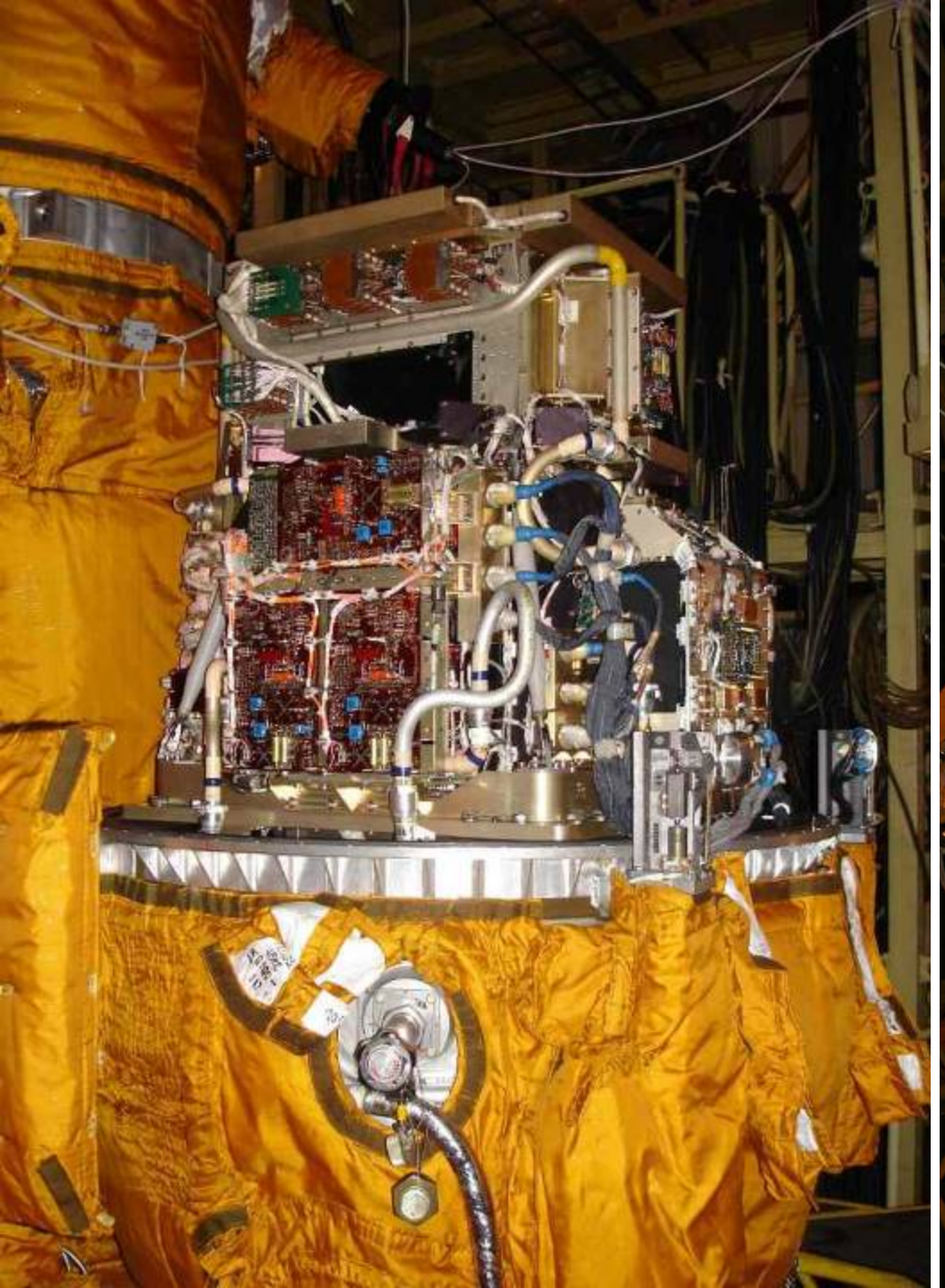
Shower-tail catcher

Resurs-DK1 satellite

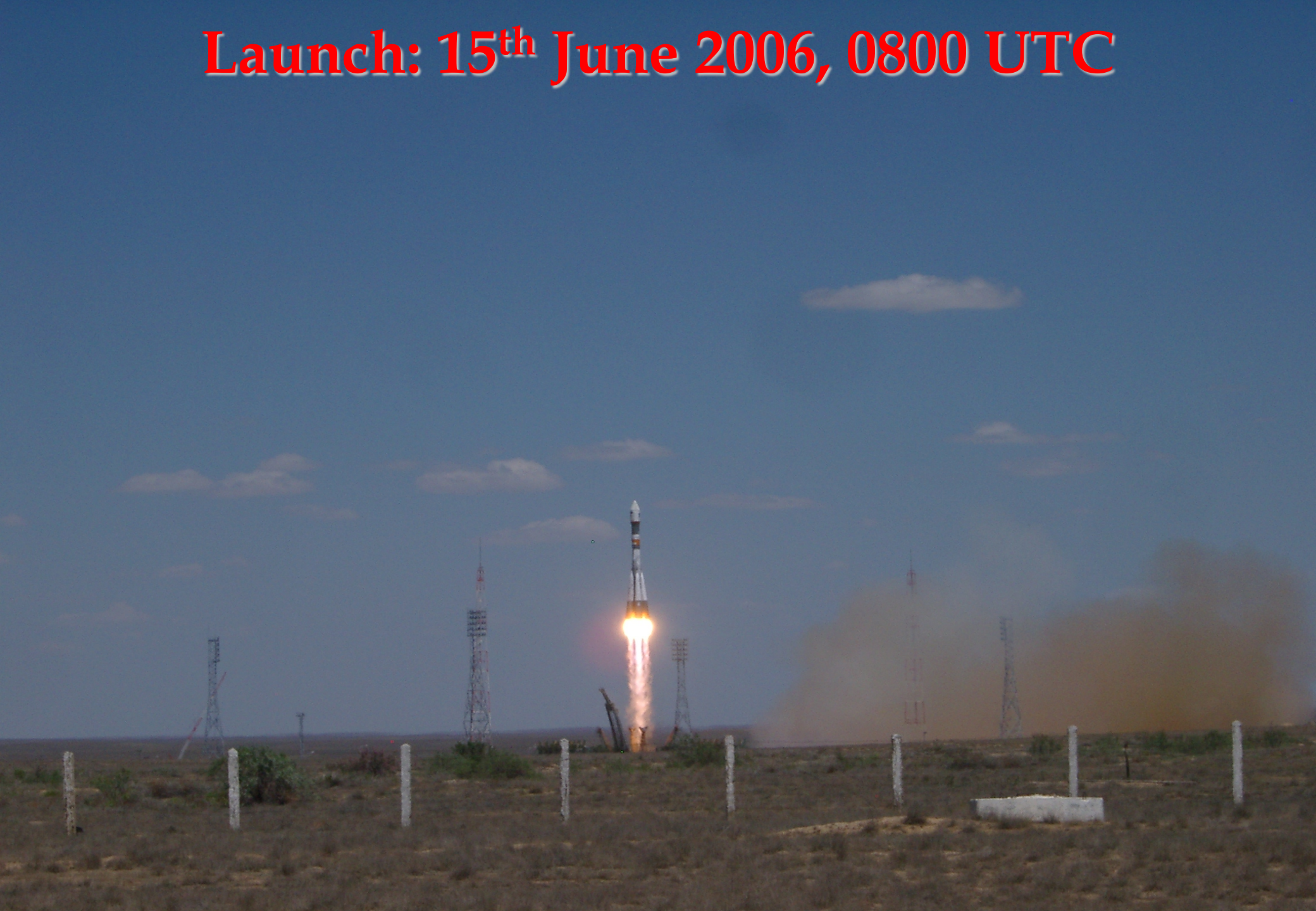


- **Main task:** multi-spectral remote sensing of earth's surface
- Built by TsSKB Progress in Samara, Russia
- **Lifetime >3 years (assisted)**
- Data transmitted to ground via high-speed radio downlink
- **PAMELA mounted inside a pressurized container**

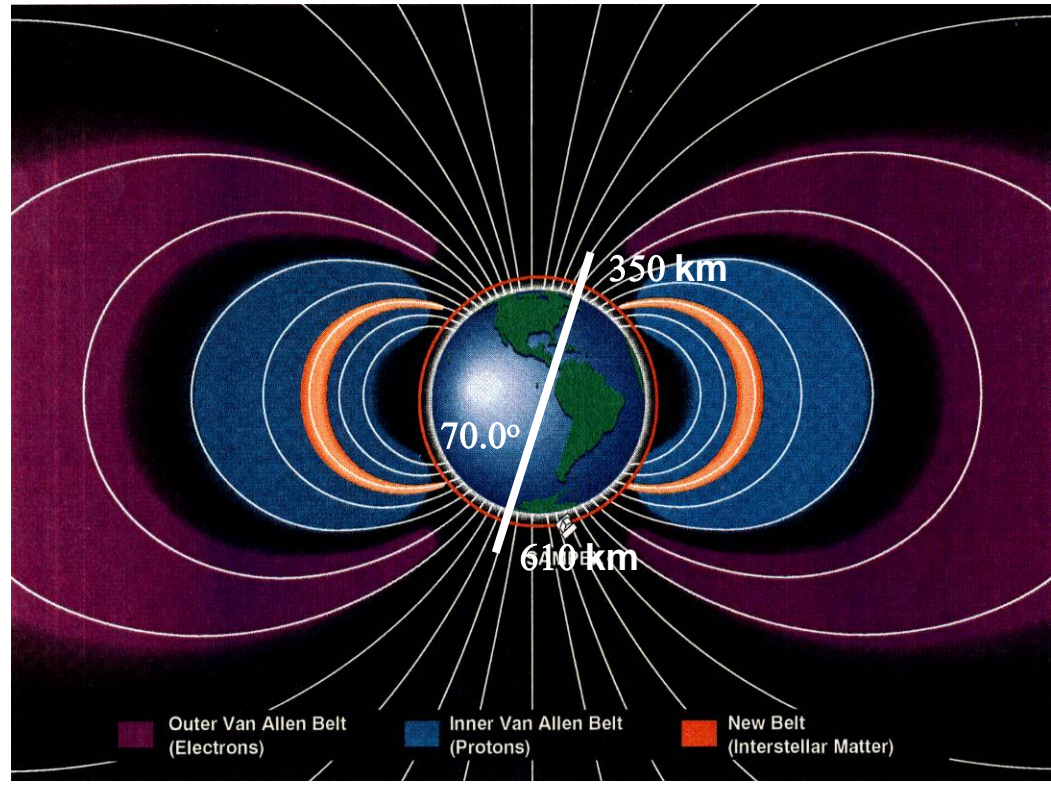
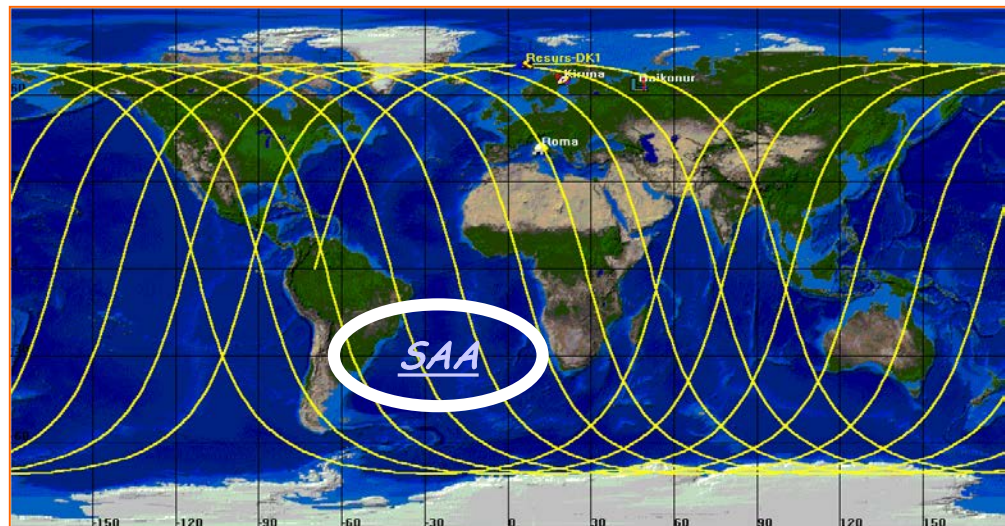
Mass: 6.7 tonnes
Height: 7.4 m
Solar array area: 36 m²



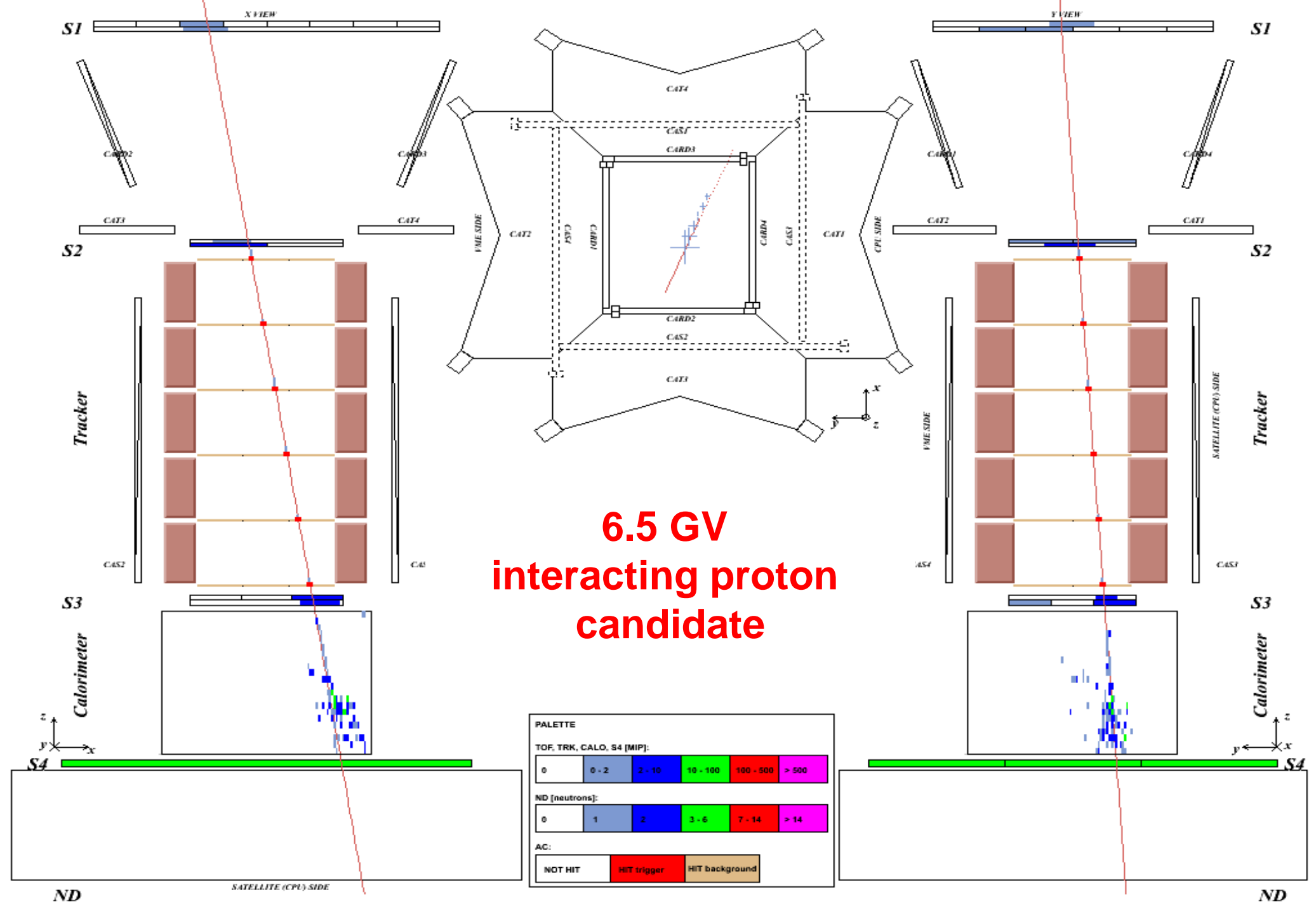
Launch: 15th June 2006, 0800 UTC

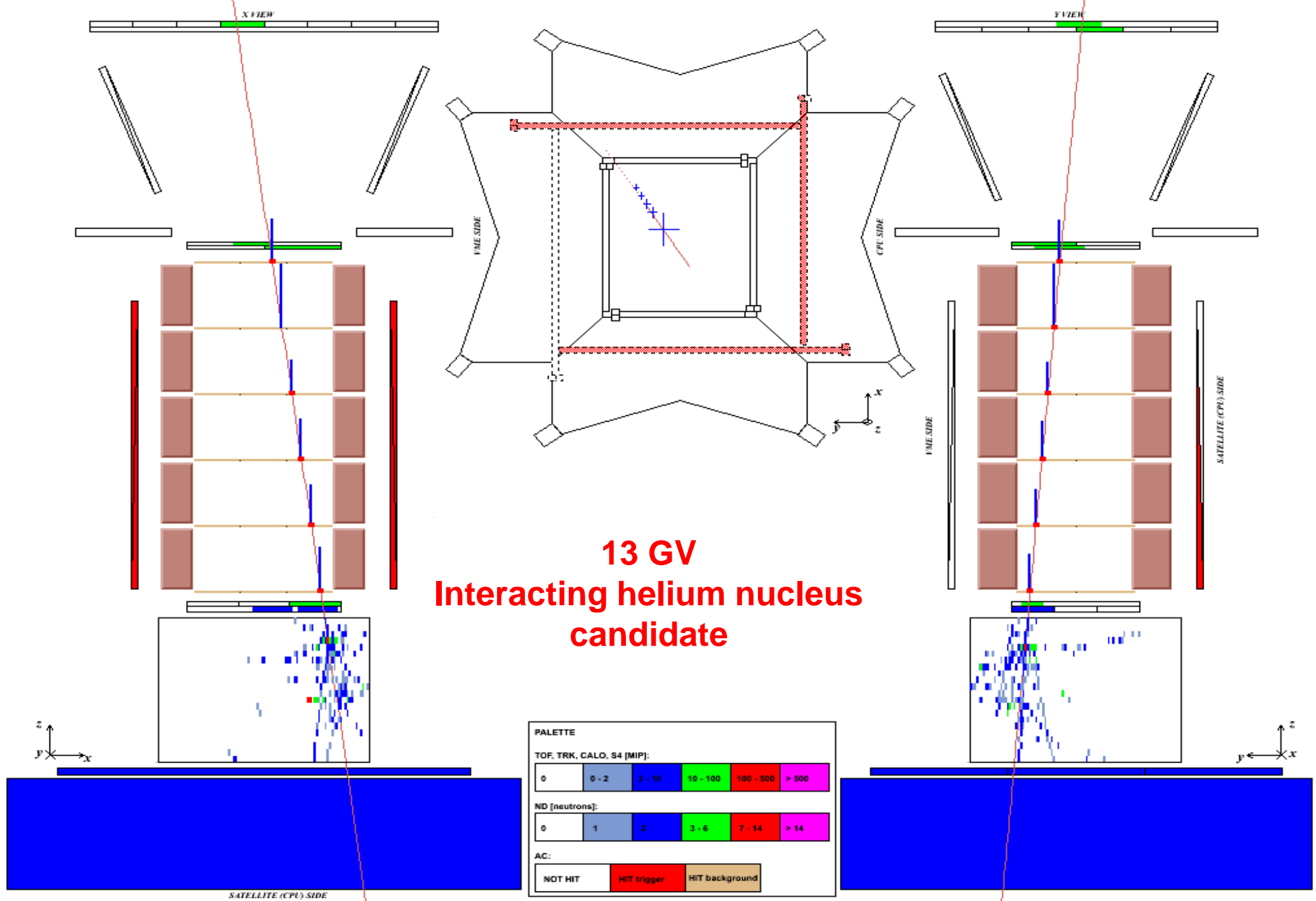


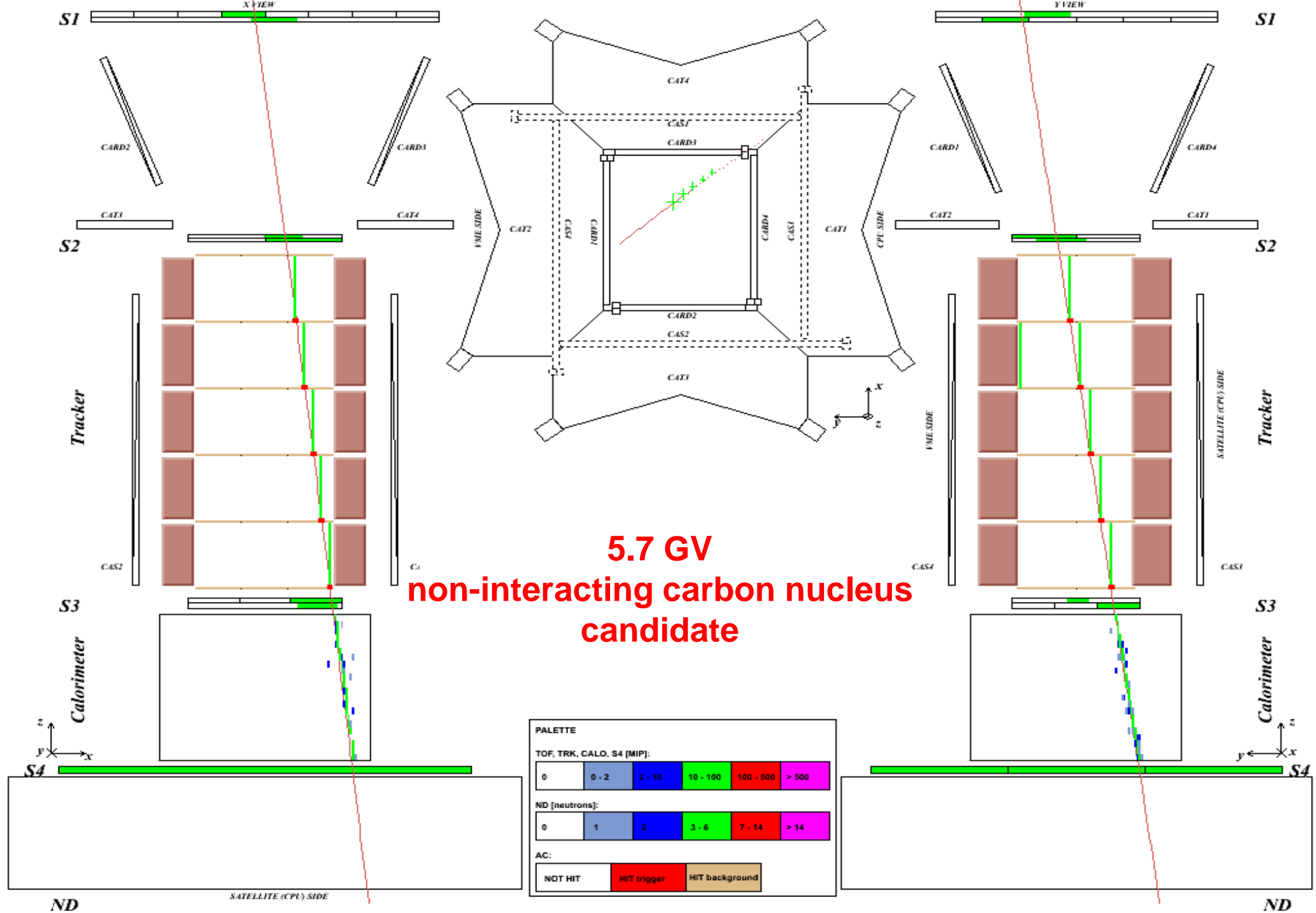
Orbit characteristics

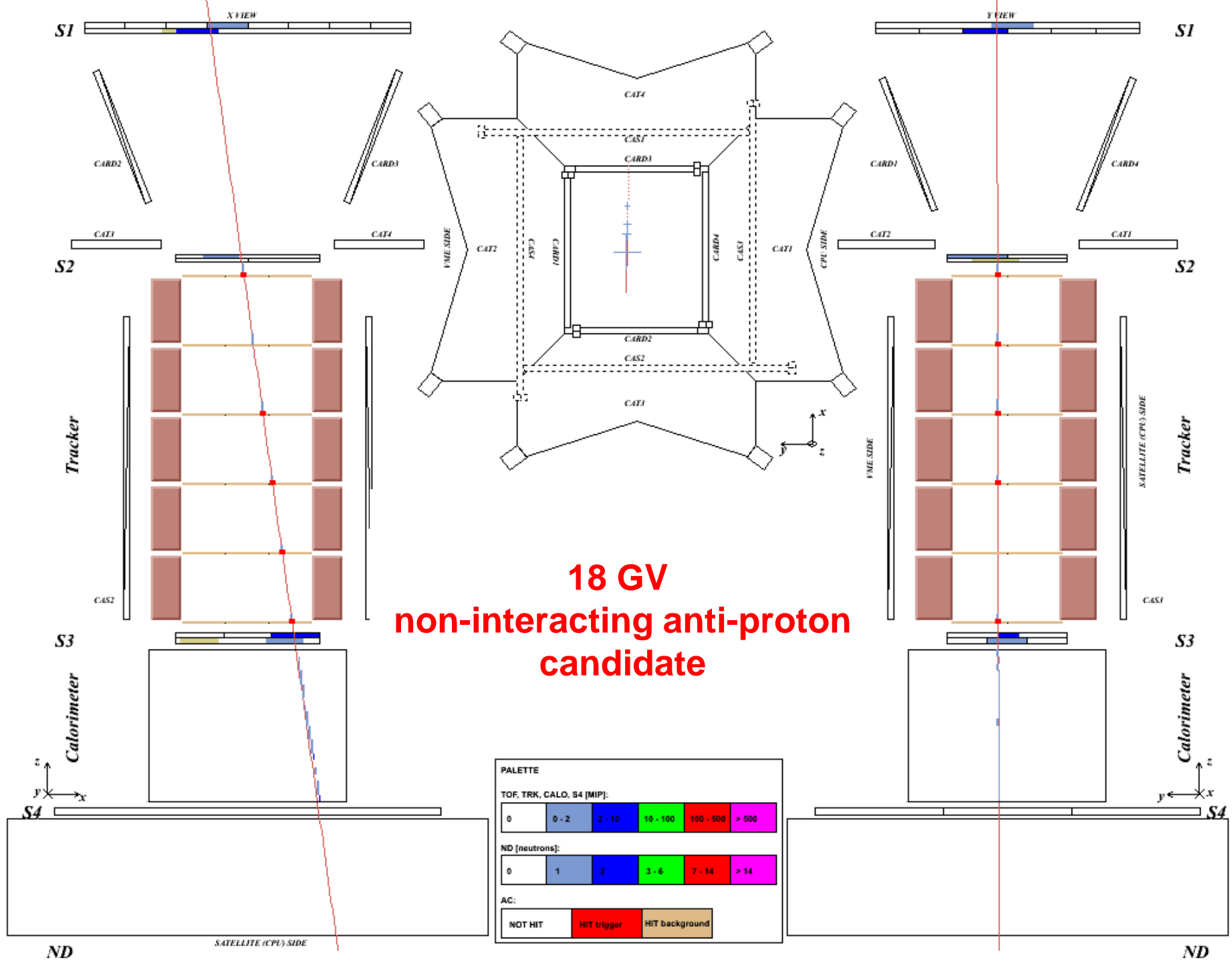


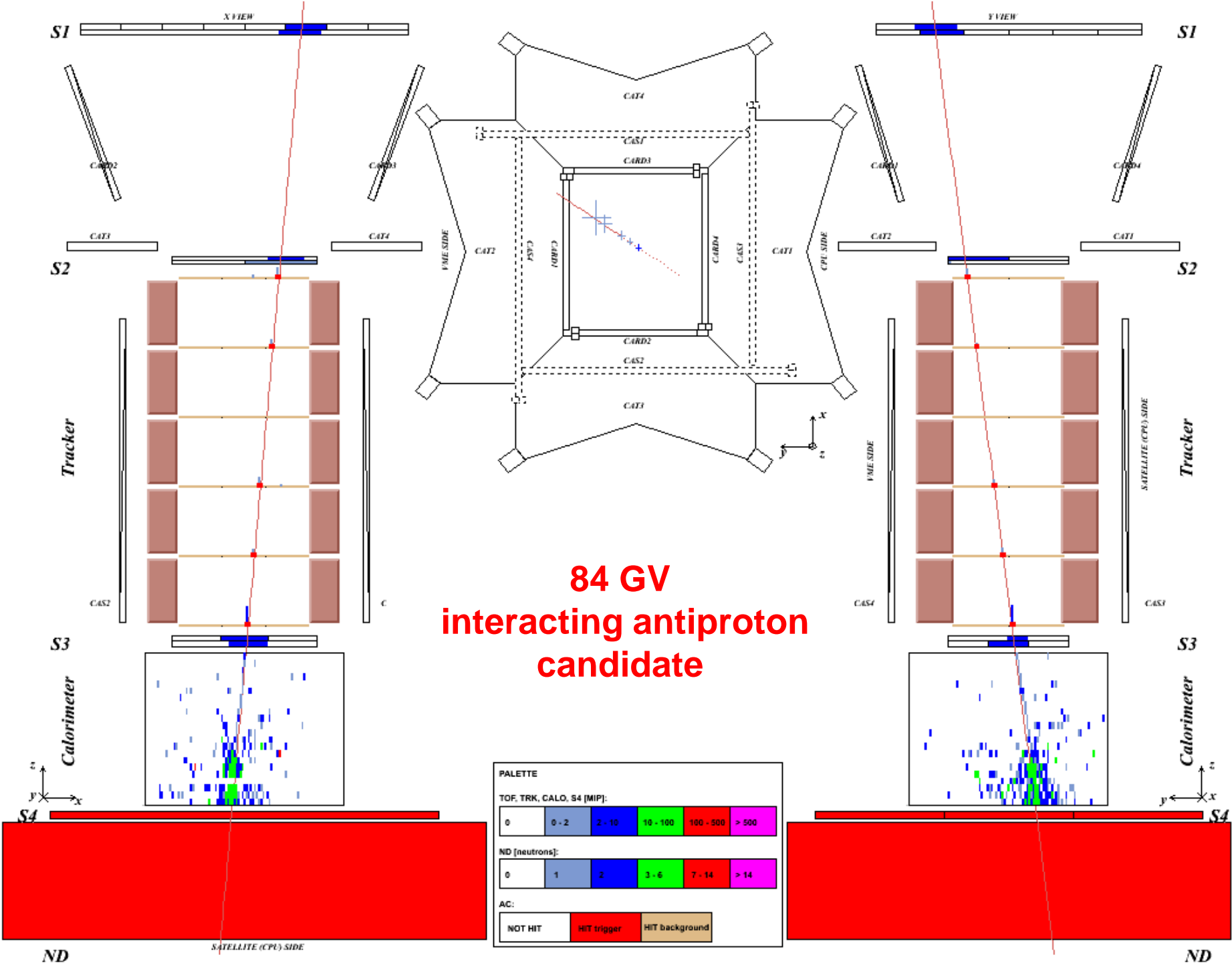
- Quasi-polar (70.0°)
- Elliptical (350 km - 600 km)
- PAMELA traverses the South Atlantic Anomaly
- At the South Pole PAMELA crosses the outer (electron) Van Allen belt

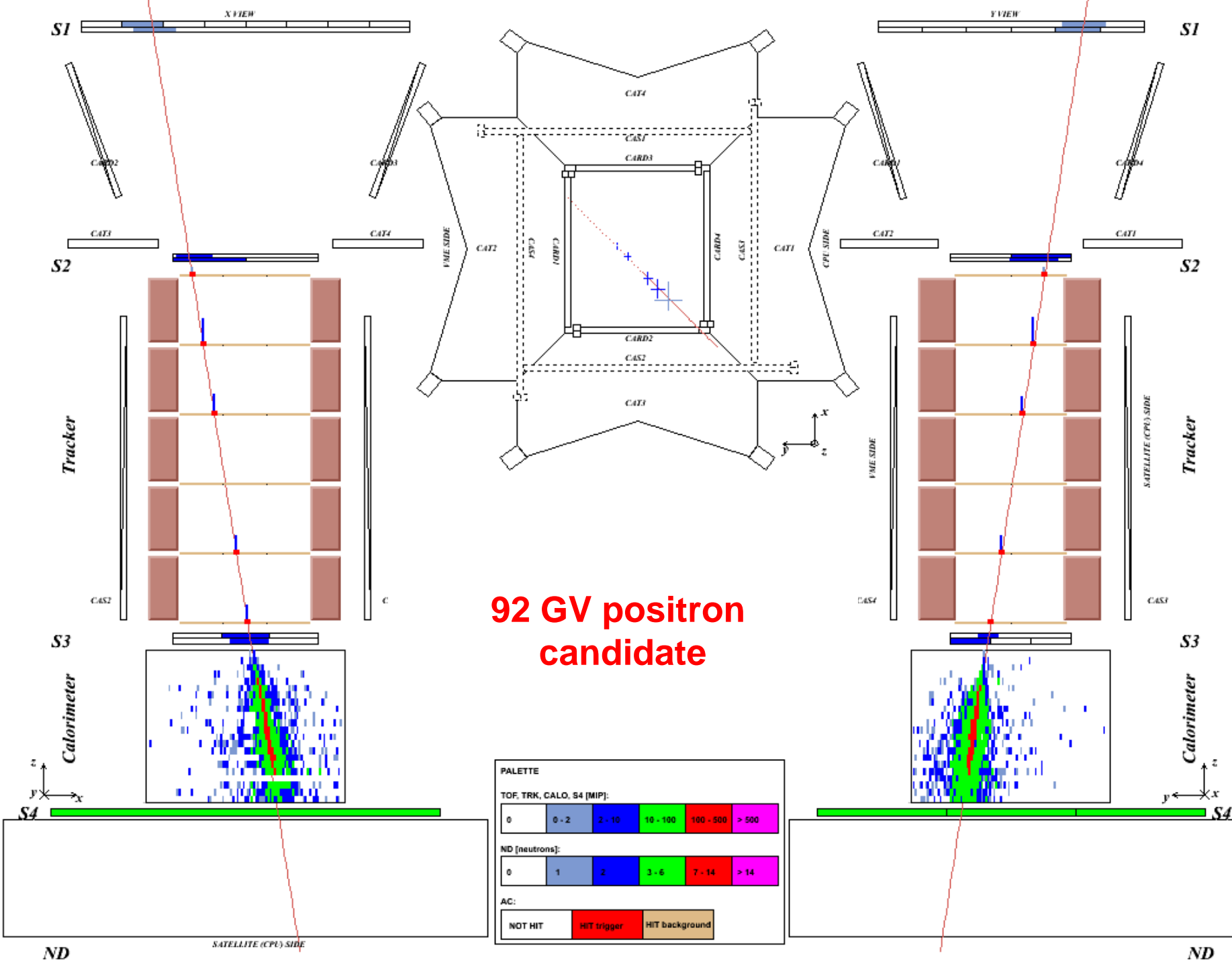






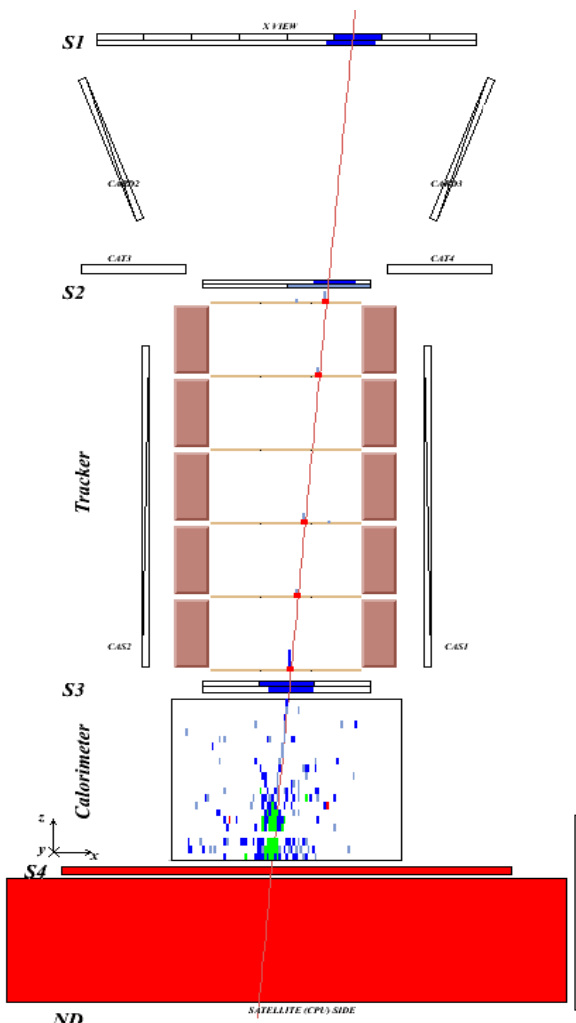






Antiprotons

Antiproton / positron identification



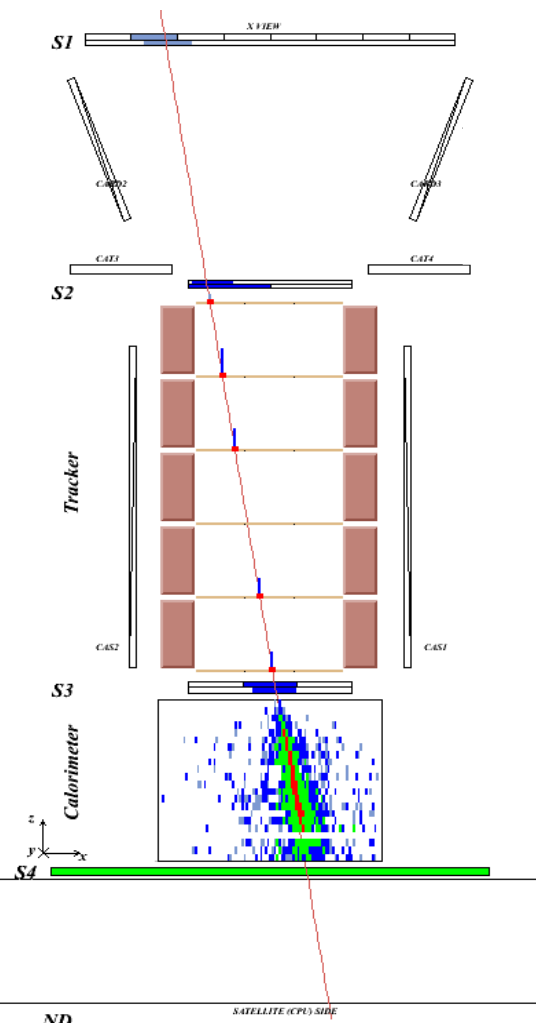
Antiproton
(NB: $e^-/p \sim 10^2$)

Time-of-flight:
trigger, albedo
rejection, mass
determination (up
to 1 GeV)

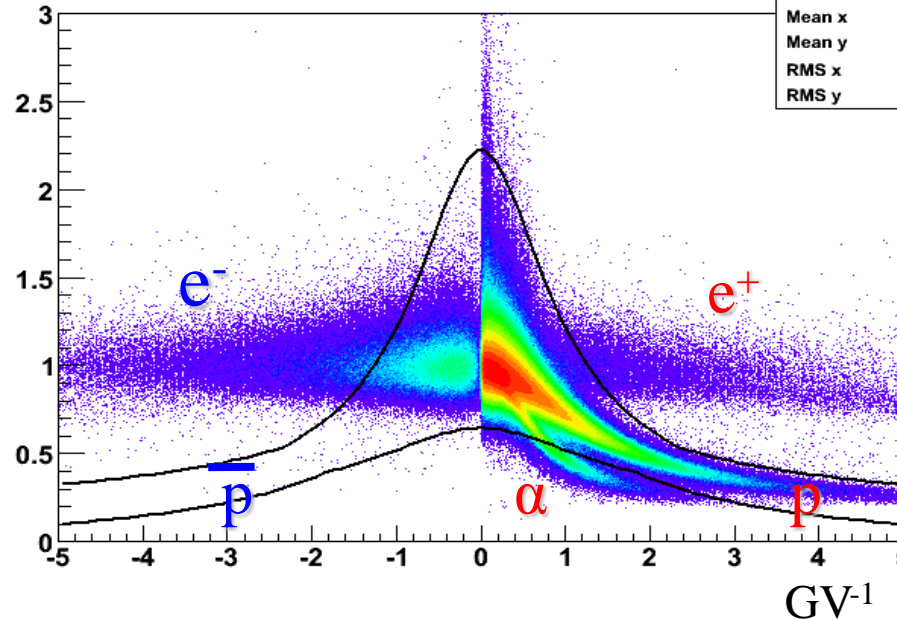
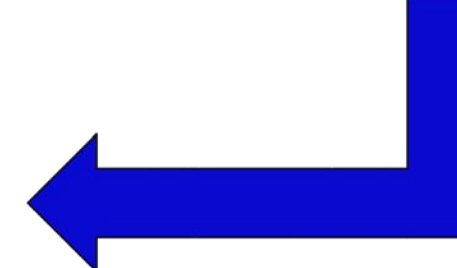
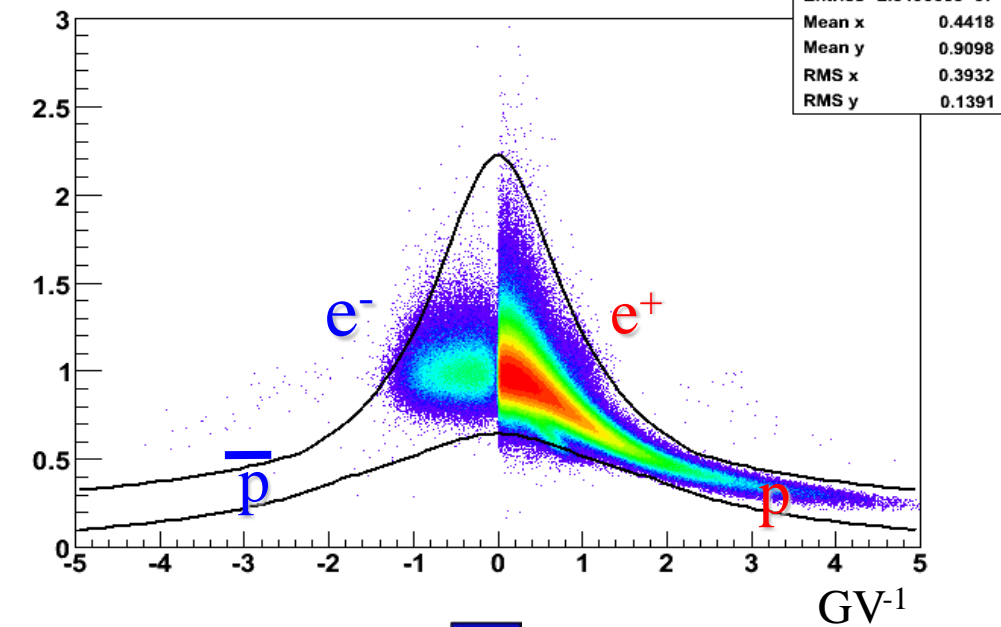
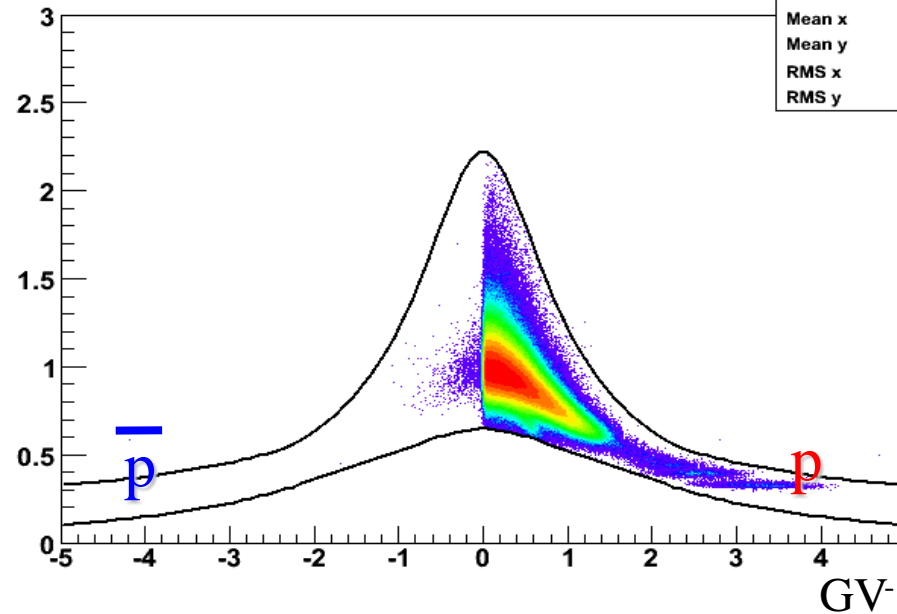
Bending in
spectrometer:
sign of charge

Ionisation energy loss
(dE/dx):
magnitude of charge

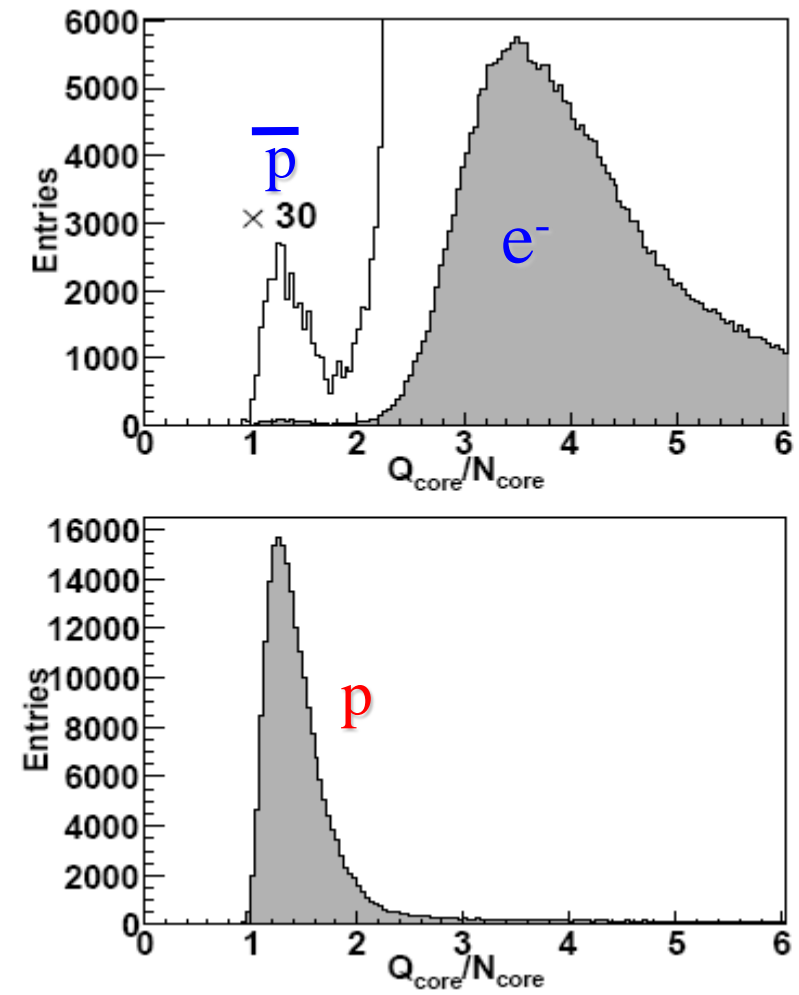
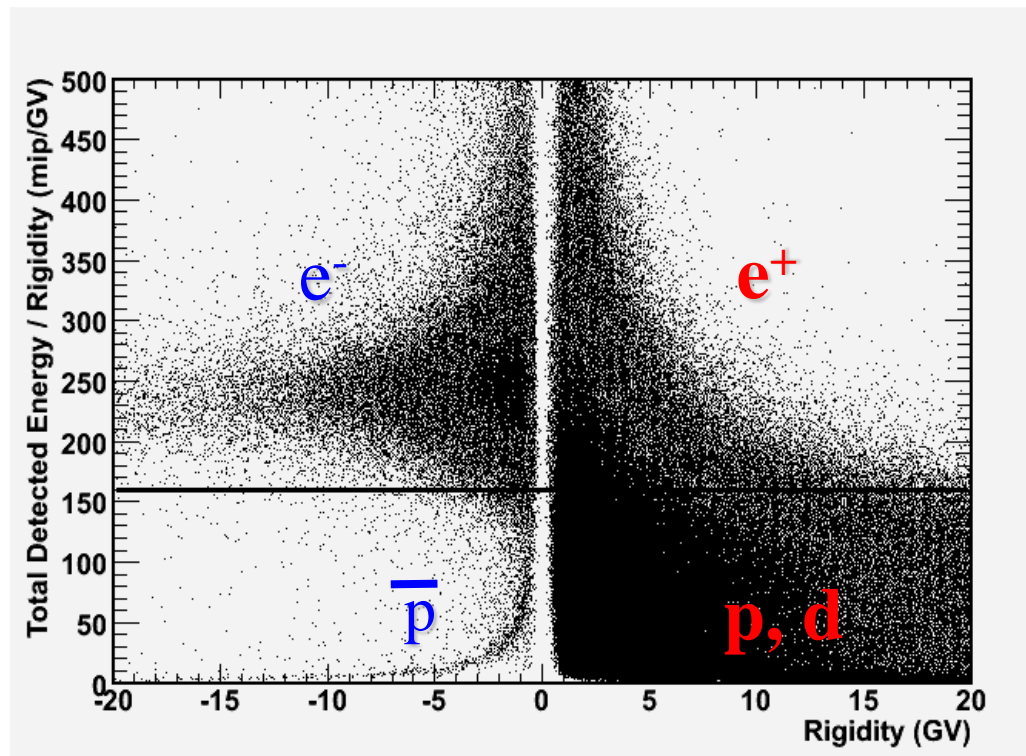
Interaction pattern in
calorimeter:
electron-like or
proton-like, electron
energy



Positron
(NB: $p/e^+ \sim 10^{3-4}$)

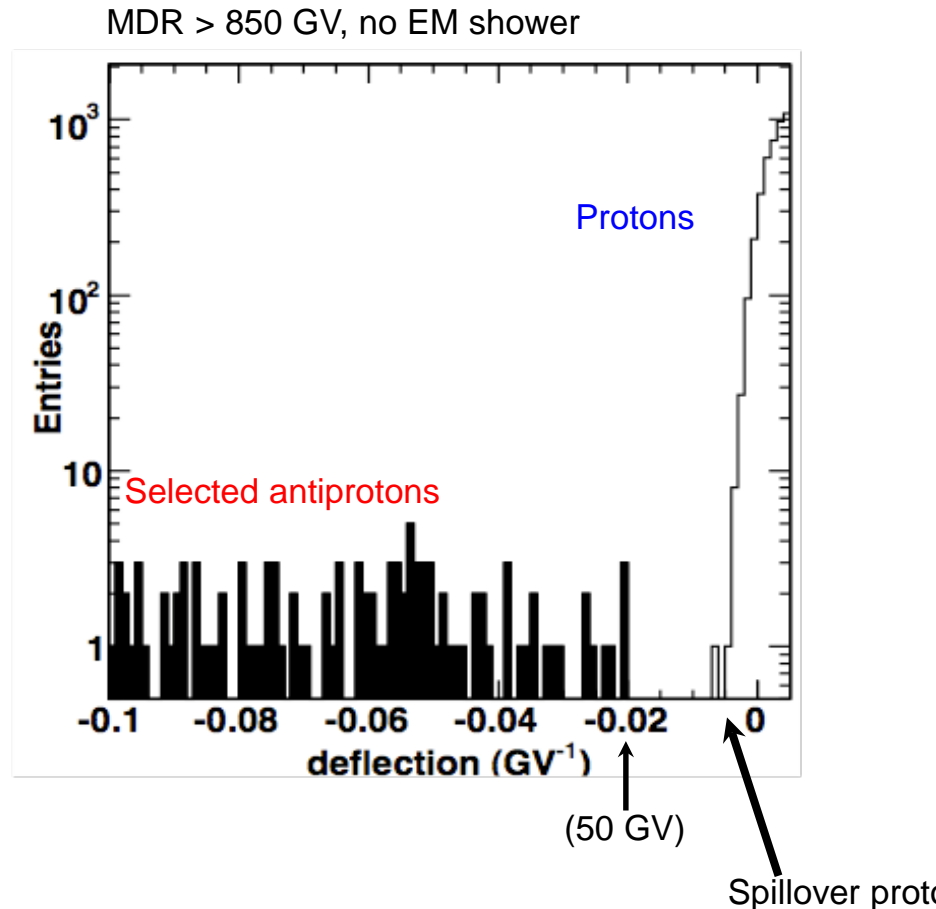
beta vs deflection**beta vs deflection -- after Z1 sel (Trk+ToF)****beta vs deflection -- after Z1&&BETA sel -- no electrons**

Calorimeter Selection

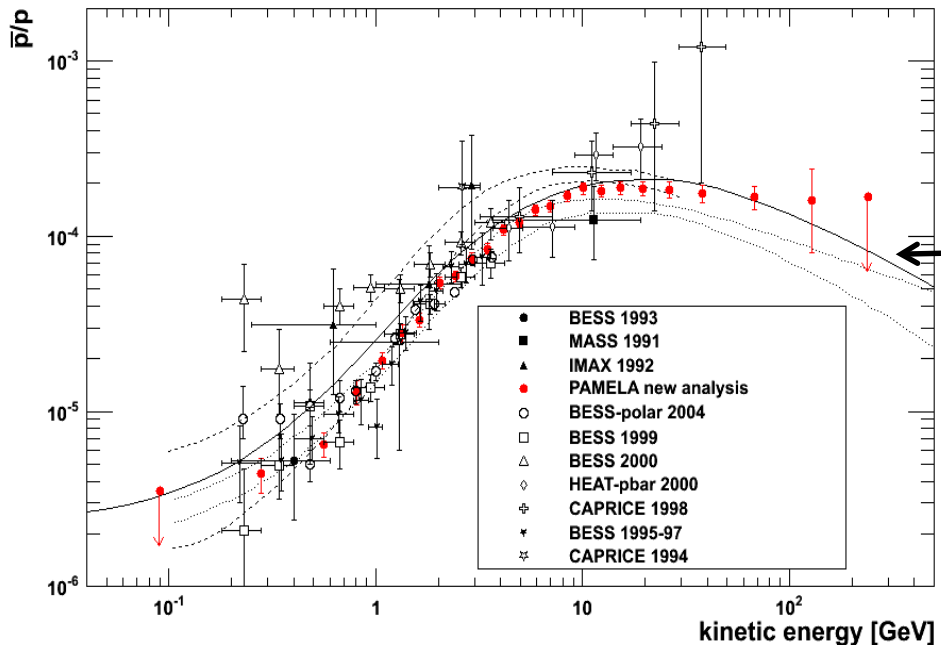


Proton Background

- Spectrometer tracking information is crucial for high-energy antiproton selection
- Finite spectrometer resolution - high rigidity protons may be assigned wrong sign-of-charge
- Also background from scattered protons
- Eliminate ‘spillover’ using strict track cuts (χ^2 , lever arm, no δ -rays, etc)
- MDR > 10 \times reconstructed rigidity
- Spillover limit for antiprotons expected to be ~200 GeV.

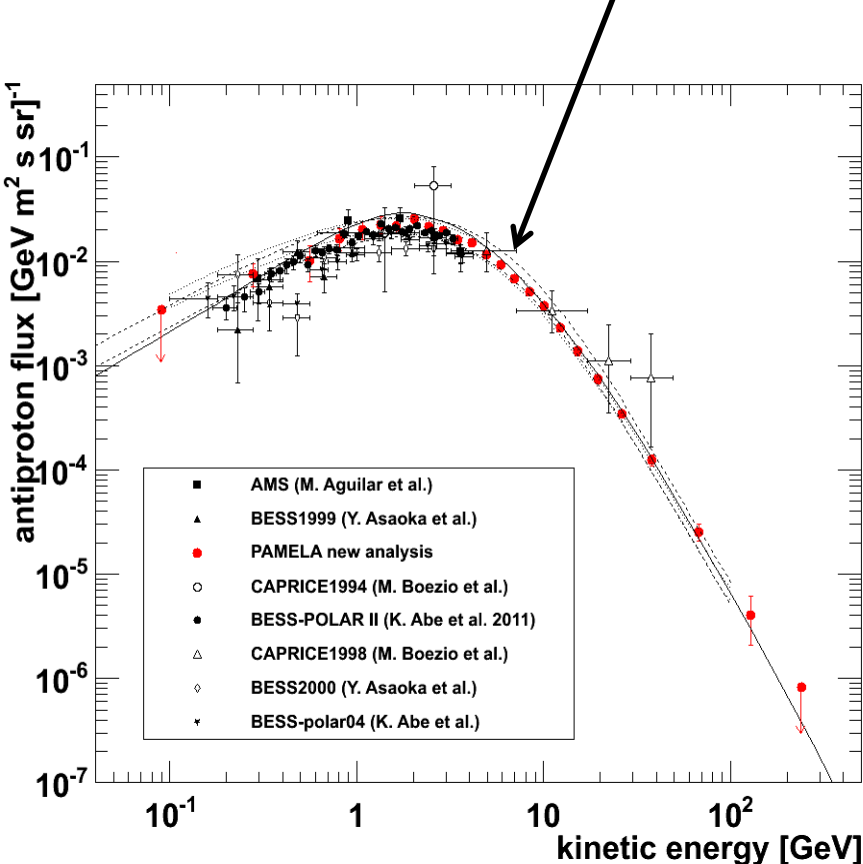


PAMELA Antiparticle Results: Antiprotons



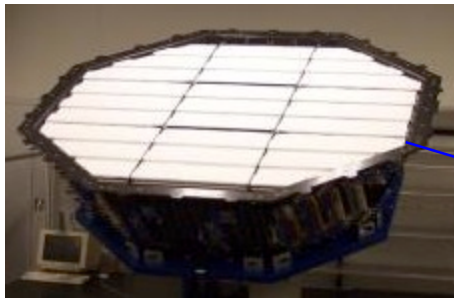
O. Adriani et al,
PRL 102 (2009) 051101;
PRL 105 (2010) 121101;
Phys. Rep. 544 (2014) 323.

Secondary production
calculations



AMS : A TeV precision, multipurpose spectrometer

Transition Radiation Detector
Identify electrons



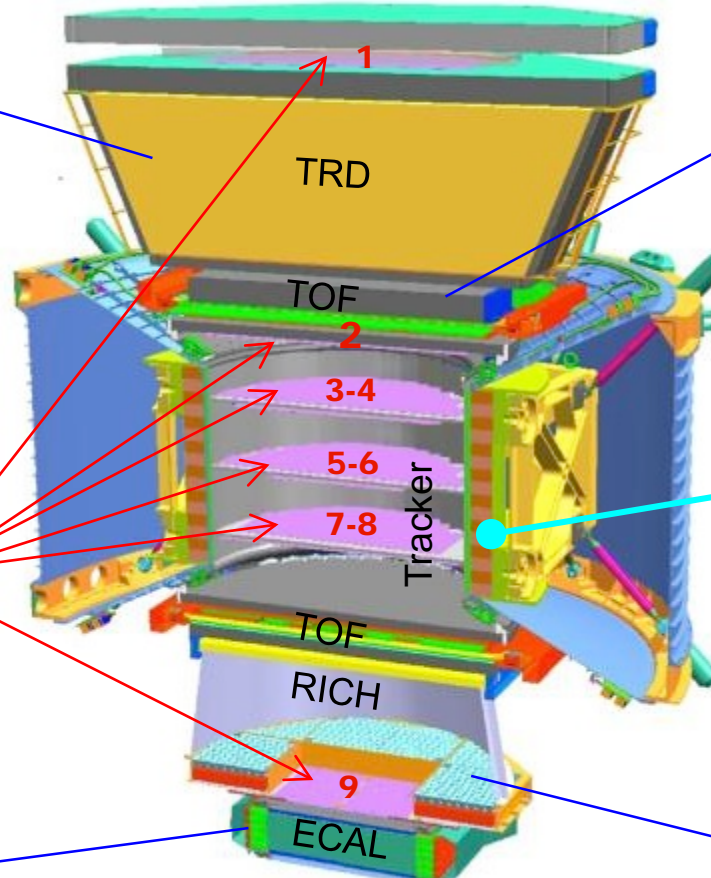
Silicon Tracker
 Z, P



Electromagnetic Calorimeter
 E of electrons



Particles are defined by their
charge (**Z**) and energy (**E**) or momentum (**P**)



Time of Flight
 Z, E



Magnet
 $\pm Z$

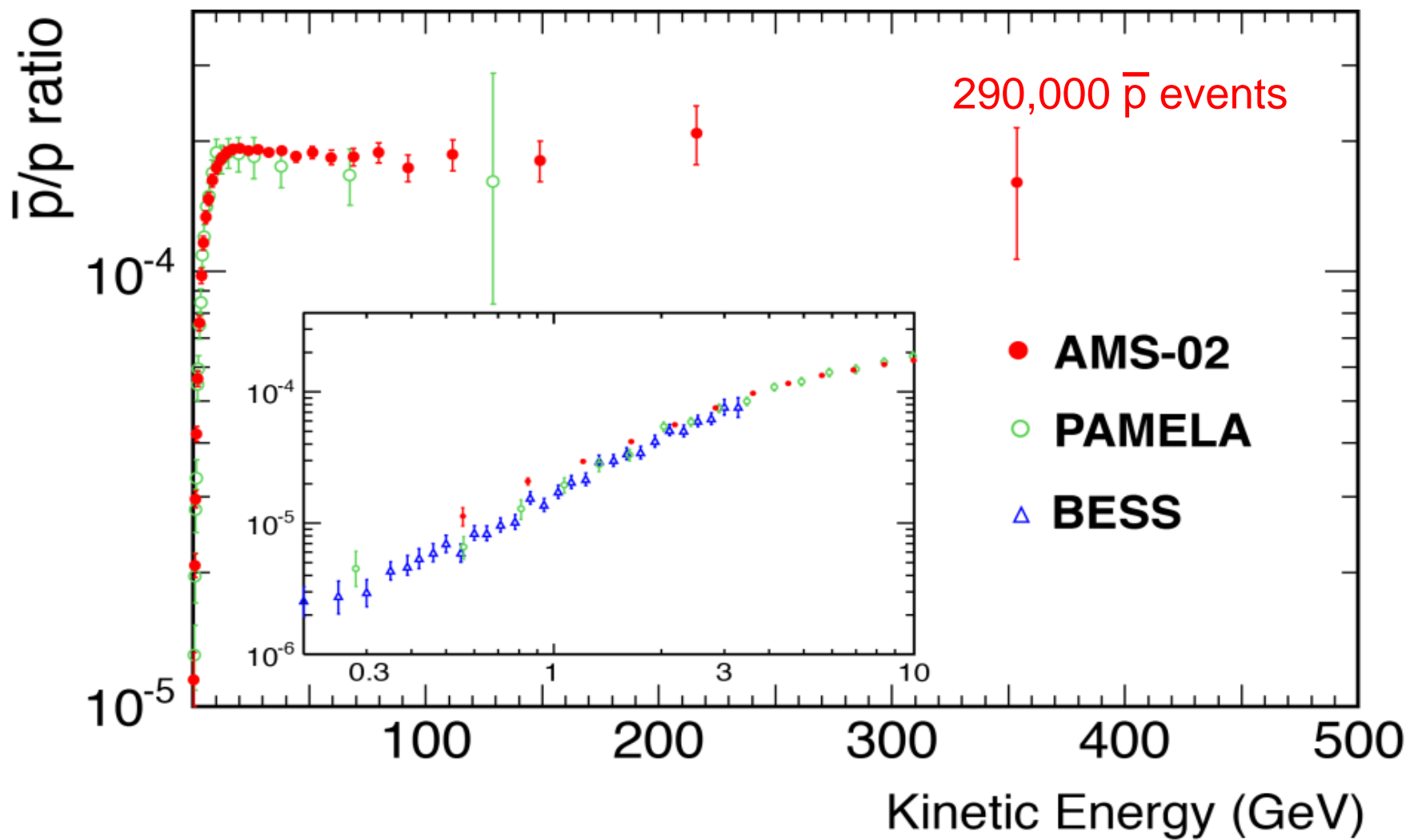


Ring Imaging Cherenkov
 Z, E



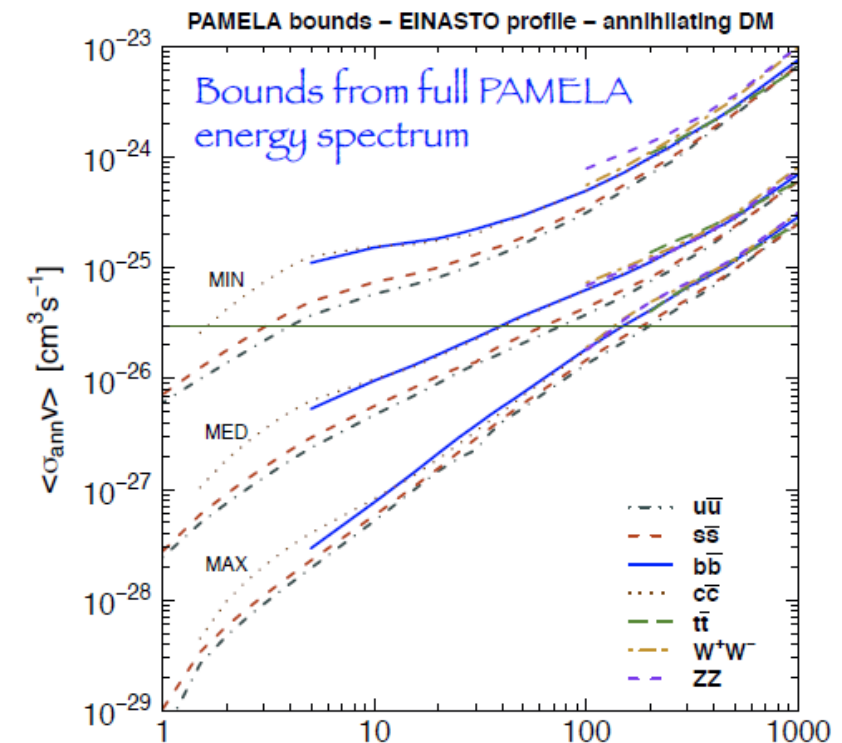
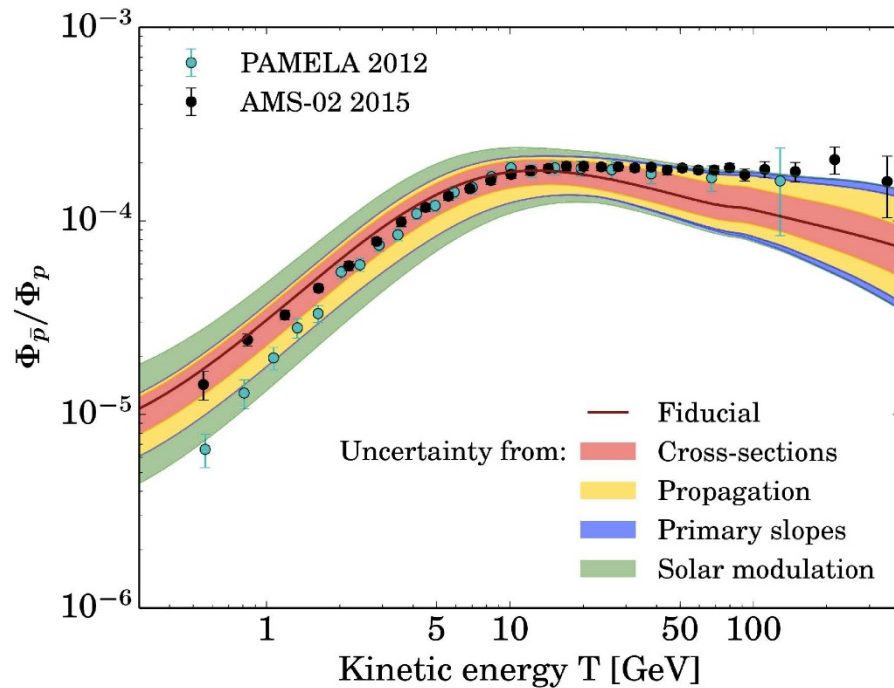
*The Charge and Energy (momentum)
are measured independently by many
detectors*

AMS-02 vs PAMELA & BESS



Cosmic-Ray Antiprotons and DM limits

PAMELA and preliminary AMS-02 antiproton data constrains on various dark matter models and astrophysical uncertainties.

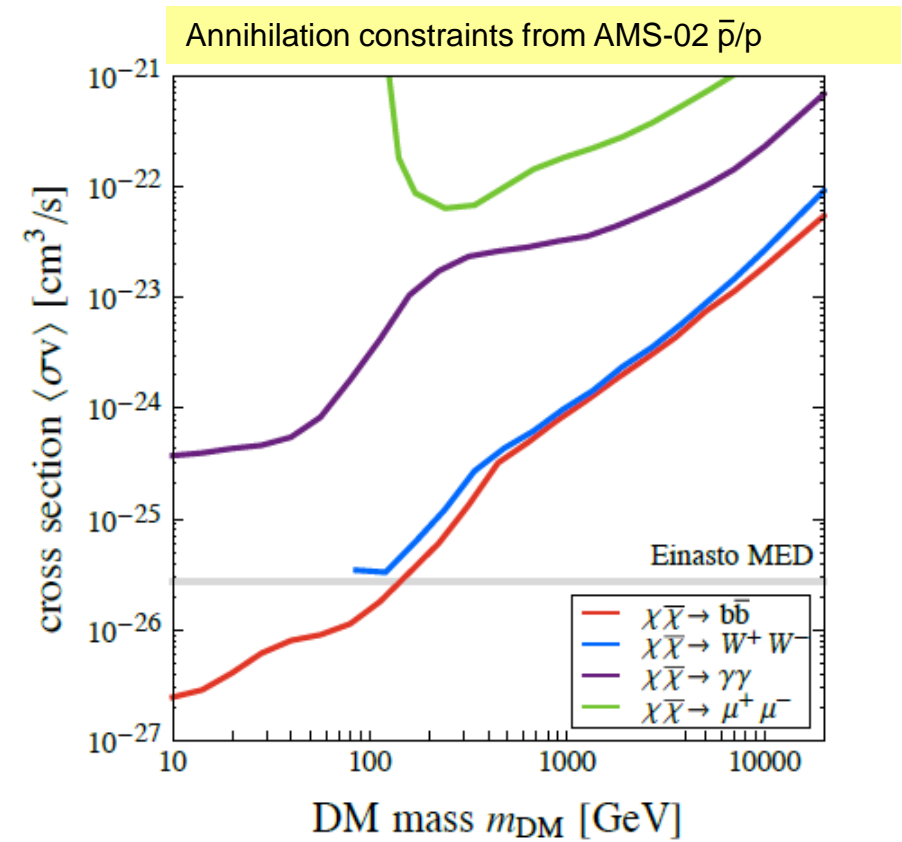
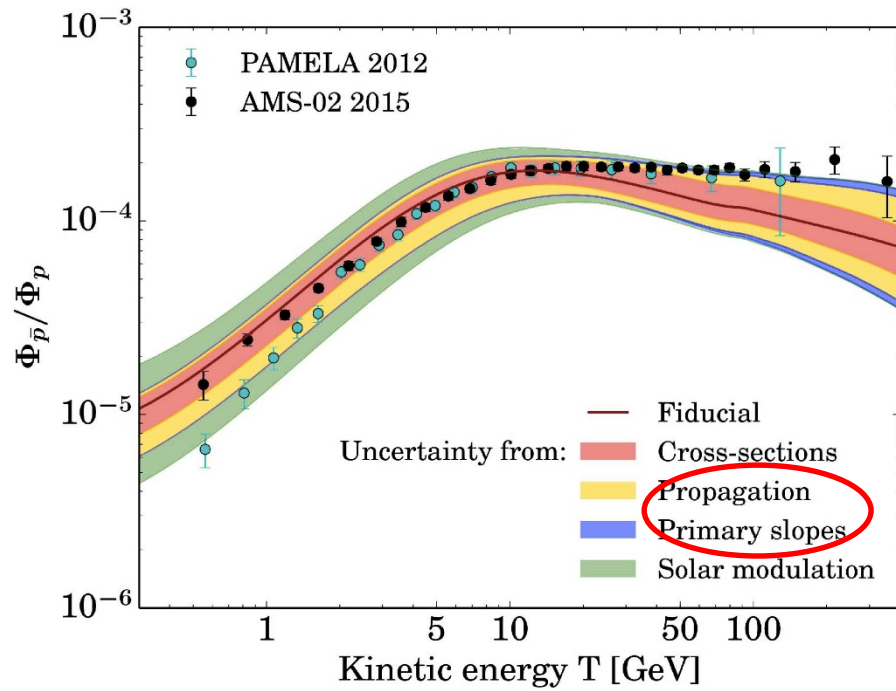


G. Giesen et al., JCAP 1509 (2015) 023,
arXiv: 1504:04276

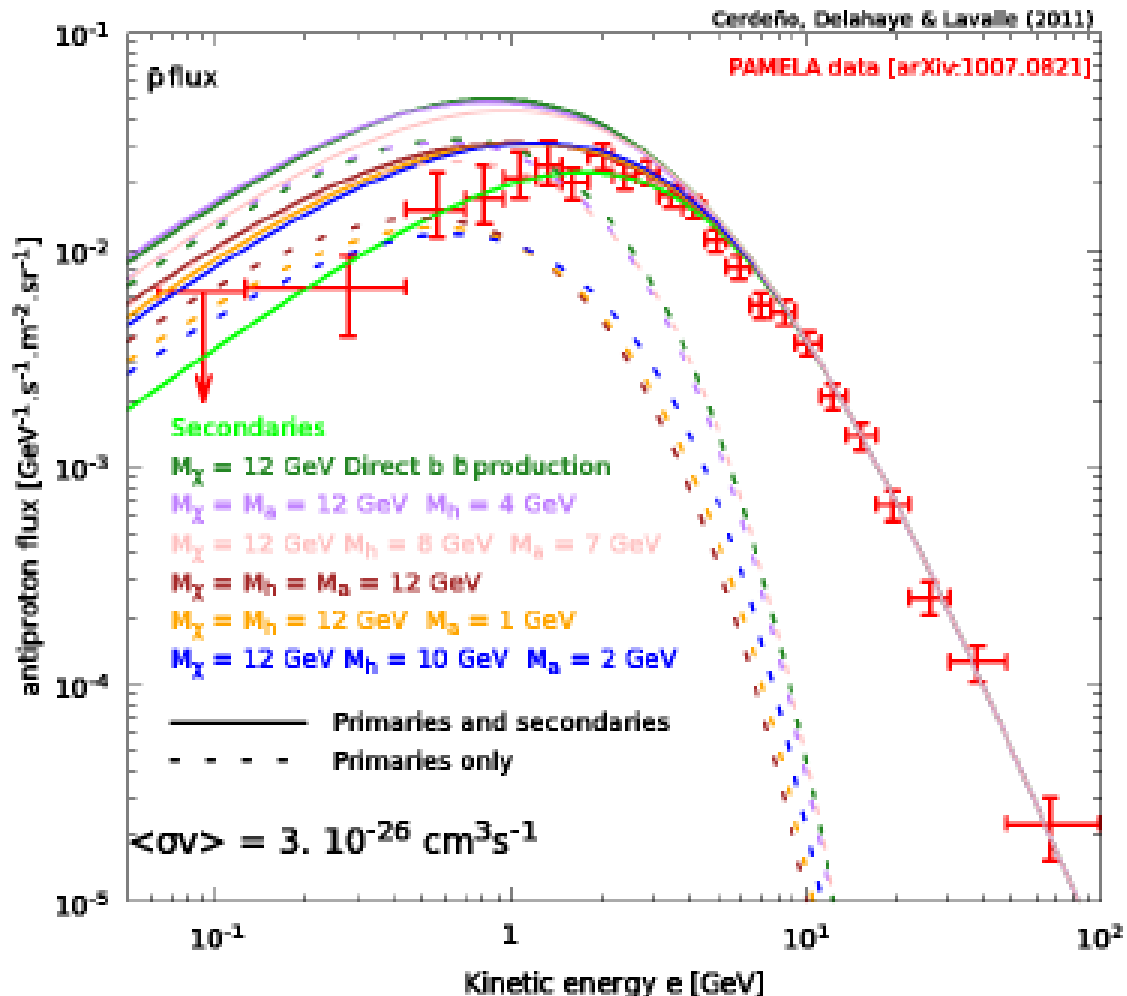
Fornengo, Maccione, Vittino, JCAP
1404 (2014) 04, 003

Cosmic-Ray Antiprotons and DM limits

PAMELA and preliminary AMS-02 antiproton data constrains on various dark matter models and astrophysical uncertainties.



Cosmic-Ray Antiprotons and DM limits

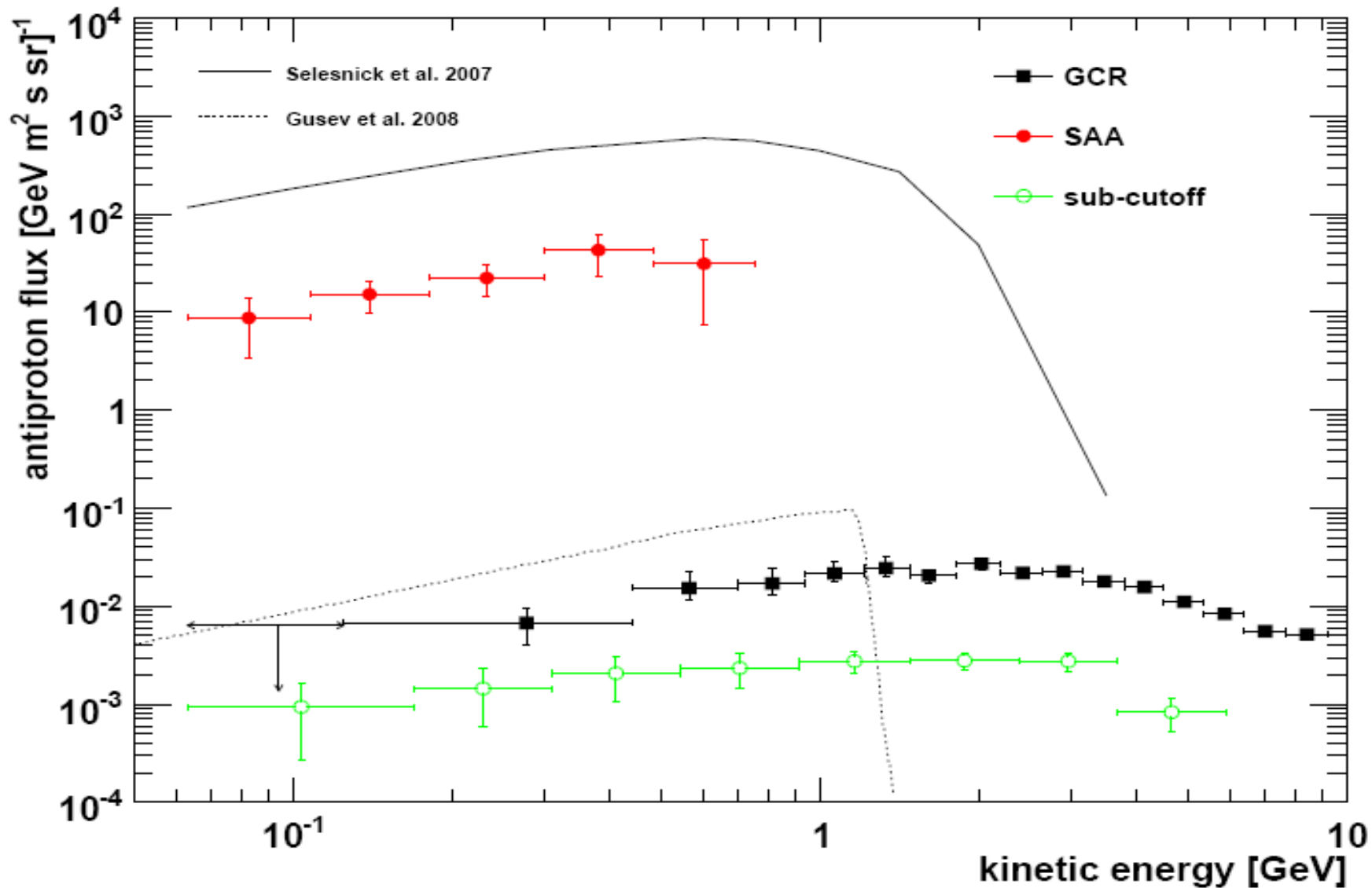


D. G. Cerdeno, T. Delahaye & J. Lavalle,
Nucl. Phys. B 854 (2012) 738
Antiproton flux predictions for a 12 GeV
WIMP annihilating into different mass
combinations of an intermediate two-
boson state which further decays into
quarks.

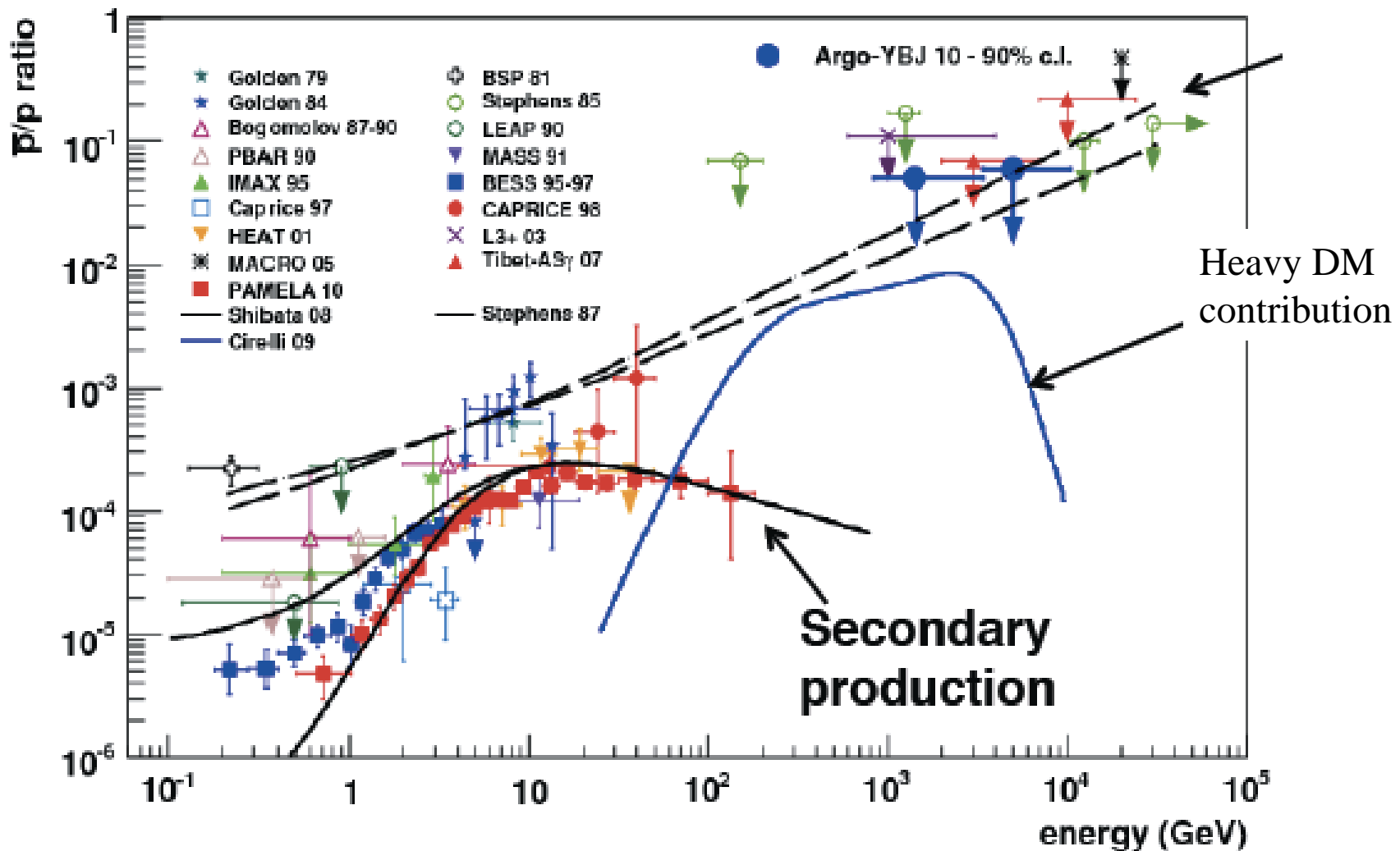
See also:

- M. Asano, T. Bringmann & C. Weniger, Phys. Lett. B 709 (2012) 128.
- M. Garny, A. Ibarra & S. Vogl, JCAP 1204 (2012) 033
- R. Kappl & M. W. Winkler, PRD 85 (2012) 123522

PAMELA trapped antiprotons

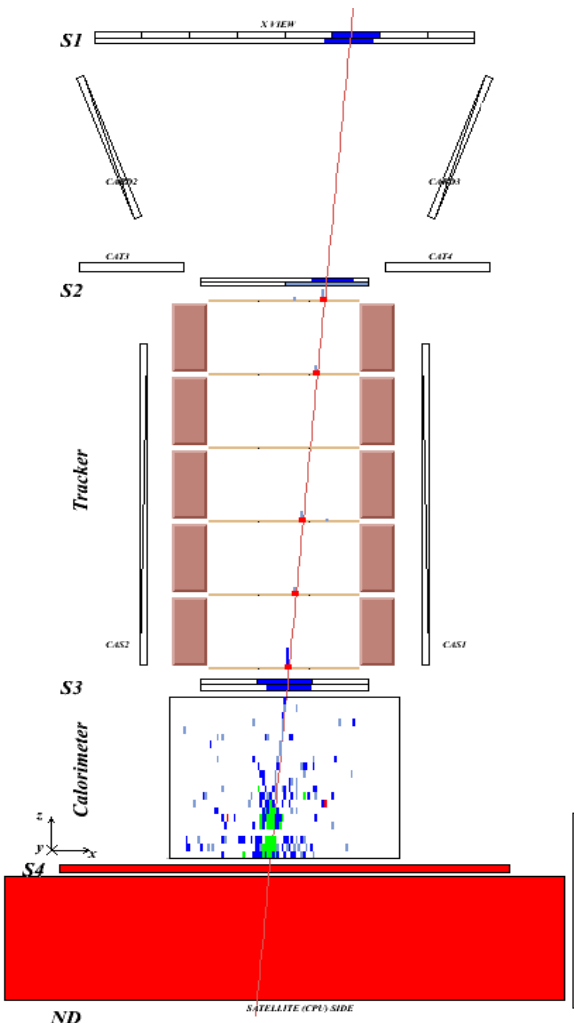


Antiproton to Pion Flux Ratio



Positrons

Proton / positron discrimination



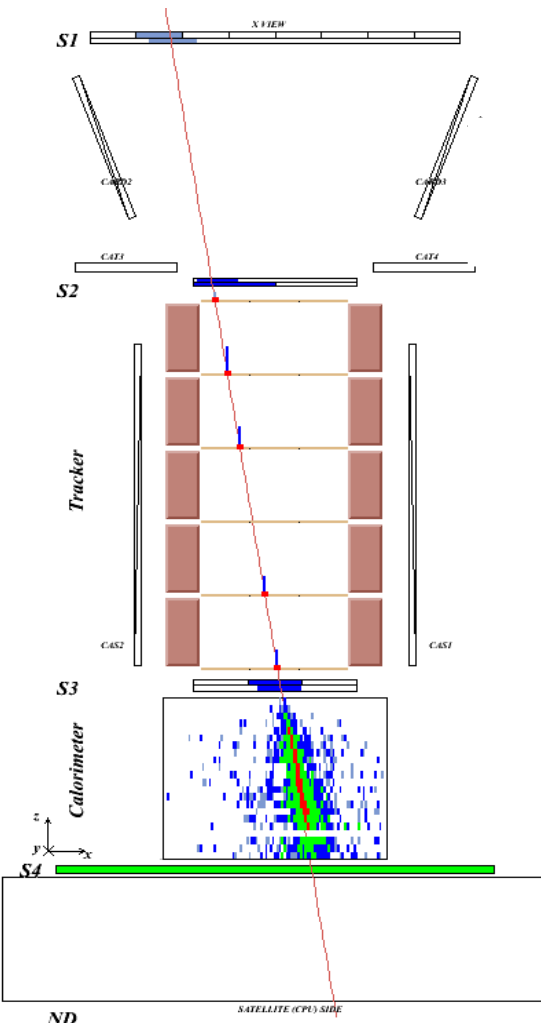
Proton

Time-of-flight:
trigger, albedo
rejection, mass
determination (up to
1 GeV)

Bending in
spectrometer: **sign**
of charge

Ionisation energy loss
(dE/dx):
magnitude of charge

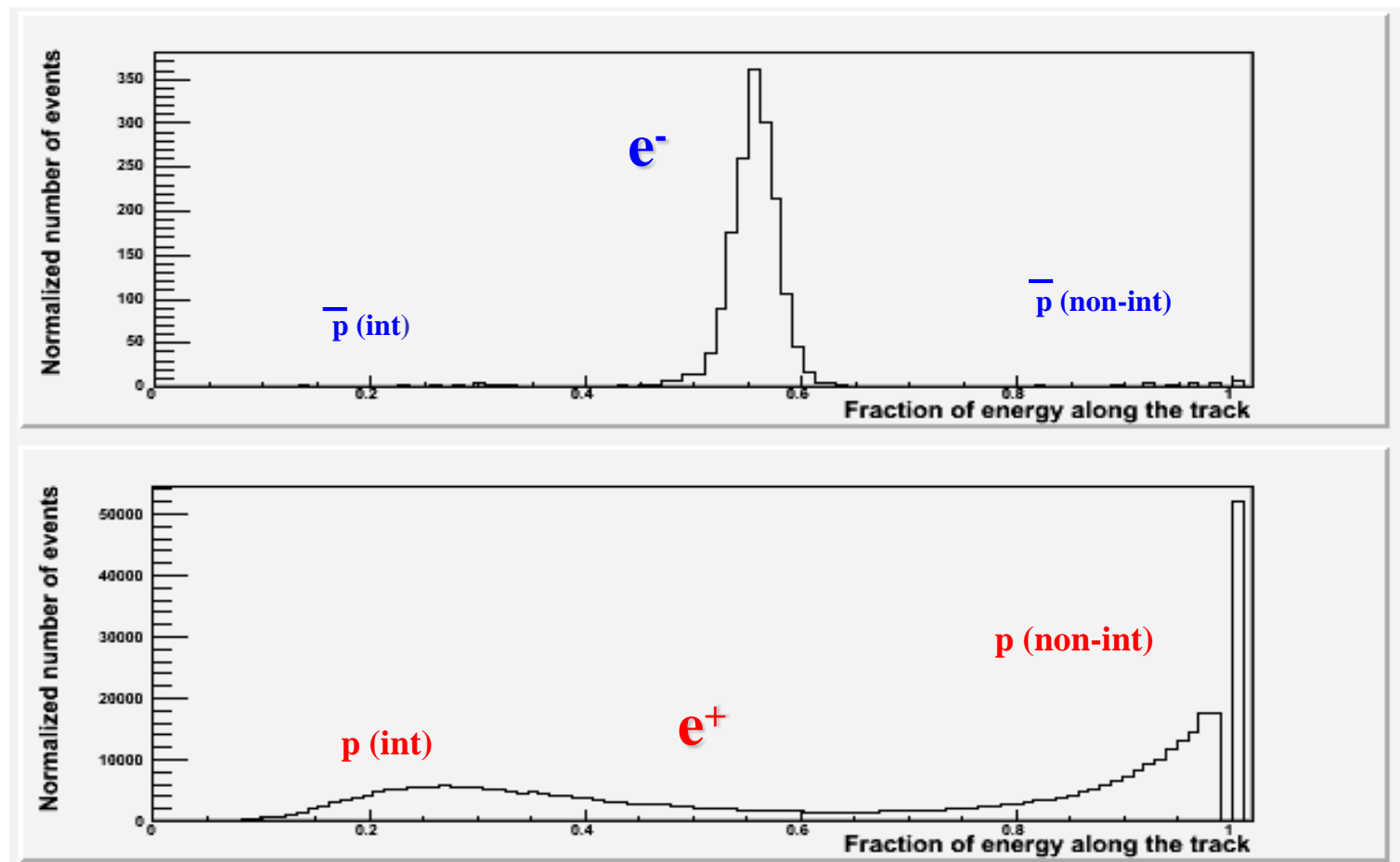
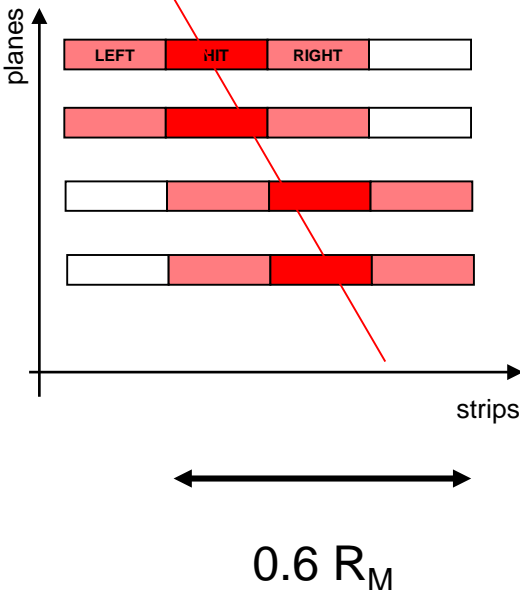
Interaction pattern in
calorimeter: **electron-**
like or proton-like,
electron energy



Positron

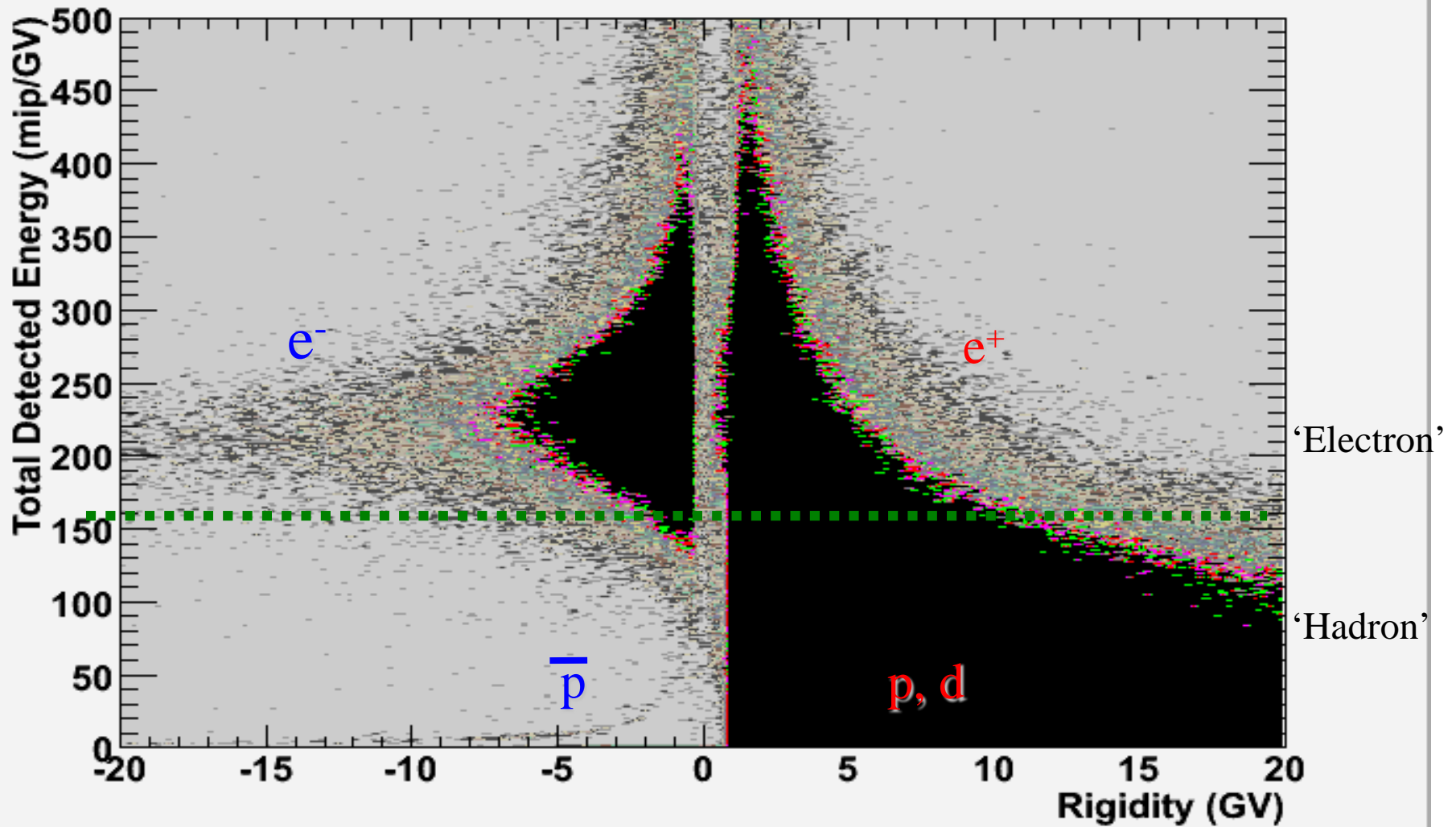
Positron selection with calorimeter

Fraction of energy released along the calorimeter track (left, hit, right)



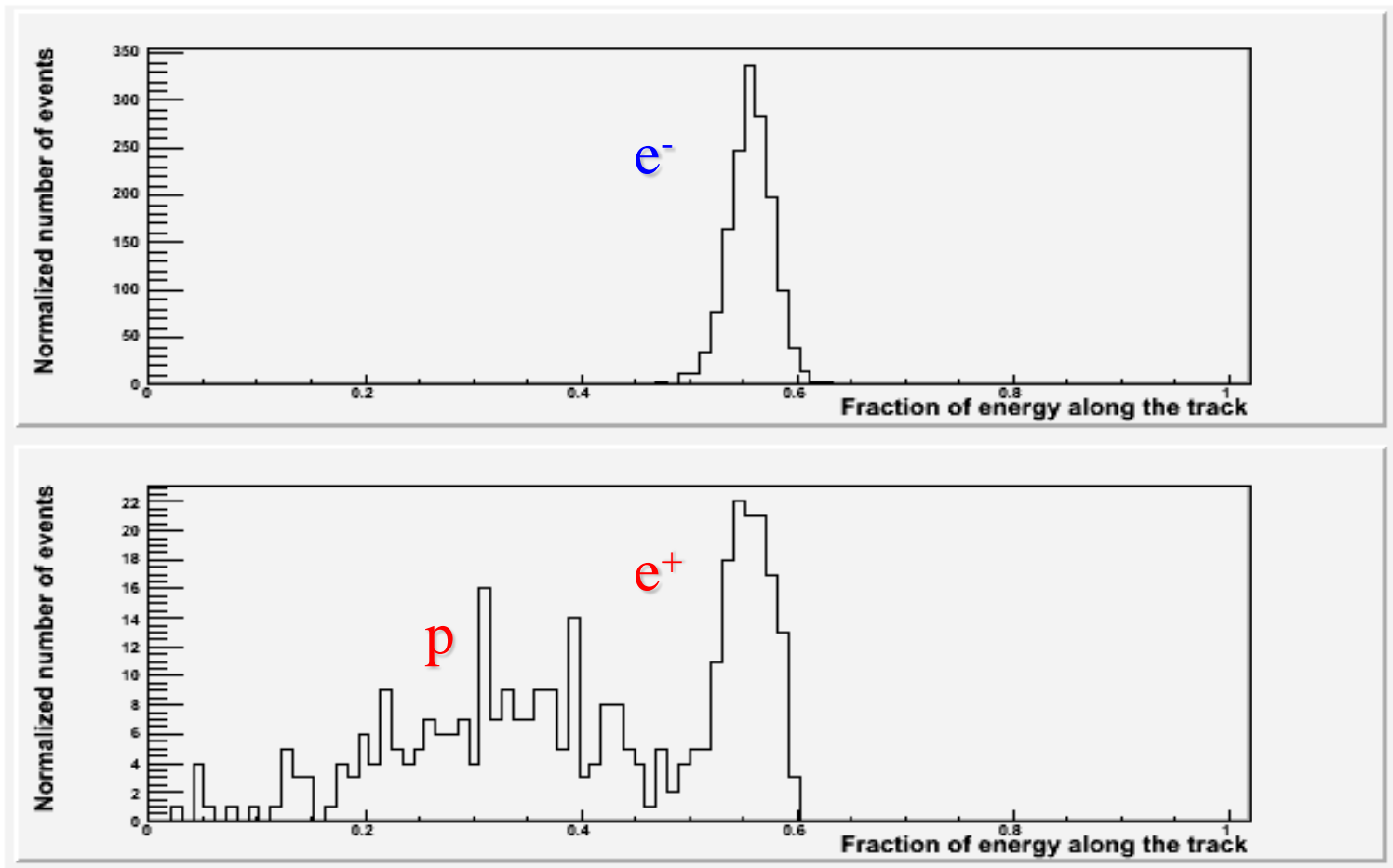
Rigidity: 20-30 GV

Antiparticle selection



Positron selection with calorimeter

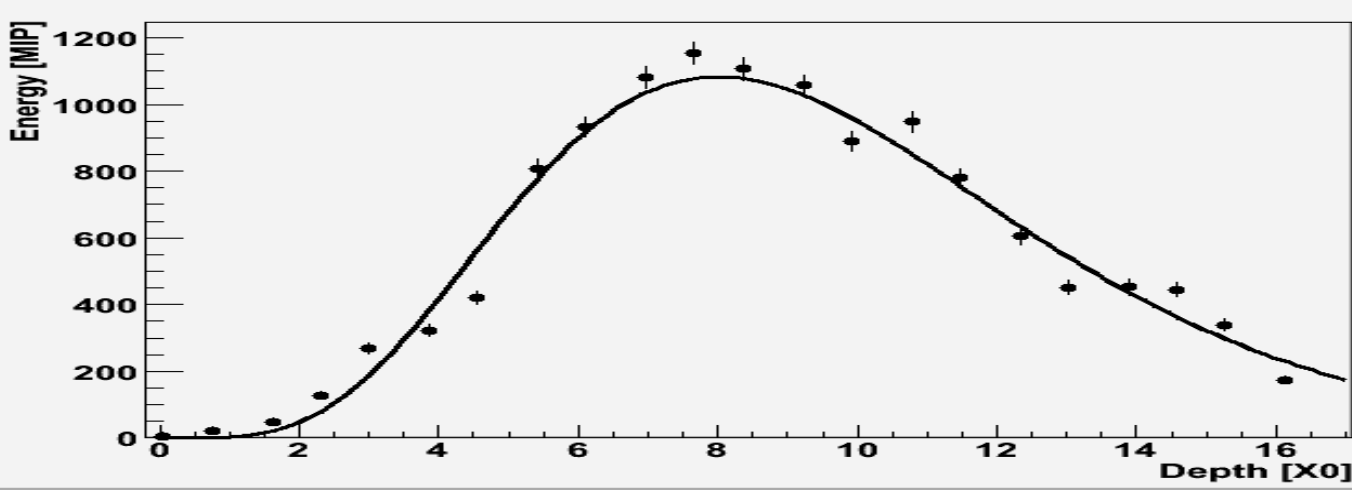
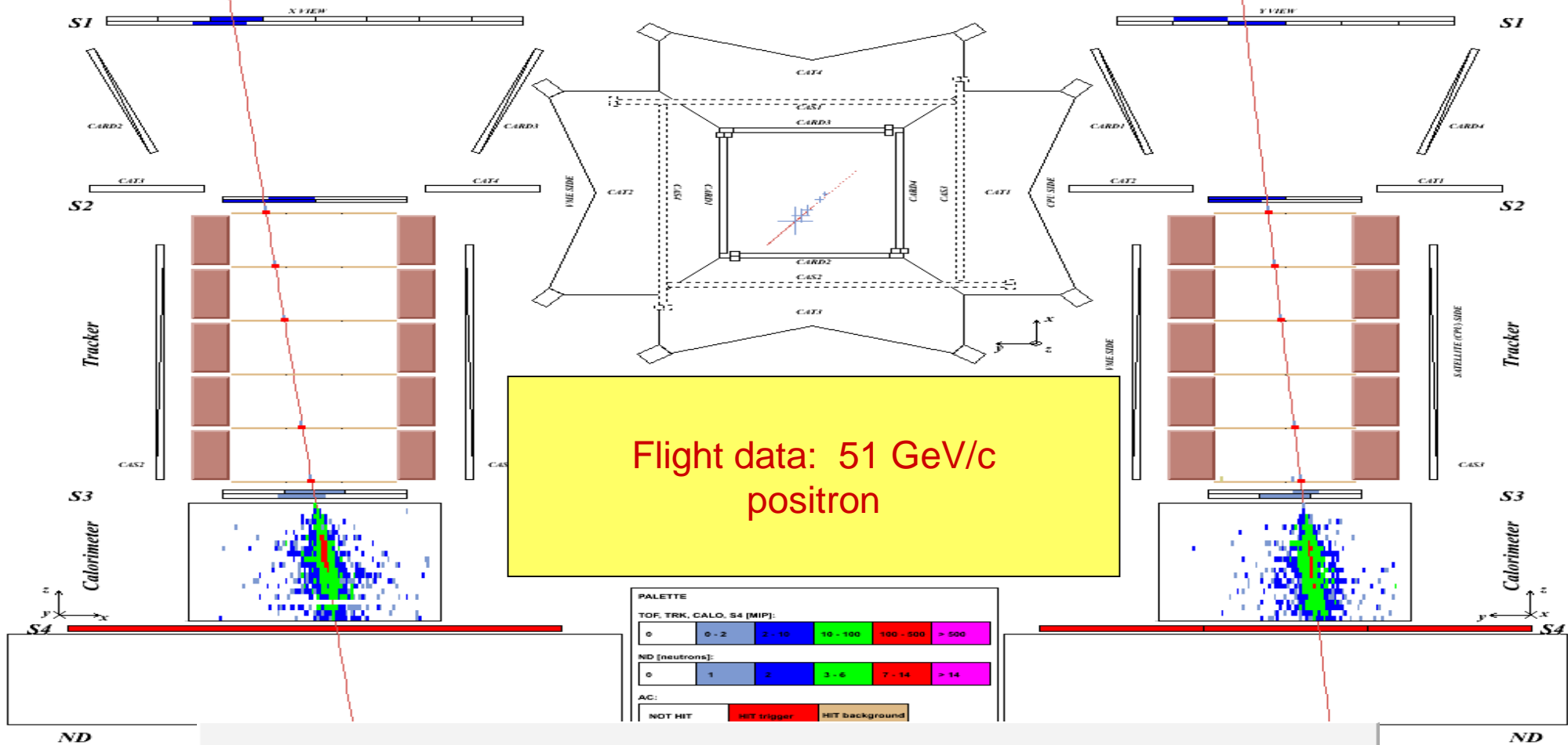
Rigidity: 20-30 GV



Fraction of charge released along the
calorimeter track (left, hit, right)

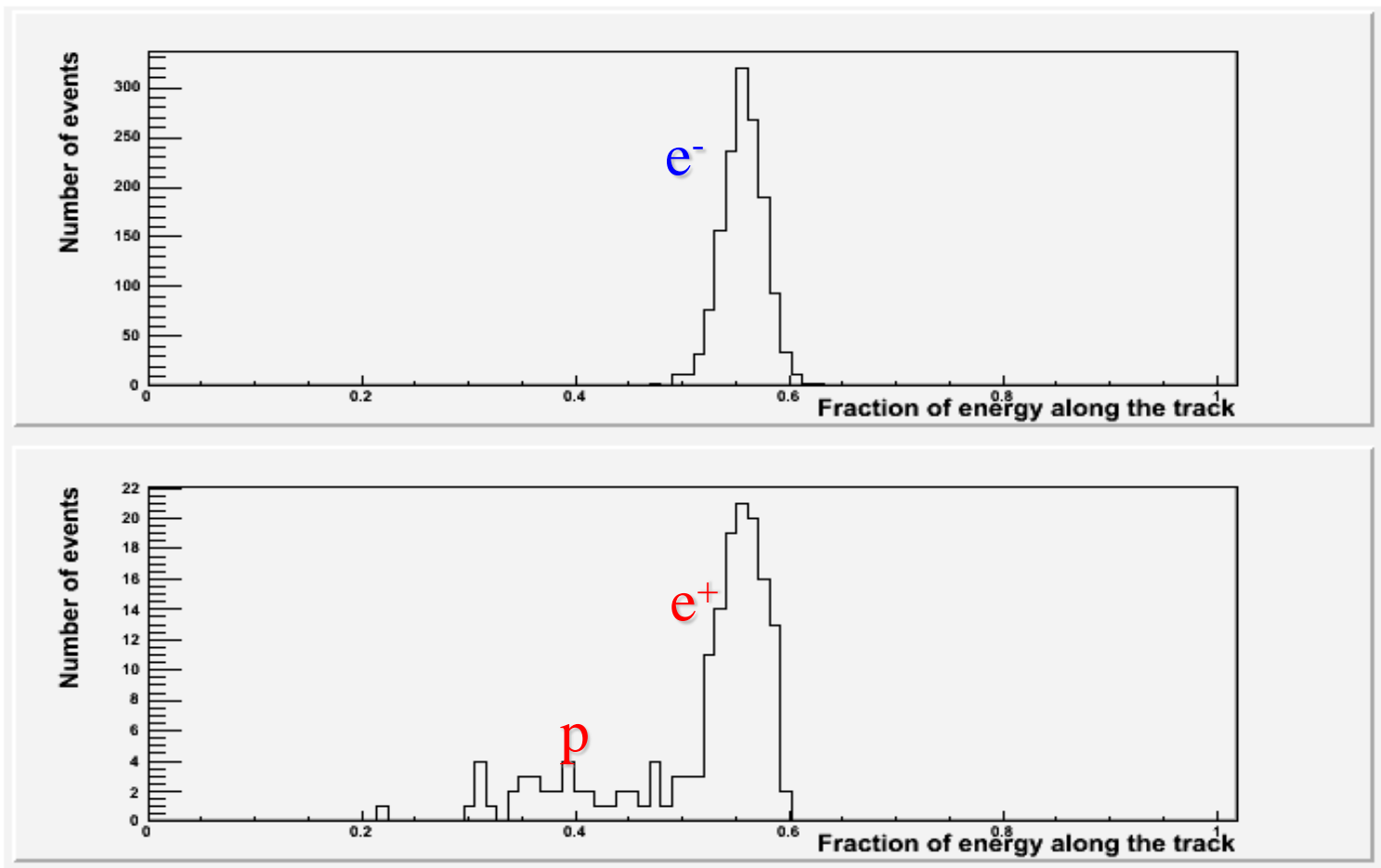


- Energy-momentum match
- Starting point of shower



Positron selection with calorimeter

Rigidity: 20-30 GV

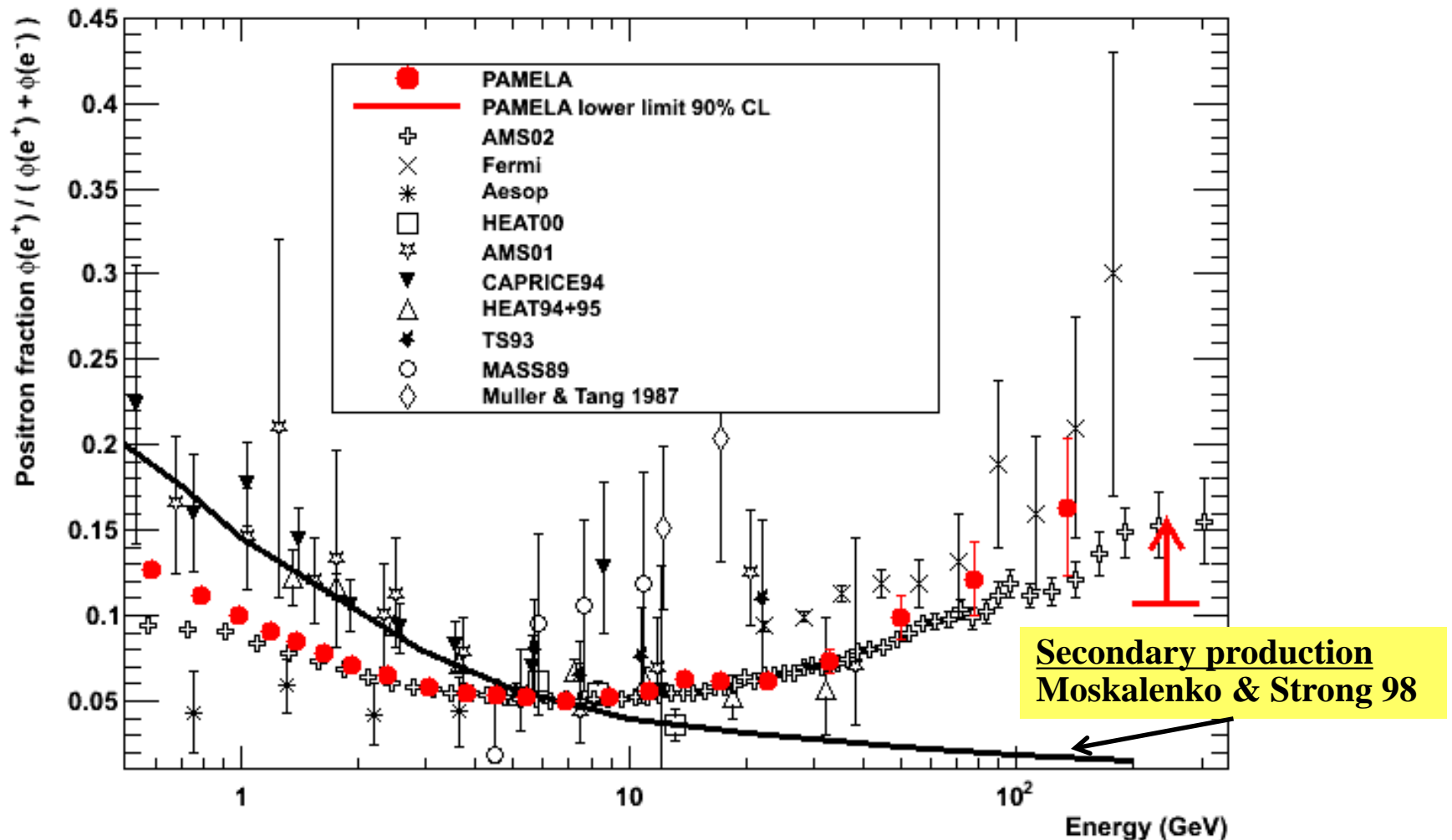


Fraction of charge released along the
calorimeter track (left, hit, right)

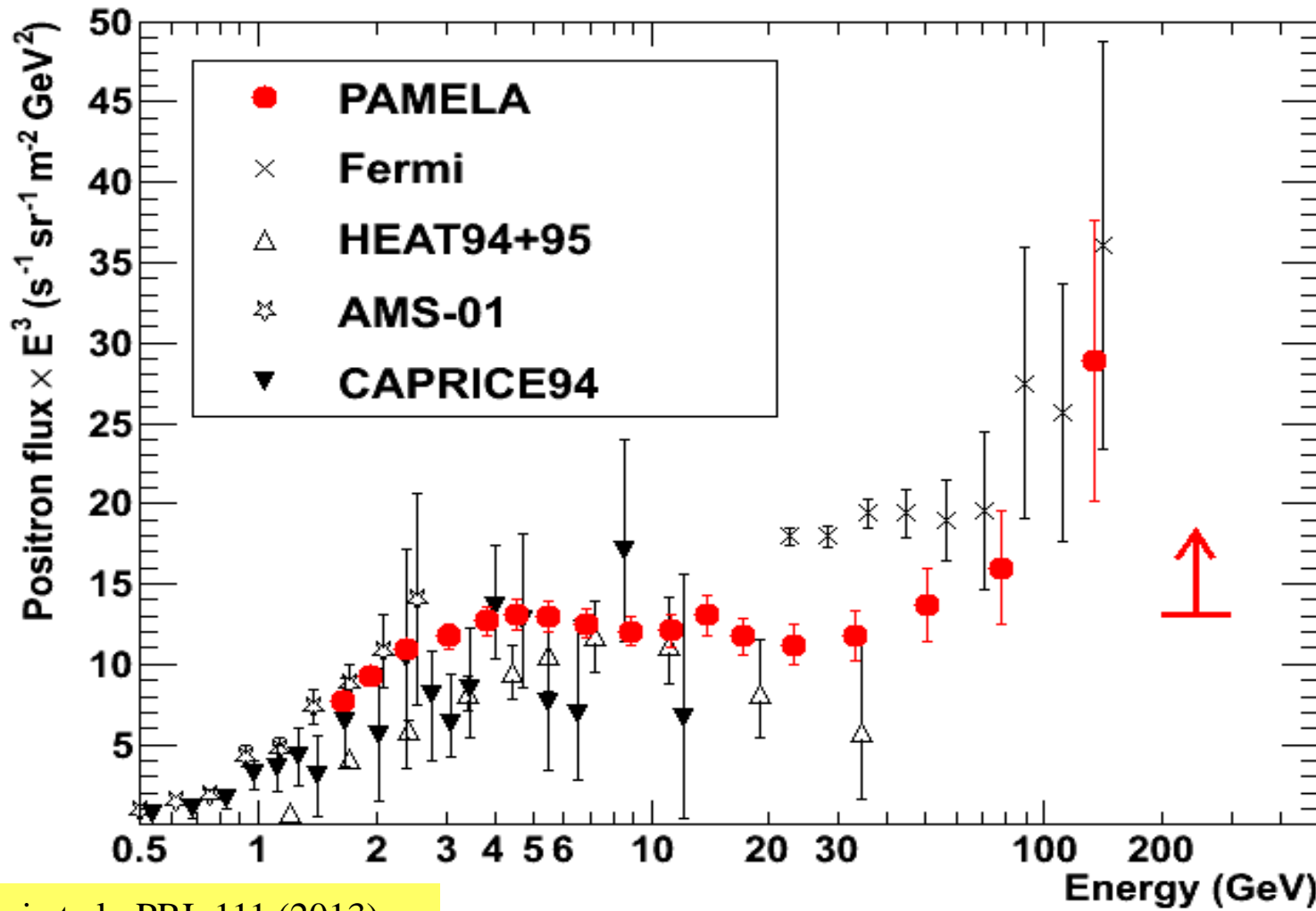


- Energy-momentum match
- Starting point of shower
- Longitudinal profile

Positron to Electron Fraction

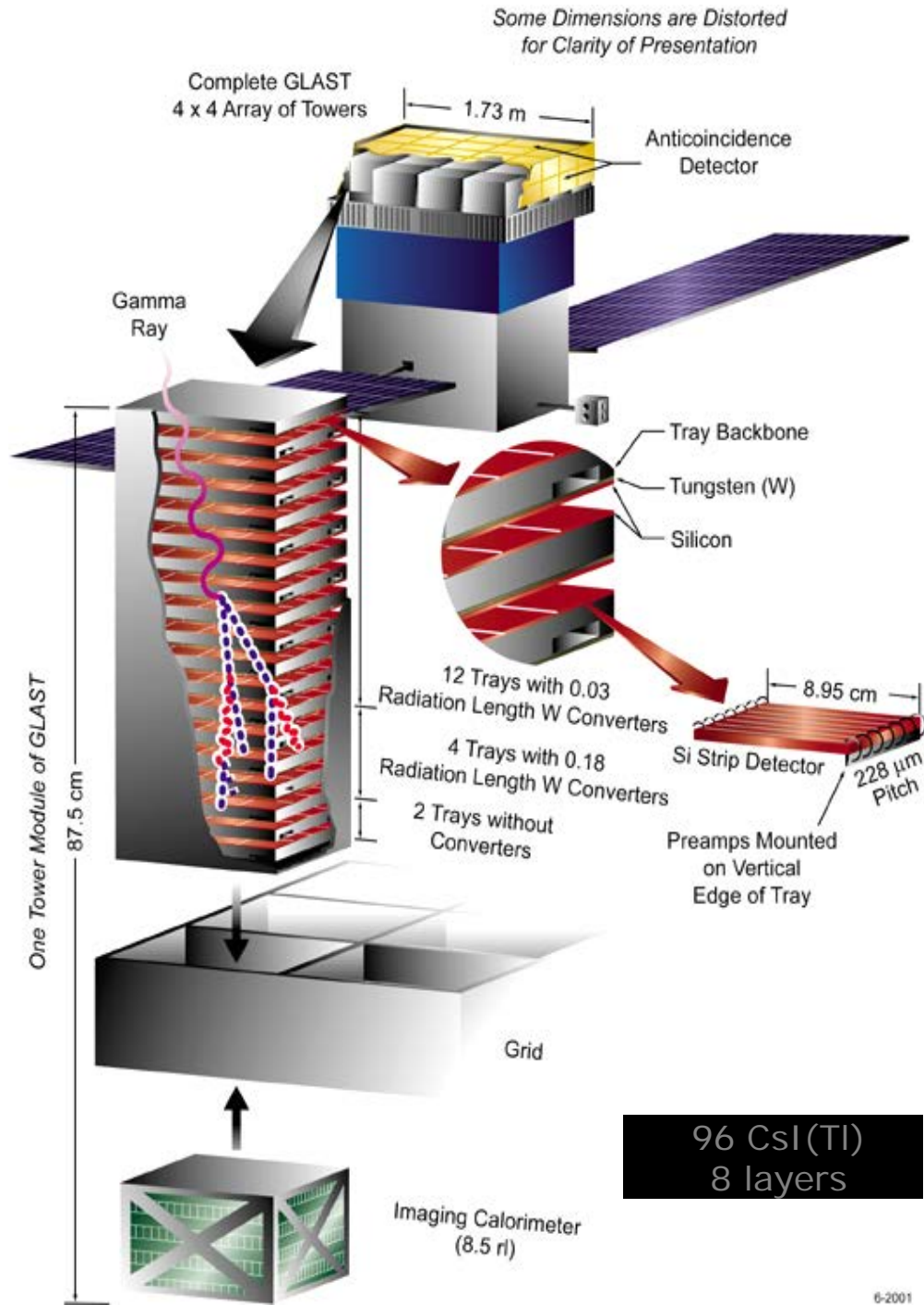


Positron Energy Spectrum

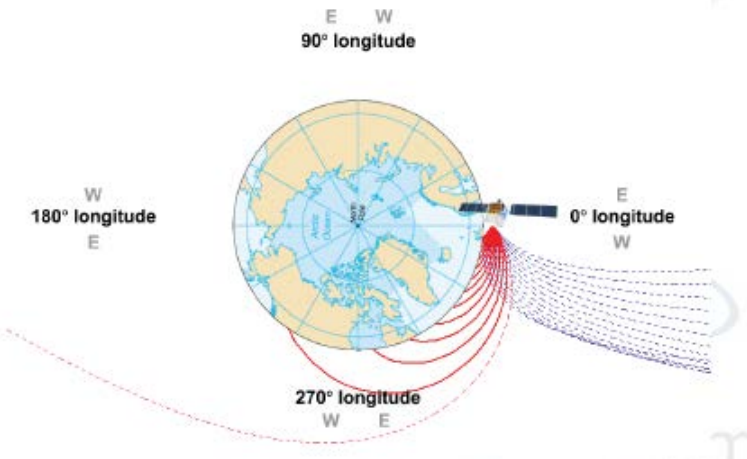
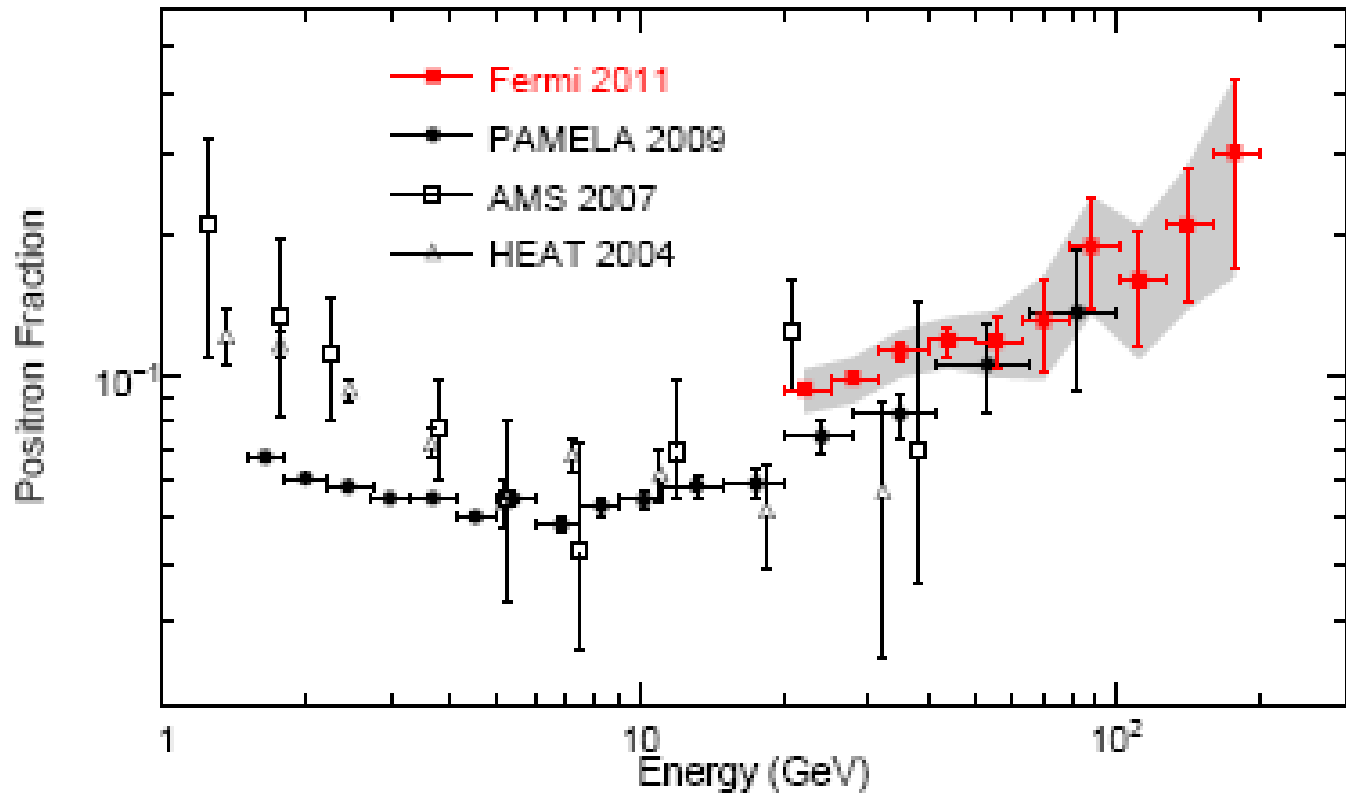


GLAST/ FERMI Gamma-Ray Large Area Space Telescope

3000 kg, 650 W
1.8 m x 1.8 m x 1 m
20 MeV – 300 GeV

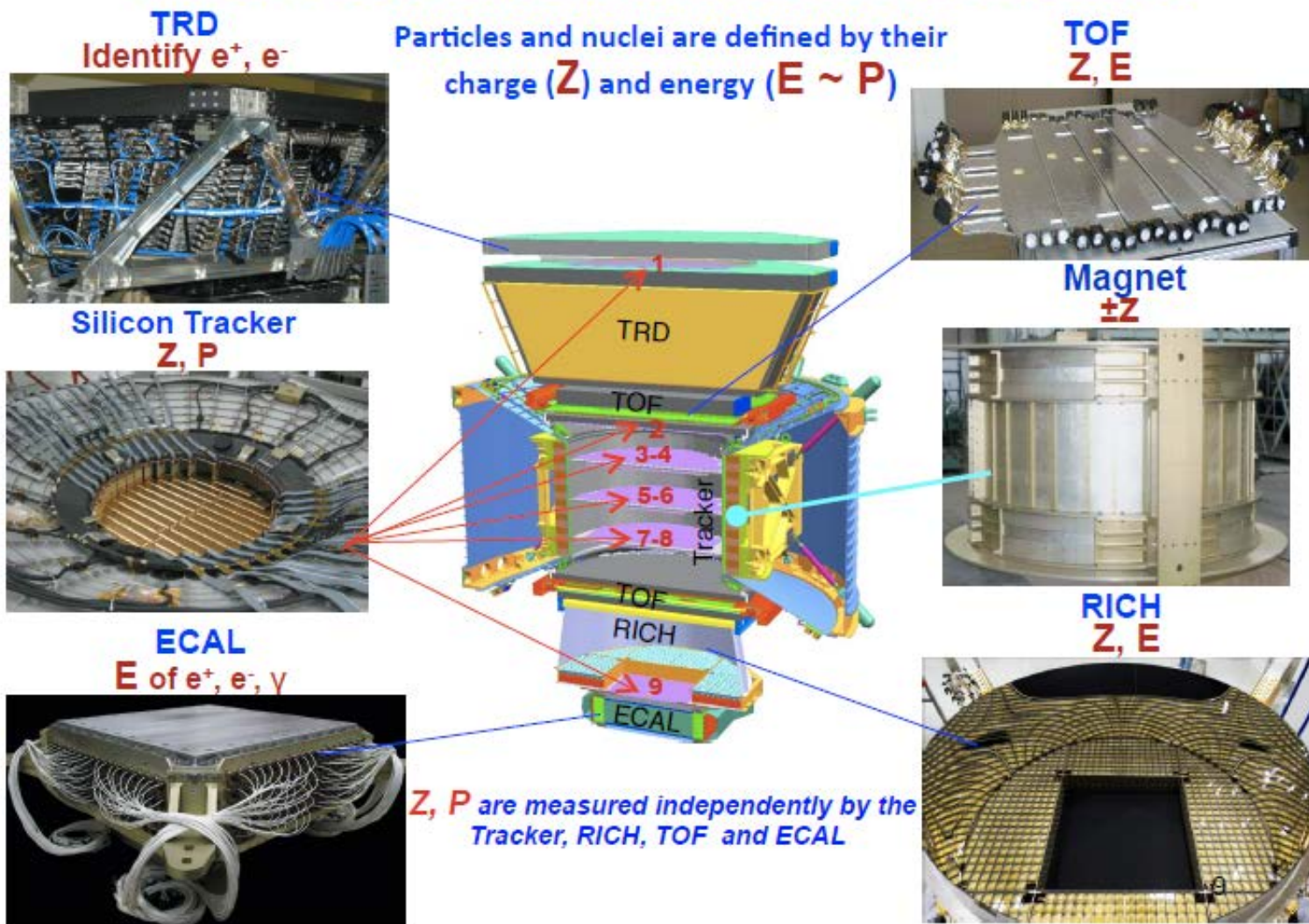


Fermi Positron Fraction

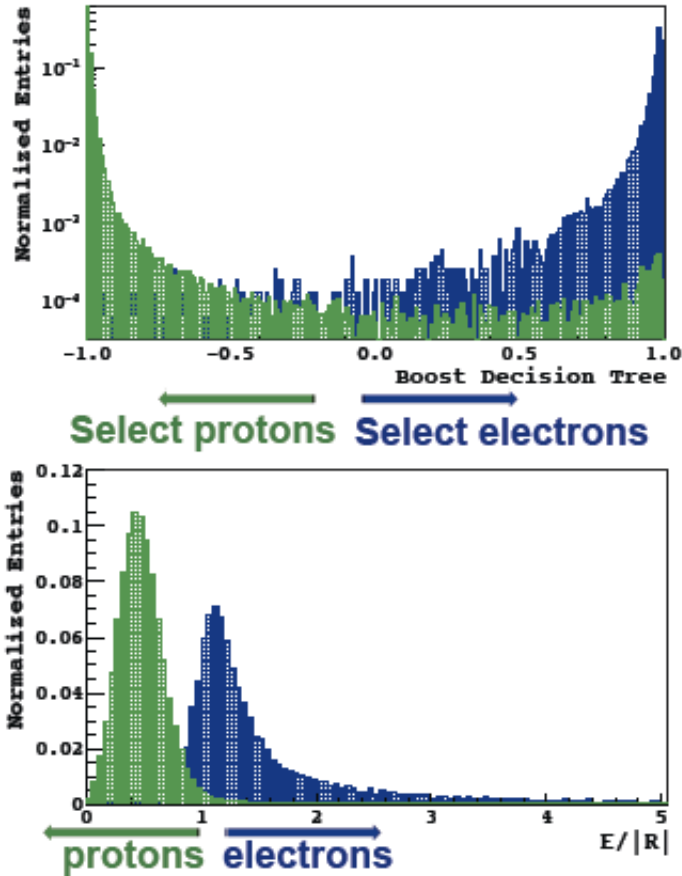


M. Ackermann, Phys.Rev.Lett. 108
(2012) 011103; astro-ph: 1109.0521

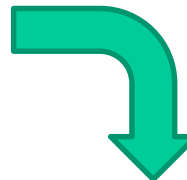
AMS: A TeV precision, multipurpose spectrometer



AMS Positron Selection

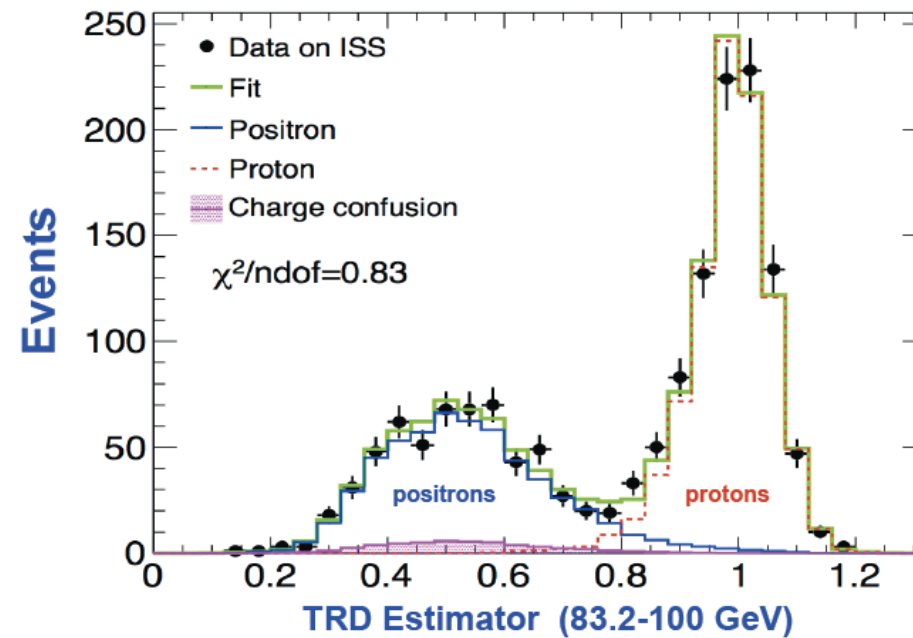


e/p separation with calorimeter+tracker

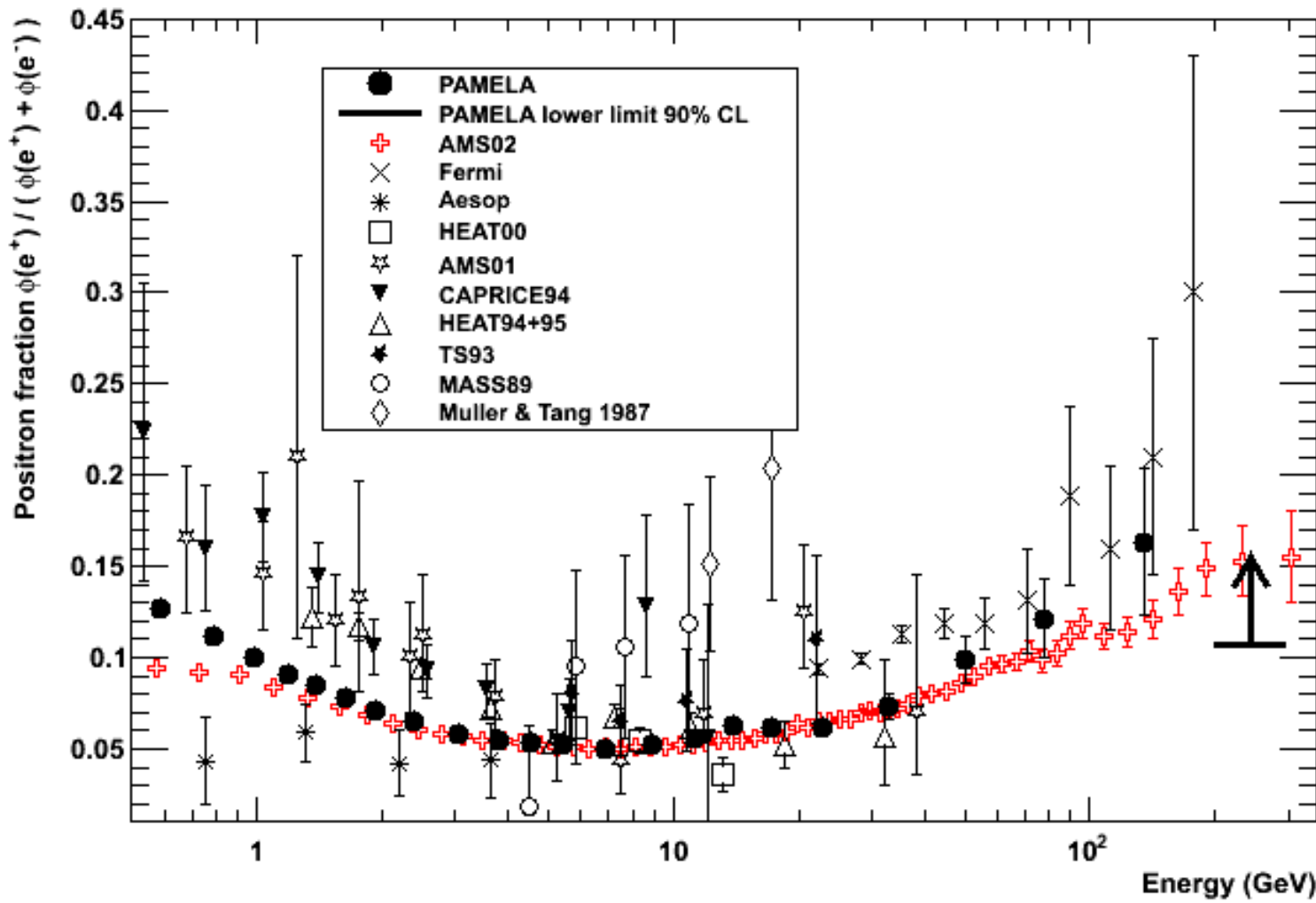


Example of Positron Selection:

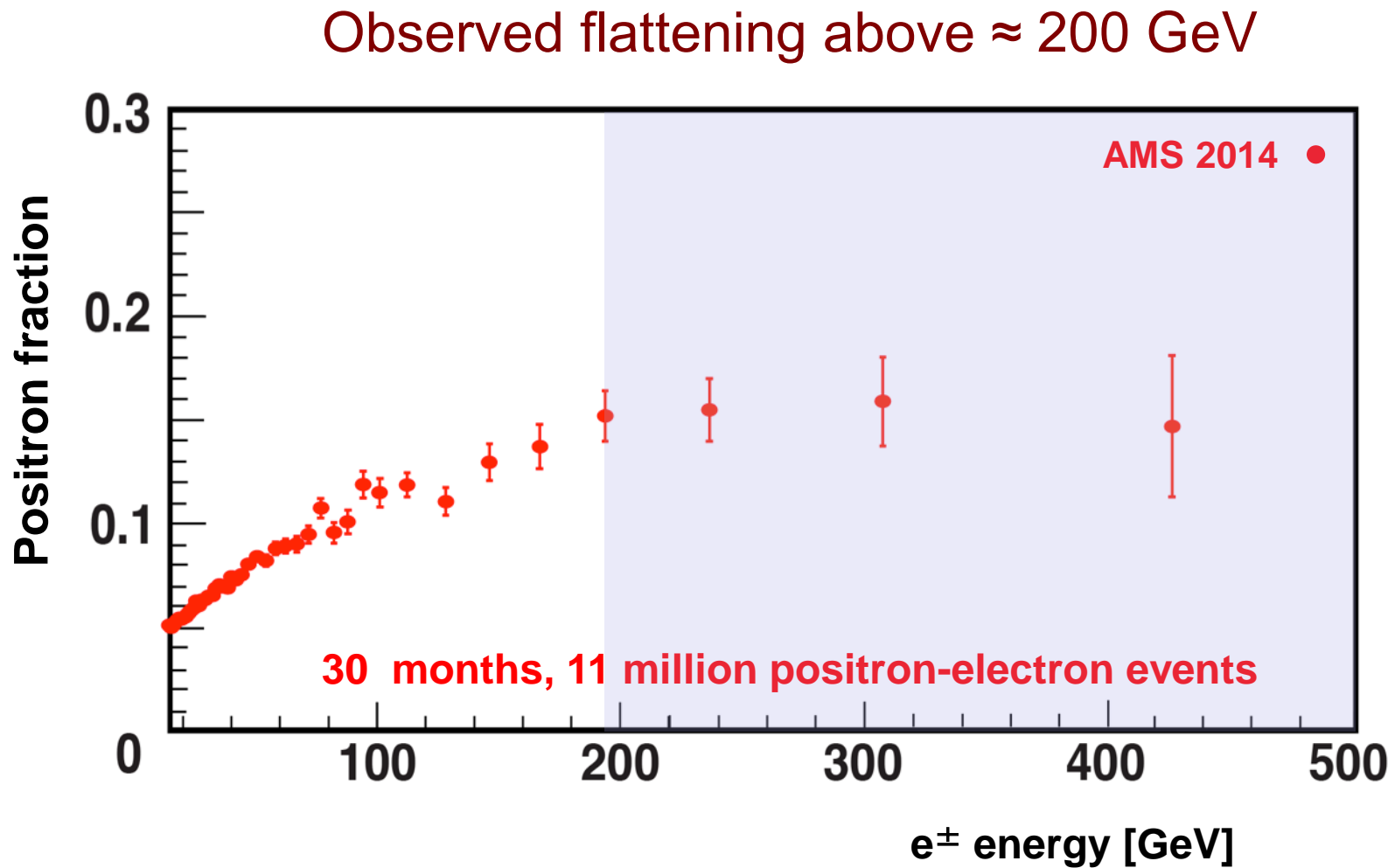
The TRD Estimator shows clear separation between **protons** and **positrons** with a small **charge confusion** background



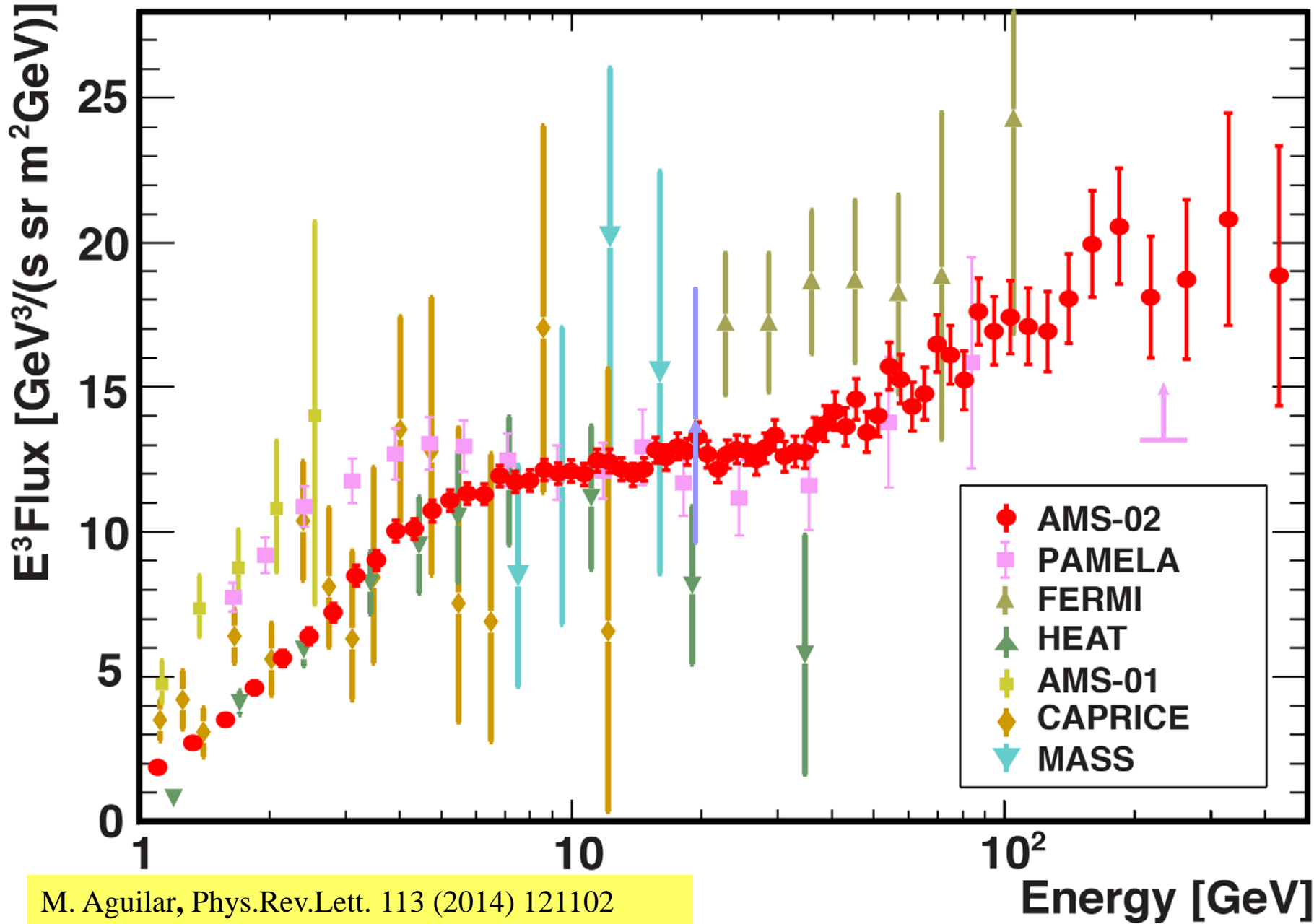
AMS Positron Fraction



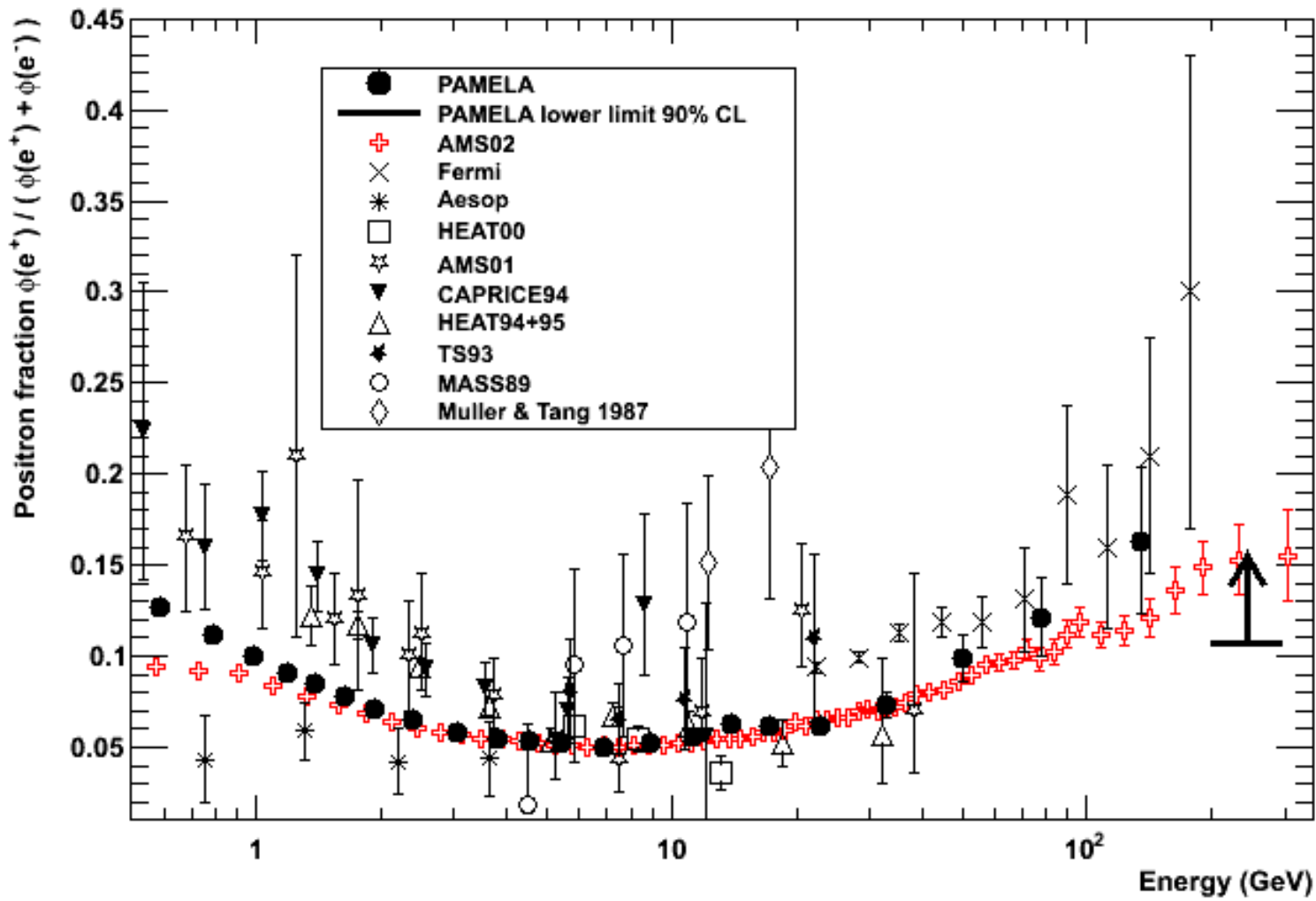
2014: New Results on Positron Fraction



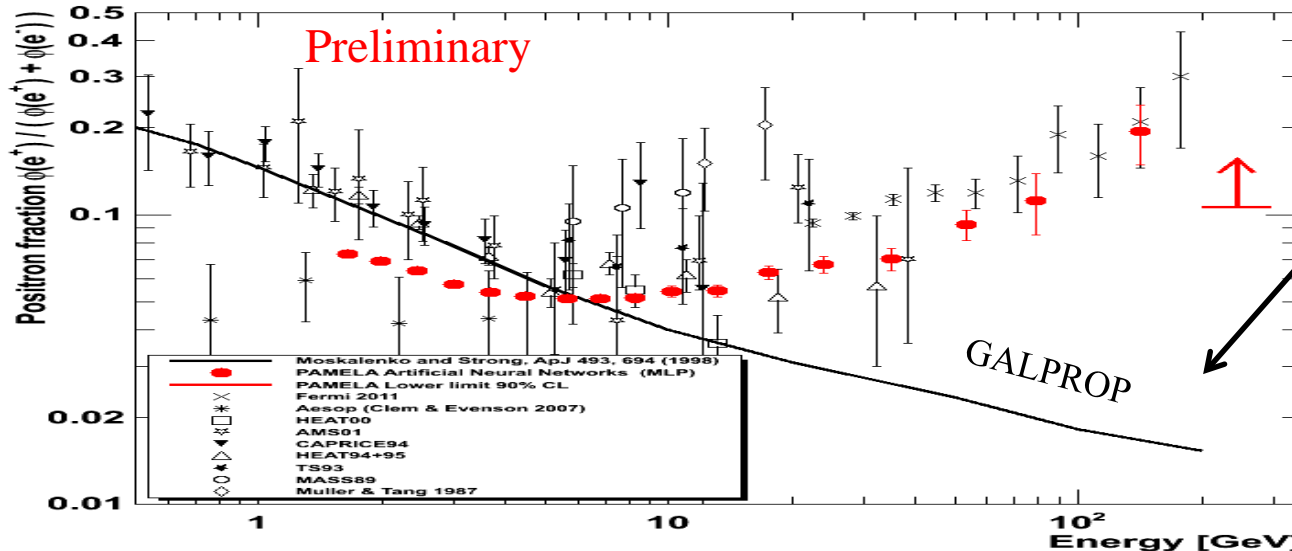
Positron Flux Data with AMS



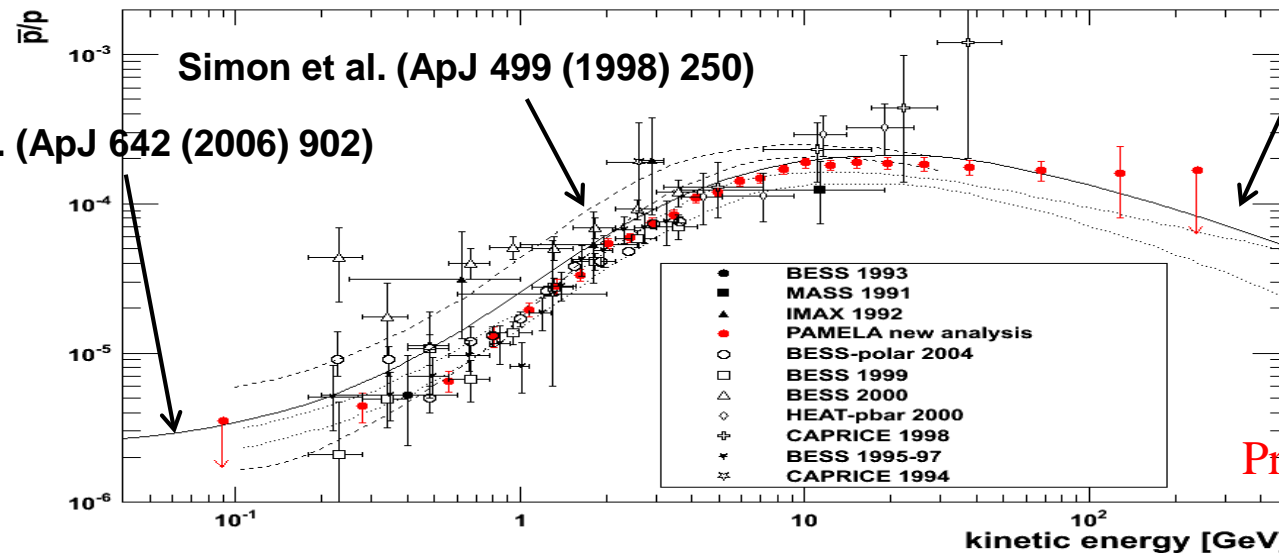
AMS Positron Fraction



A Challenging Puzzle for CR Physics



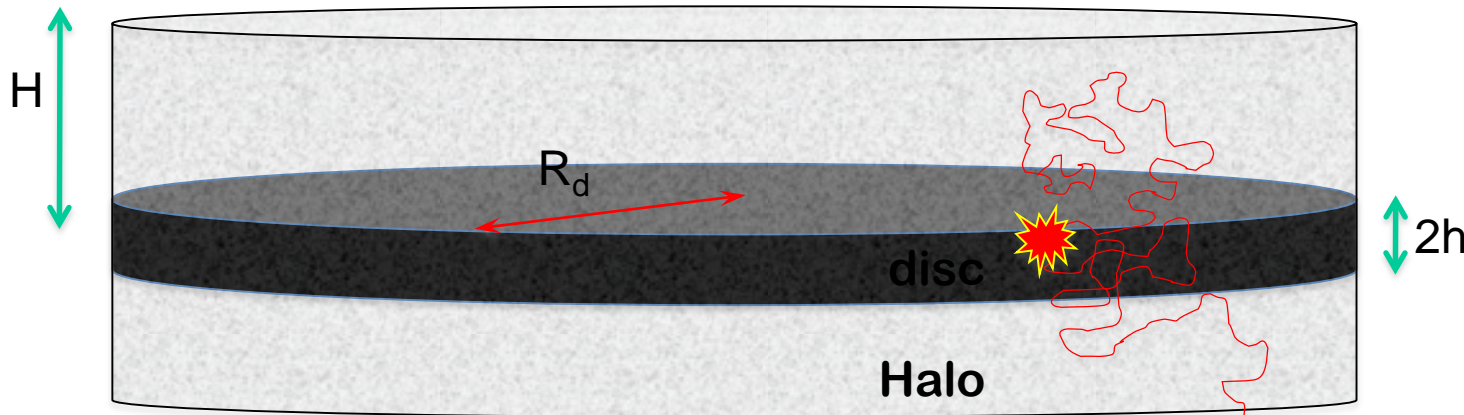
CR Positron spectrum significantly harder than expectations from secondary production



Donato et al.
(PRL 102
(2009) 071301)

But antiprotons in CRs are in agreement with secondary production

Secondary positrons (1)



PRIMARY COSMIC RAY SPECTRUM AT EARTH

$$n_{CR}(E) = \frac{N(E) \mathcal{R}}{2\pi R_d^2} \frac{H}{D(E)} \equiv \frac{N(E) \mathcal{R}}{2H\pi R_d^2} \frac{H^2}{D(E)} \propto E^{-\gamma-\delta}$$

SPECTRUM OF PRIMARY ELECTRONS AT EARTH

$$n_e(E) \approx \frac{N(E) \mathfrak{R} \tau_{loss}(E)}{\sqrt{D(E) \tau_{loss}(E)}} \propto E^{-\gamma-1/2-\delta/2}$$

IF ENERGY LOSSES
ARE DOMINANT
UPON DIFFUSION
(TYPICALLY $E > 10$ GeV)

Secondary positrons (2)

INJECTION RATE OF SECONDARY POSITRONS

$$q_{e^+}(E')dE' = n_{CR}(E)dE \ n_H \sigma_{pp} c \propto E^{-\gamma-\delta}$$

EQUILIBRIUM SPECTRUM OF SECONDARY POSITRONS (AND ELECTRONS) AT EARTH

$$n_{e^+}(E) \approx \frac{q_{e^+}(E)\tau_{loss}(E)}{\sqrt{D(E)\tau_{loss}(E)}} \propto E^{-\gamma-1/2-3\delta/2}$$

POSITRON
FRACTION

$$\frac{\Phi_{e^+}}{\Phi_{e^+} + \Phi_{e^-}} \approx \frac{\Phi_{e^+}}{\Phi_{e^-}} \propto E^{-\delta}$$

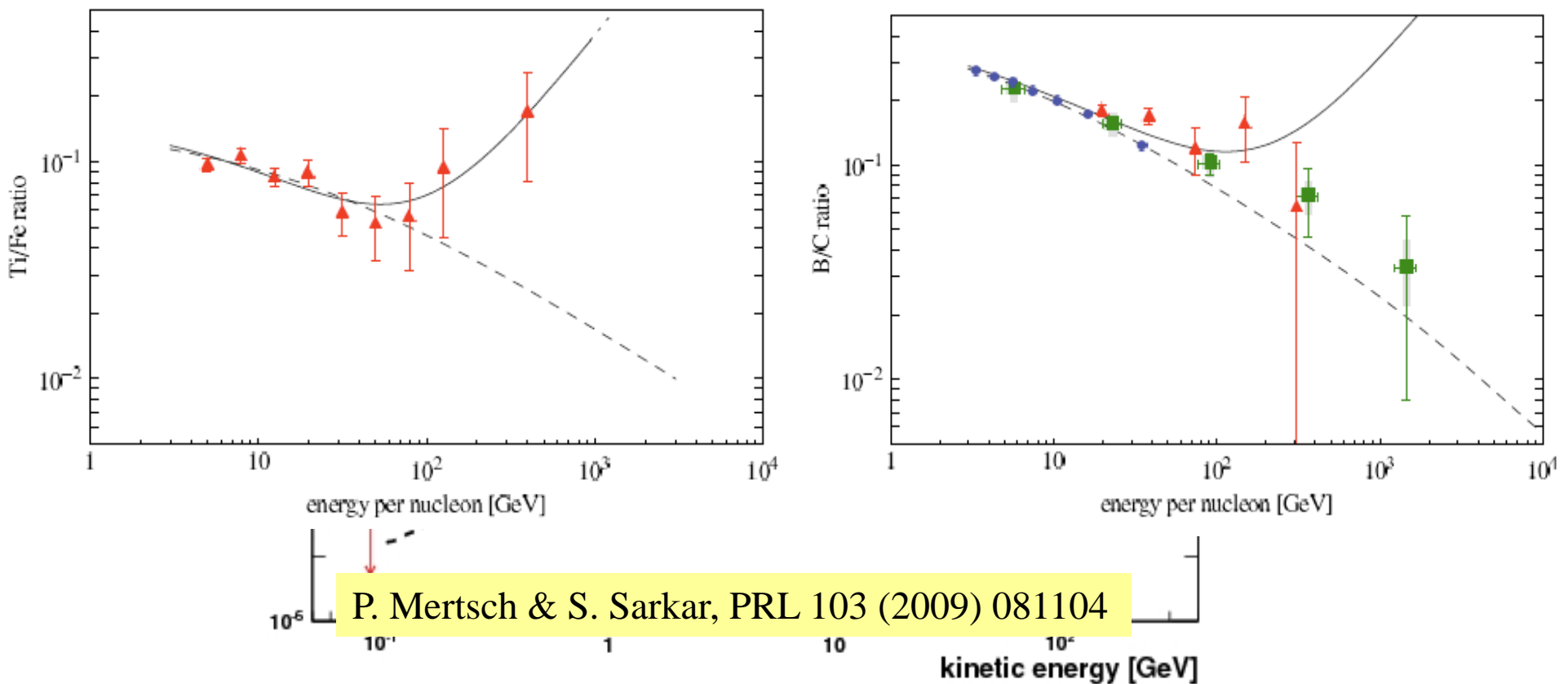
MONOTONICALLY
DECREASING
FUNCTION OF
ENERGY

Implications

A rising positron fraction requires:

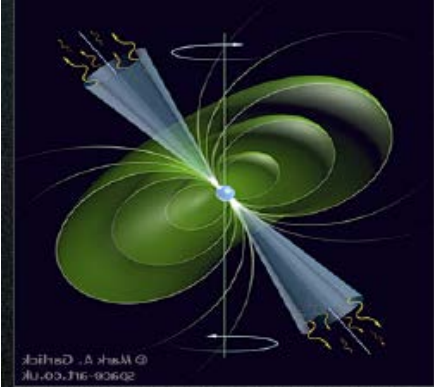
1. An additional component of positrons with spectrum flatter than CR primary electrons
2. A diffusion coefficient with a weird energy dependence
(BUT this should reflect in the CR spectrum as well)
3. Subtleties of Propagation

A Challenging Puzzle for CR Physics



P.Błasi, PRL 103 (2009) 051104 (see also Y. Fujita et al., PRD 80 (2009) 063003, M. Ahlers et al. PRD 80 (2009) 123017) Positrons (and electrons) produced as secondaries in the sources (e.g. SNR) where CRs are accelerated.

But also other secondaries are produced: significant increase expected in the p/p and secondary nuclei ratios.



Astrophysical Explanation: Pulsars

Mechanism: the spinning B of the pulsar strips e^- that accelerated in the outer magnetosphere emit g that produce e^\pm . But pairs are trapped in the cloud. After $(4\text{-}5)\times 10^4$ years pulsars leave remanent and pairs are liberated (e.g. P. Blasi & E. Amato, arXiv:1007.4745).

Young ($T < 10^5$ years) and nearby ($< 1\text{kpc}$)
If not: too much diffusion, low energy, too low flux.

Geminga: 157 parsecs from Earth and 370,000 years old

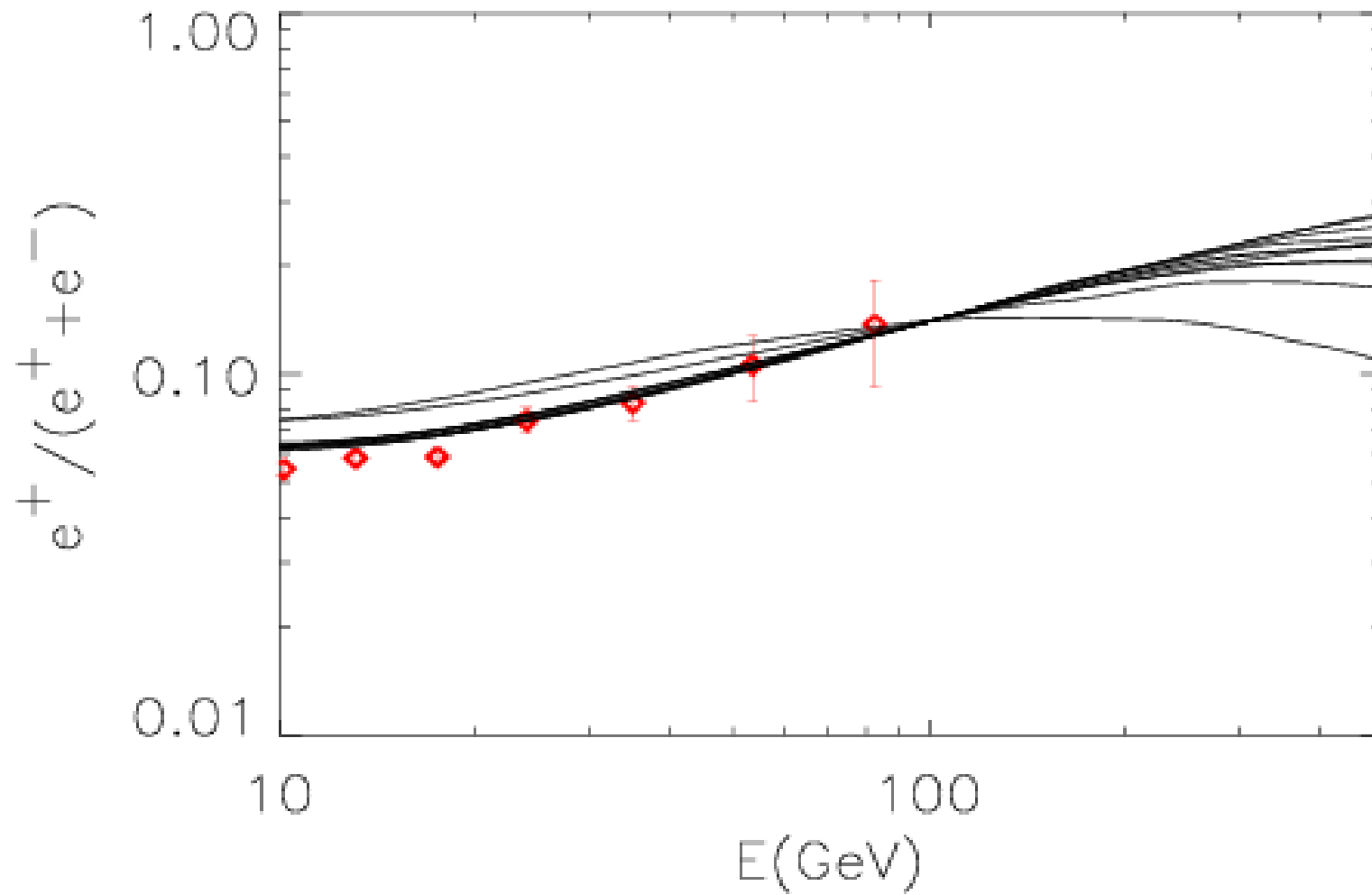
B0656+14: 290 parsecs from Earth and 110,000 years old.

Not a new idea, e.g.: Harding & Ramaty, ICRC 2 (1987), Boulares, ApJ 342 (1989), Atoyan et al. PRD 52 (1995)

CRAB NEBULA



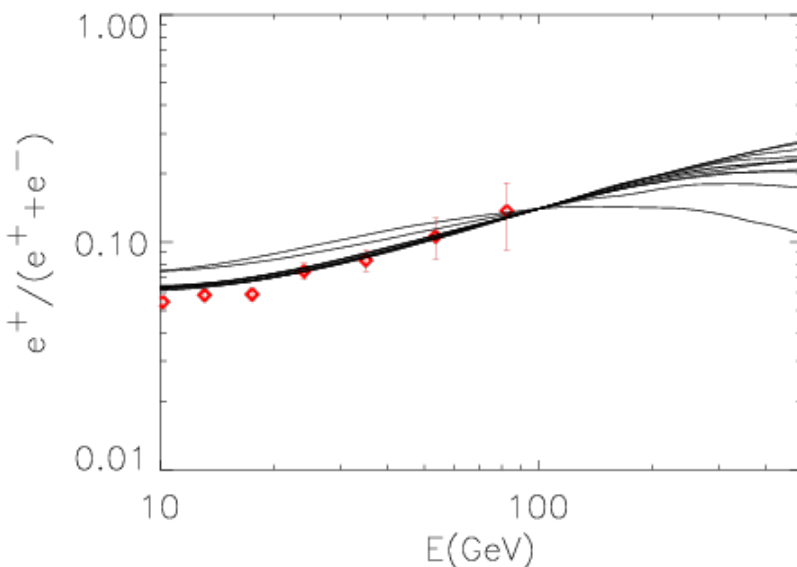
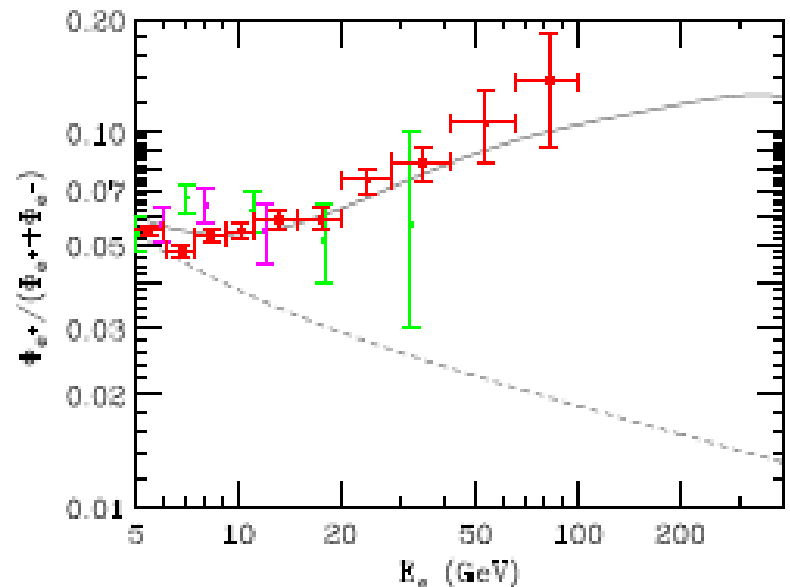
A Challenging Puzzle for CR Physics



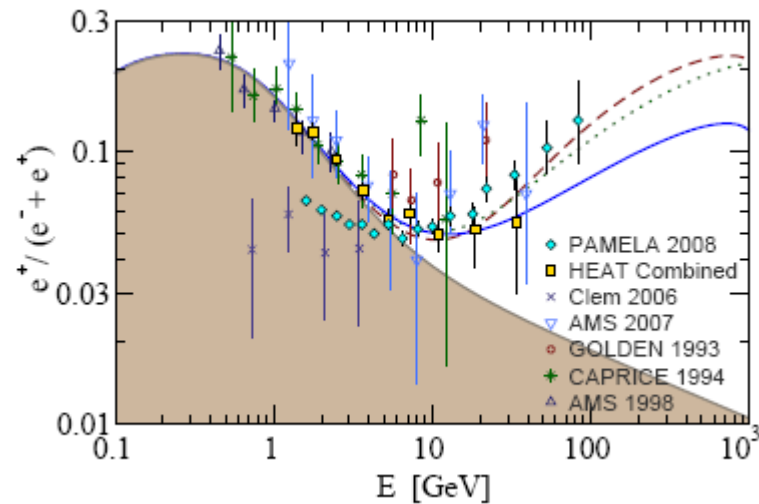
P. Blasi & E. Amato, arXiv:1007.4745

Contribution from pulsars varying the injection index and location of the sources.

Pulsar Explanation



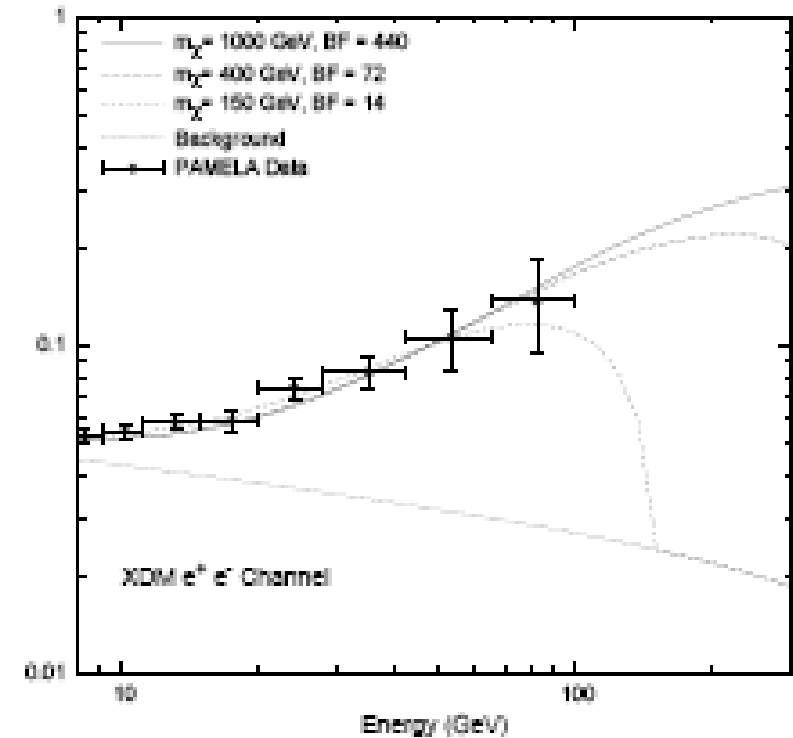
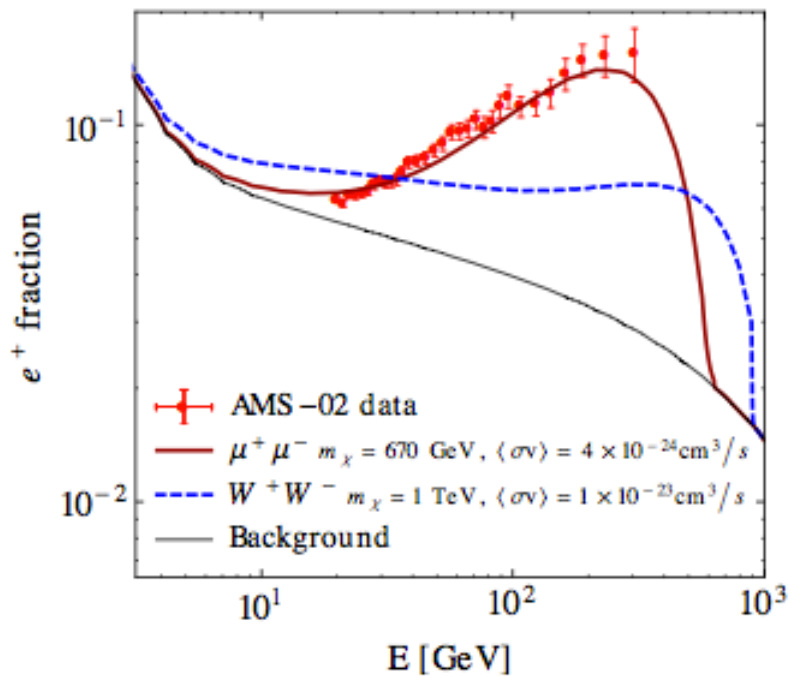
D. Hooper, P. Blasi, and P. Serpico, JCAP 0901:025,2009; arXiv:0810.1527
Contribution from diffuse mature & nearby young pulsars.



H. Yuksel et al., PRL 103 (2009) 051101; arXiv:0810.2784v2
Contributions of e^- & e^+ from Geminga assuming different distance, age and energetic of the pulsar

P. Blasi & E. Amato, arXiv:1007.4745
Contribution from pulsars varying the injection index and location of the sources.

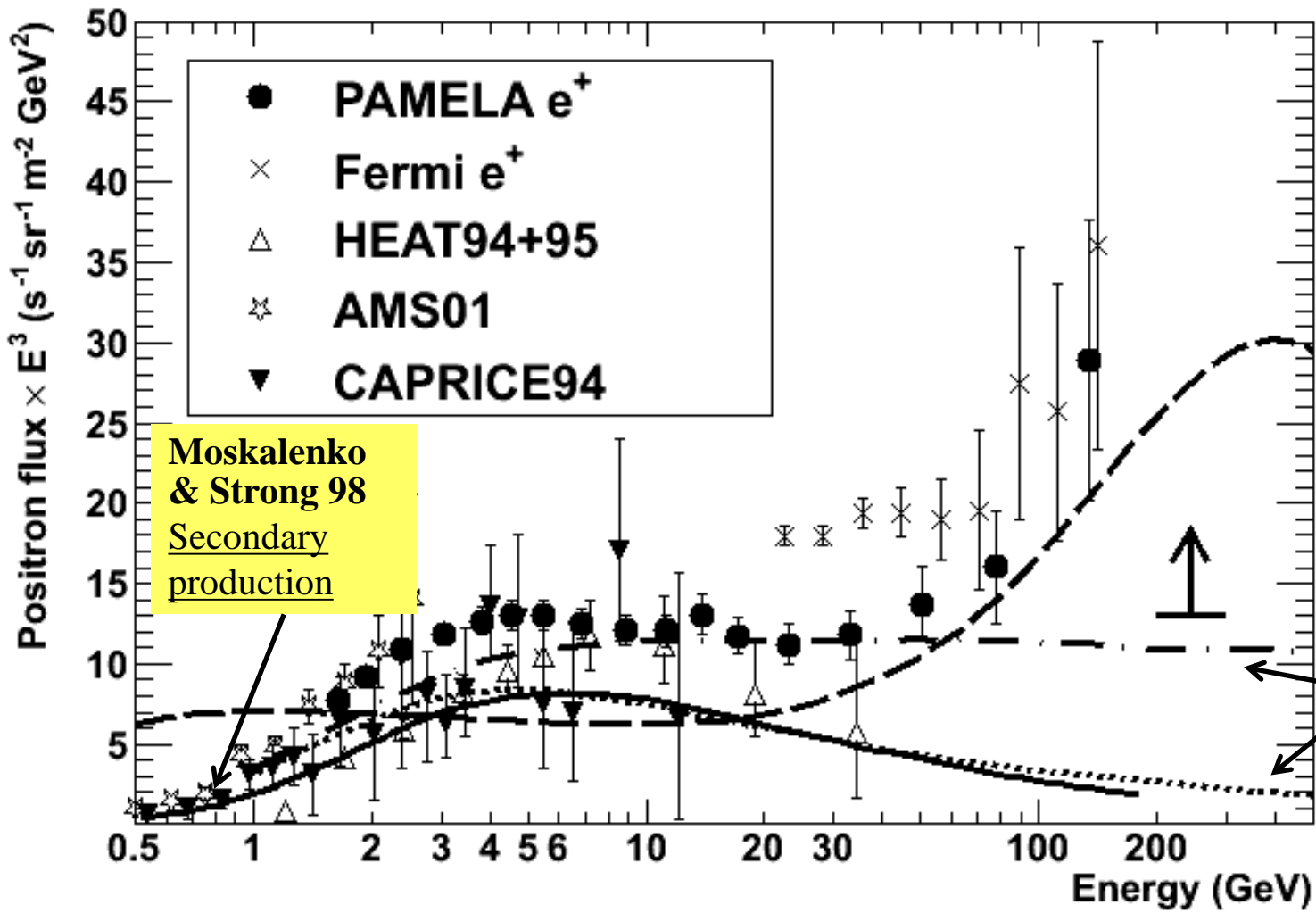
Dark Matter Explanation



J. Kopp, Phys. Rev. D 88 (2013)
076013; arXiv:1304.1184

I. Cholis et al., Phys. Rev. D 80 (2009)
123518; arXiv:0811.3641v1

Positron Energy Spectrum

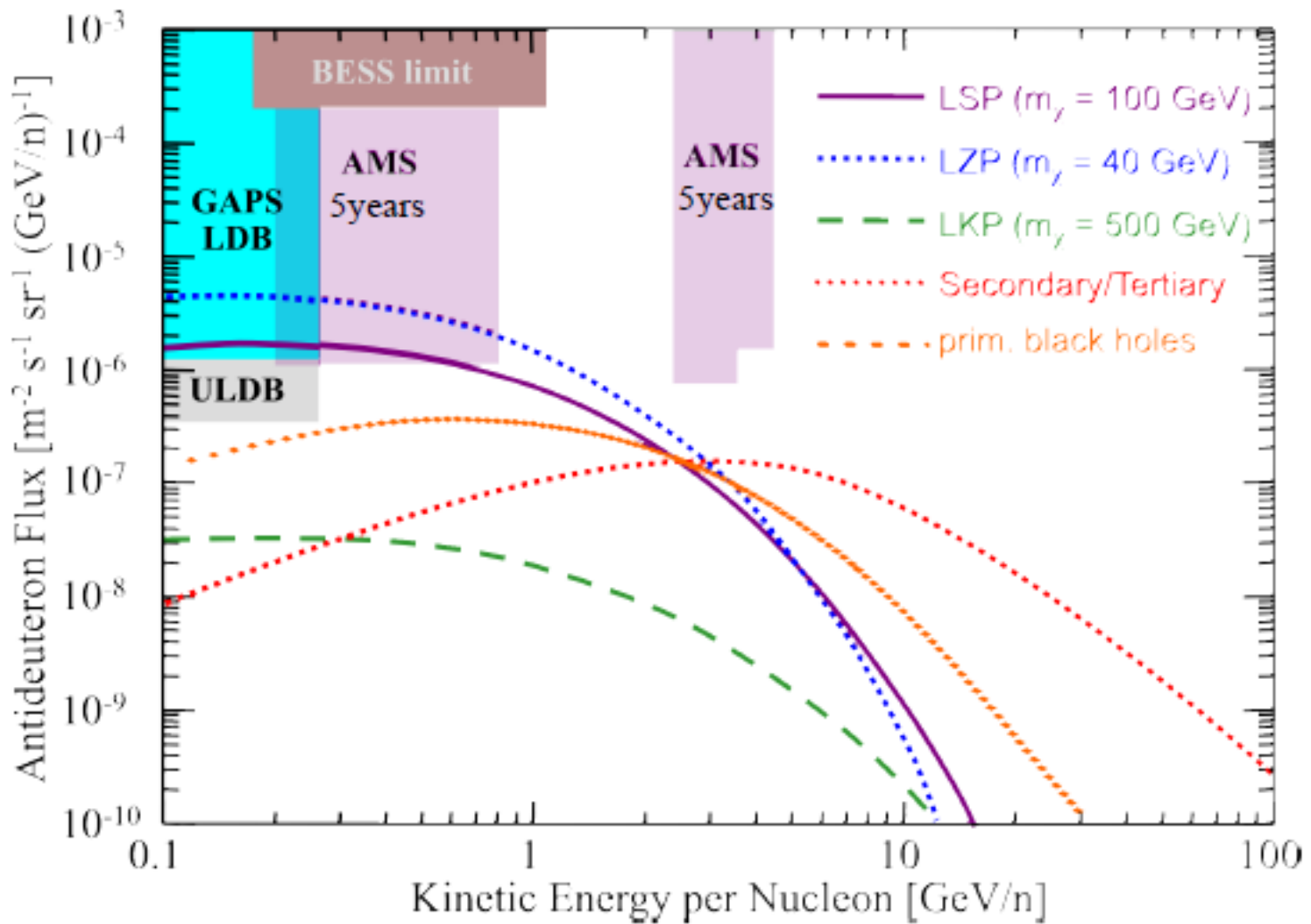


D. P. Finkbeiner et al., JCAP 1105, 002 (2011).
Secondary+primary production (from dark matter annihilation)

T. Delahaye et al., A&A 524 (2010) A51
Secondary & Secondary+Primary production (from Astrophysical Sources)

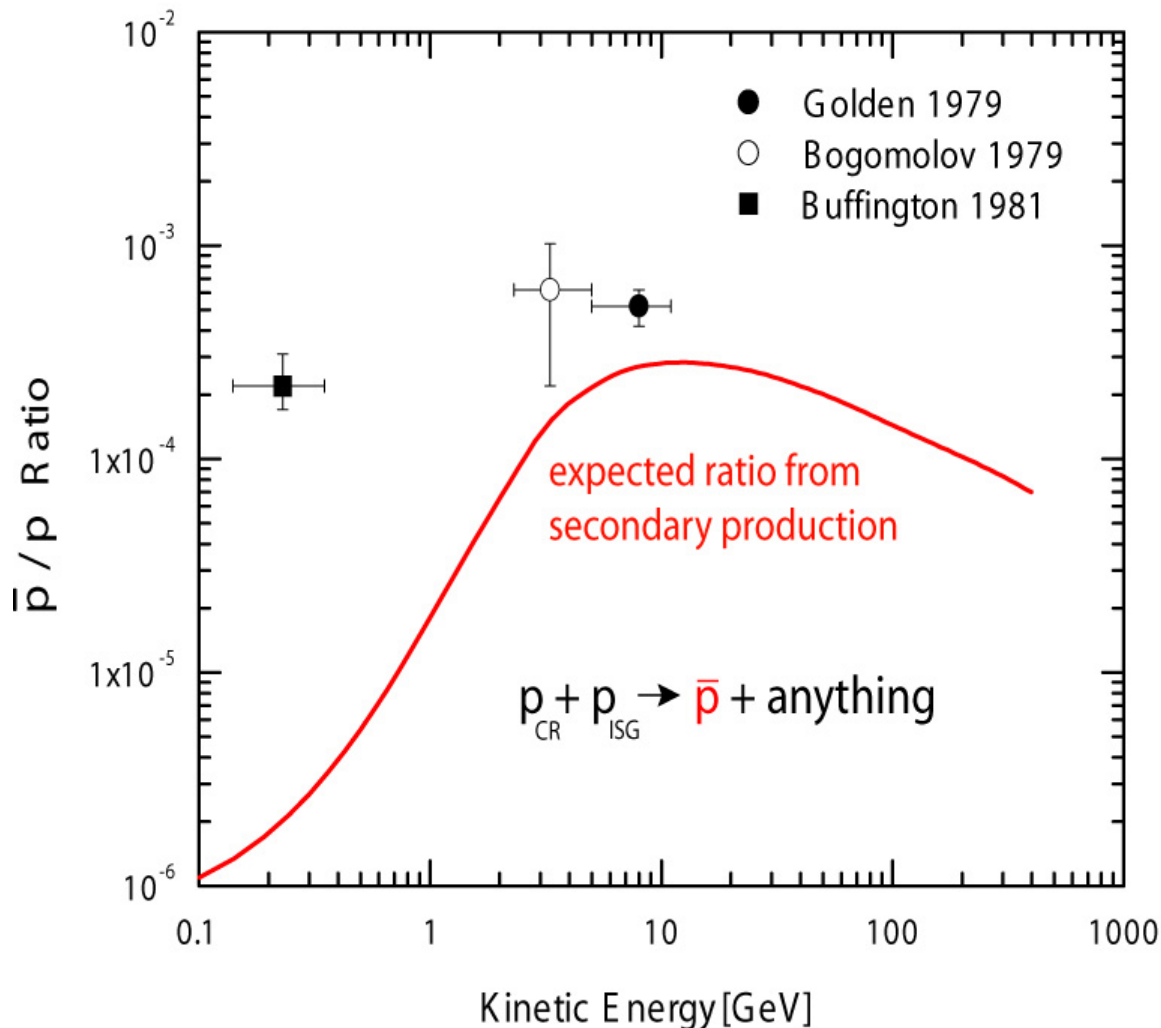
Antideuterons

P. Von
Doetinchem,
UCLA Dark
Matter 2012



Conclusions

The first historical measurements on galactic antiprotons



Conclusions

